Volume 34, Issue 01, 2021 **ISSN 1096-9411**

Dental Anthropology

A Publication of the Dental Anthropology Association

Dental Anthropology

Volume 34, Issue 01, 2021

Dental Anthropology is the Official Publication of the Dental Anthropology Association.

Contact for Manuscripts

Dr. Marin A. Pilloud
Department of Anthropology
University of Nevada, Reno
E-mail address: mpilloud@unr.edu
Website: journal.dentalanthropology.org

Address for Book Reviews

Dr. Daniel H. Temple
Department of Sociology and Anthropology
George Mason University
E-mail address: dtemple3@gmu.edu

Published at

University of Nevada, Reno
Reno, Nevada 89557

The University of Nevada, Reno is an EEO/AA/Title IX/Section 504/ADA employer

Editorial Assistant

Rebecca L. George

Production Assistant

Daniel E. Ehrlich

Growth Rates of Accessory Human Enamel: A Histological Case Study of a Modern-Day Incisor from Northern England

Christopher Aris[1*] and Emma Street[2]

[1] University of Kent, Canterbury, UK
[2] No affiliations

Keywords: incisor, enamel, daily secretion rates

ABSTRACT This study investigates enamel growth of a modern-day human upper first incisor (S197) possessing a talon cusp (accessory cusp). Growth rates collected from the accessory enamel are compared to data collected from the primary cusp and cusps of a standard incisor sample from the same population. Upper first incisors (n=12) and S197 were analysed using histological methods. Daily secretion rates (DSRs) were calculated for inner, mid, and outer regions of cuspal and lateral sites. Additional DSRs were calculated for equivalent regions of S197's accessory cusp. S197's primary cusp DSRs were significantly faster than the accessory cusp for all lateral regions, but significantly slower in the inner and mid cuspal regions. S197's primary cusp DSRs were also significantly slower than the standard incisor sample for all regions except the lateral cuspal. The DSRs of the standard sample were significantly faster than those of S197's accessory cusp for all lateral regions, but significantly slower in the inner cuspal region. This case study displays that human teeth possessing accessory cusps can present varying DSRs to teeth lacking accessory enamel from the same population, and that accessory enamel growth may not follow the same pattern of increasing DSRs along the length of enamel prisms.

The study of modern human enamel growth rates via histological analysis is common within the study of biological anthropology and bioarchaeology, commonly focusing on the variation between cusps of the same tooth (e.g. Mahoney, 2008), within single populations (e.g. Schwartz et al., 2001), and between populations (e.g. Smith et al., 2007; Aris et al., 2020a, 2020b). A common trend between these lines of research is the exclusive use of what are deemed as dental samples containing no evidence of pathology, stress markers, or growth of accessory enamel (defined here as: growth of enamel outside of the features typically used to define and identify human tooth types). While past research has touched on how some human enamel growth features vary between individuals suffering from stress and those not suffering from stress resulting in dental morphologies, these typically concern the accuracy of making certain calculations relating to enamel growth (Lukacs & Guatelli-Steinberg, 1994; Guatelli-Steinberg & Lukacs, 1999), and the development of non-accessory enamel (defined here as: growth of the enamel features which define how human tooth types are identified and classified) in individuals presenting evidence of stress on their dental morphology (e.g. Fitzgerald & Saunders, 2005). Comparison of enamel growth rates collected from teeth presenting accessory enamel to those with no evidence of stress markers or non-metric traits from the same population, and comparison of accessory enamel growth to the growth of non-accessory enamel within the same tooth, have yet to be conducted. This project aims to begin to address these issues and widen our understanding of accessory enamel growth in modern-day humans through the case study of a modern-day upper first incisor.

Background

Amelogenesis and daily enamel growth

Amelogenesis is the process of secretion and mineralization of protein matrix by ameloblast cells (Boyde, 1989; Nanci & Smith, 1992; Smith & Nanci, 1995). During the secretory stage of amelogenesis,

*Correspondence to:
Christopher Aris
Department of Archaeology
Ella Armitage Building
University of Sheffield
Sheffield, UK
c.aris@sheffield.ac.uk

ameloblast secretion is altered according to a daily circadian rhythm, producing short-period markers along the length of enamel prisms (e.g., Asper, 1916; Gysi, 1931; Massler & Schour, 1946; Okada, 1943; Kajiyama, 1965; Dean et al., 1993; Smith & Nanci, 2003). These daily forming markers are known as cross striations (e.g. Boyde, 1963; 1990; Kajiyama, 1965; Bromage, 1991; Dean, 1995; Fitzgerald, 1995, 1998; Antoine, 2000; Antoine et al., 2009). The formation of cross striations causes alterations in the refractive index of enamel prisms, making them observable in thin sections under transmitted light (e.g. Berkovitz et al., 2002; Zheng et al., 2013).

Daily secretion rates (DSRs) can be calculated from cross striations. These rates accelerate from inner enamel regions proximal to the enamel dentine junction towards the outer enamel surface (e.g. Beynon et al., 1991 Beynon et al., 1998; Reid et al., 1998; Lacruz & Bromage, 2006; Mahoney, 2008; Aris et al., 2020a, 2020b). Daily secretion rates are also faster relative to their proximity to the dentine horn (Beynon et al., 1991). Due to DSRs varying within a tooth, analysis of these rates are undertaken for specific regions (e.g. Dean, 1998) where the crown is divided into cuspal, lateral, and cervical enamel, and then further subdivided into inner, mid, and outer regions. Typically, DSRs are broadly similar when equivalent regions are compared between cusps within a molar (Mahoney, 2008).

Analysis of DSRs for human samples have examined variations within individual teeth (Mahoney, 2008), differences between biologically male and female groups (Schwartz et al., 2001), and more recently variations between populations (Aris et al., 2020a, 2020b). Despite the breadth of these studies, they have universally used teeth absent of evidence of stress, pathology, and accessory enamel growth. Thus, our understanding of how human DSRs vary in accessory enamel in comparison to non-accessory enamel is limited.

Enamel growth patterns within pathological cases

While the DSRs of accessory enamel have not yet been analysed, certain features of enamel growth have been analysed for individuals presenting signs of stress on their dentition. These studies have focused on the possible changes in amelogenesis, which leads to the formation of enamel growth defects observable from internal and external analysis. Lukacs and colleagues have published a series of papers explaining the pattern and expression of enamel defects in modern humans. These can vary due to diet, geographic location, and climate. In particular, these papers present evidence of longer crown formation times (CFTs) in stressed individuals (Lukacs et al., 1989; Lukacs, 1991, 1992, 1999; Lukacs & Joshi, 1992; Lukacs & Pal, 1993; Lukacs & Guatelli-Steinberg, 1994; Luckas & Walimbe, 1998; Guatelli-Steinberg & Lukacs, 1999). As CFTs are directly related to the products of daily enamel growth (e.g. Massler & Schour, 1946) there is potential that accessory enamel possesses growth rates which vary from non-accessory enamel.

Fitzgerald and Saunders (2005) investigated the possibility of using enamel defects to predict the age at which stress was incurred and thus improve the way in which we interpret the influence of stress on enamel growth patterns. This concept was based on the ability to age through examining interior enamel structures, and that these structures would be notably altered during stressful events. Through the use of a large sample size (274 teeth from 127 Roman subadults), they concluded that enamel formation patterns are more highly impacted according to the severity of the cause of stress, and that there is no minimum requirement of stress level for enamel to be effected (Fitzgerald & Saunders, 2005). Multiple papers have since been published on this topic, all conclusively stating that stress impacts enamel structures, significantly increases CFTs, and reduces the reliability of DSR calculations (Reid & Dean, 2006; Holt et al., 2012; Birch & Dean, 2014; Primeau et al., 2015). As a result of these studies, we can reliably say that non-accessory enamel grows differentially in individuals presenting evidence of stress. It is therefore important to expand our understanding of how accessory enamel grows in relation to non-accessory enamel.

Material and methods

Dental sample

Upper permanent first incisors (n=13) were selected from a modern-day collection consisting of teeth extracted between 1964 and 1973 at dental surgeries in northern England and southern Scotland. All 13 samples originated from Newcastle-Upon-Tyne, including an incisor presenting an accessory enamel cusp (S197). The accessory cusp of S197 has developed on the cingulum and reached beyond half the distance to the incisal edge (Figure 1), as such it is diagnosed as a talon cusp (Edgar et al., 2016). The remaining 12 incisors made up a standard sample, with each tooth presenting no evidence of stress, pathology, or accessory enamel growth. Right teeth were selected unless it was

unavailable or the left was better preserved. The collection itself is curated at the Skeletal Biology Research Centre, University of Kent, as part of the UCL/Kent Collection. Ethical approval for the histological analysis of this dental sample was obtained from the UK National Health Service research ethics committee (REC reference: 16/SC/0166; project ID: 203541).

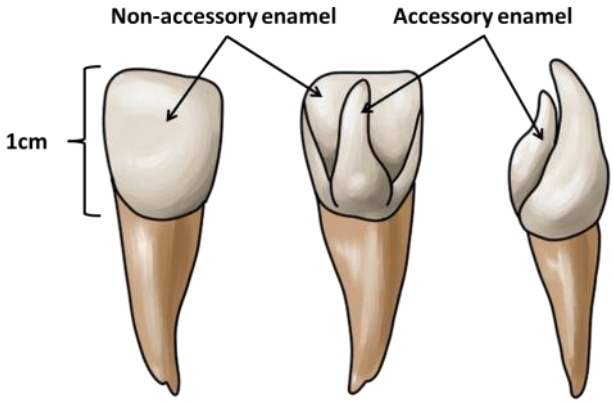

Figure 1. Depictions of upper first permanent incisor S197 prior to sectioning highlighting the regions defined as accessory and non-accessory enamel. Moving left to right the images display the tooth from the labial, lingual, and mesial directions.

Sample preparation

Resin casts were produced for each incisor prior to any destructive analysis, and were produced using standard methods (Aris, 2020). The casts reproduced the surface morphology of the tooth crown allowing for future study of microwear, crown morphology, and enamel surface features including linear enamel hypoplasia and perikymata.

Thin sections were produced using standard histological procedures (e.g. Schwartz et al., 2005; Mahoney, 2008; Aris, 2020). The incisors were embedded in an epoxy resin and hardener mixture (Buehler®) to minimise the chance of the teeth fracturing during sectioning. Embedded samples were then cut at a low speed using a diamond-edged wafering blade (Buehler® IsoMet 1000 Precision Cutter) at a longitudinal angle through the apex of the incisal crowns. The samples were then mounted on glass microscope slides and lapped using progressively finer grinding pads (Buehler®) until around 120µm in thickness. Ground samples were polished using 0.3µm aluminium oxide powder until evidence of lapping was removed from the mounted dental samples. Polished samples were then placed within an ultrasonic bath for two minutes in order to remove any remaining debris before being dehydrated using 90% and 100% ethanol-based solutions (Fisher scientific®). The dehydrated sections were finally cleared using Histoclear® and mounted with a glass cover slip using a mounting medium (DPX®). All sections were examined using polarised light microscopy (Olympus BX53 Upright Microscope). Analysis and image capture was conducted using micro imaging software (cellSens) (see below for detail).

Daily secretion rates

The DSRs for the incisors were calculated for the inner, mid, and outer areas of the lateral and cuspal enamel sites of each tooth using standard methods (e.g. Beynon et al., 1991a; Schwartz et al., 2001; Mahoney, 2008; Aris et al., 2020a, 2020b). Each region within the cuspal and lateral sites was determined by dividing the length of the enamel regions into three equidistant portions, following the longitudinal axis of local enamel prisms (Figure 2). The lateral enamel areas were determined within the section of imbricational enamel equidistant between the dental cervix and dentine horn. Regions of cuspal enamel were determined within the appositional enamel starting near the dentine horn. Additional DSRs were calculated for isolated regions of S197's accessory cusp (see Figure 2). These regions were selected in a fashion as to mirror the cuspal and lateral regions of the primary cusp.

Within each enamel region a measurement was made of five consecutive cross striations along the length of an enamel prism. This measurement was subsequently divided by five, giving a mean daily rate of matrix secretion (µm/day). This process was repeated to produce six mean DSRs for each region. For the standard incisor sample these results were then similarly divided to give a grand mean and standard deviation, following the standard statistical and methodological approaches of studying human enamel growth rates (e.g. Beynon et al., 1991 Beynon et al., 1998; Reid et al., 1998; Lacruz & Bromage, 2006; Mahoney, 2008; Aris et al., 2020a, 2020b). For S197 the six mean DSRs for each region were kept separate for future analysis. All cross striation measurements were taken between 20x and 40x magnification (Figure 3).

Statistical analysis

Independent sample T-tests were used to compare mean equivalent regional DSRs between the selected samples. First, the same DSRs of the primary cusp and accessory cusp of S197 were compared.

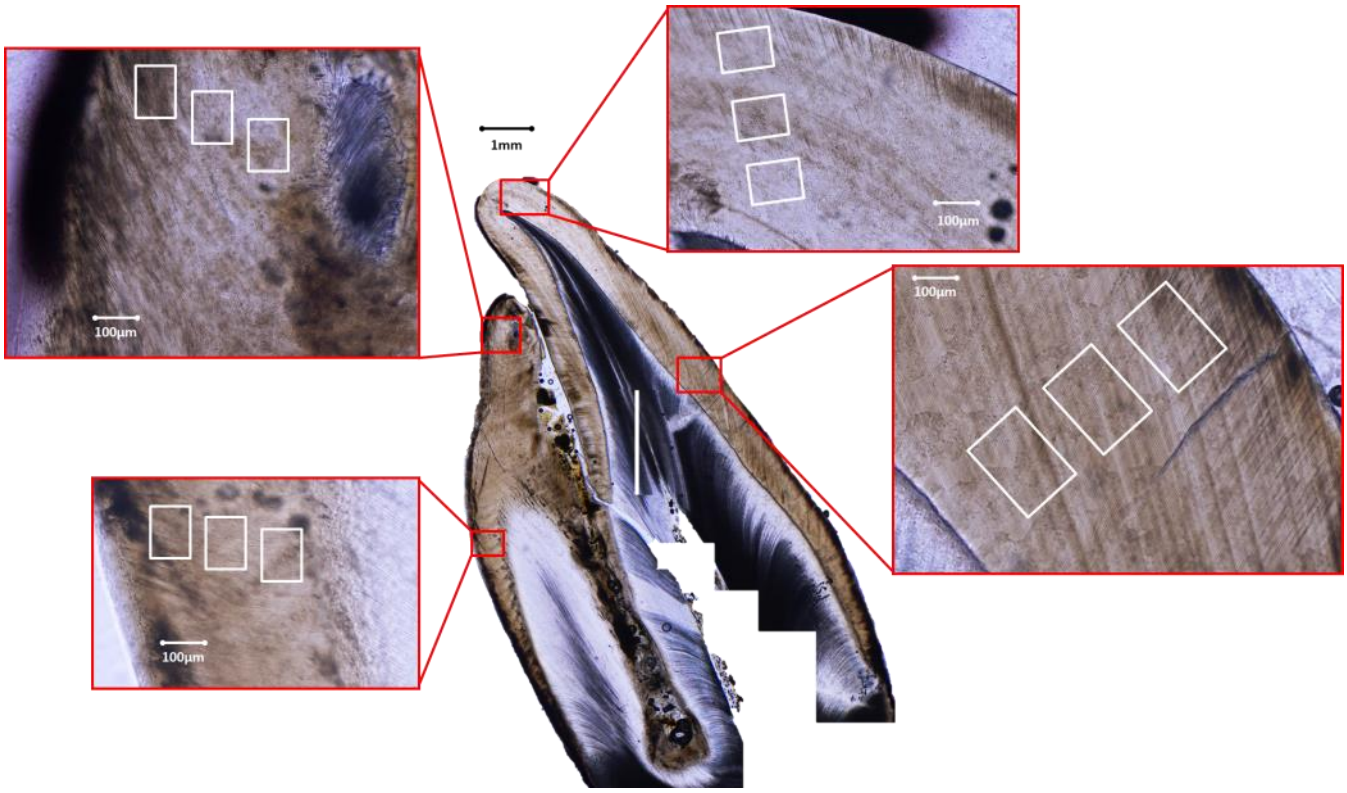

Figure 2. Cross section of Sample 197 displaying the regions from which DSRs were collected. Right superimpositions show the cuspal (top) and lateral (bottom) sites of the primary cusp. Left superimpositions show the cuspal (top) and lateral (bottom) sites of the accessory enamel. White squares represent the inner, mid, and outer regions of each site respectively moving from the enamel dentine junction towards the outer enamel surface. Daily secretion rates were collected from healthy clinical teeth from equivalent cuspal and lateral sites to the right superimpositions.

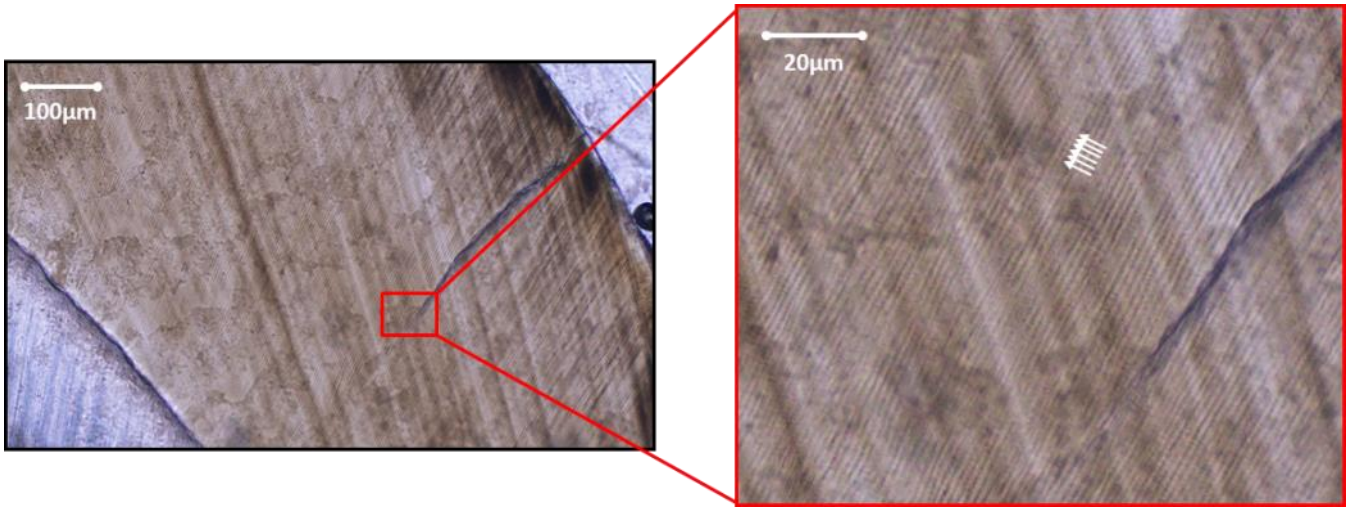

Figure 3. Cross section of the cuspal enamel site of the primary cusp of Sample 197. The right superimposition displays a portion of the mid cuspal region, and the white arrows indicate individual cross striations.

Second, the DSRs collected from the primary cusp enamel of S197 were compared to those of the standard clinical sample. Third, the DSRs of the accessory enamel of S197 were compared to those of the standard clinical sample. All statistical analyses were conducted using SPSS 24.0.

Results

Accessory enamel DSRs compared to primary cusp DSRs

Table 1 displays the results of comparing the mean DSRs of the primary cusp enamel to those of the accessory cusp enamel, all collected from S197. For the inner and mid regions of the lateral enamel the primary cusp enamel presented significantly faster DSRs. These were faster by a mean rate of 0.53µm/day (p<0.00) in the inner region, and 0.47µm/day (p=0.01) in the mid region. Conversely, accessory enamel presented significantly faster DSRs for the inner and mid cuspal enamel regions. These were faster by a mean rate of 2.14µm/day (p<0.00) in the inner region, and 1.02µm/day (p<0.00) in the mid region.

Non-accessory enamel DSRs compared to rest of population

Table 2 displays the results of comparing the mean DSRs of the primary cusp enamel of S197 to those of the standard clinical sample. For all regions of the lateral enamel, the standard sample presented significantly faster DSRs. These were faster by a mean rate of 0.27µm/day (p=0.01) in the inner region, 0.51µm/day (p<0.00) in the mid region, and 0.37µm/day (p=0.02) in the outer region. The standard sample also presented significantly faster DSRs for the inner and mid cuspal enamel regions. These were faster by a mean rate of 0.69µm/day (p<0.00) in the inner region, and 0.65µm/day (p<0.00) in the mid region.

Accessory enamel DSRs compared to rest of population

Table 3 displays the results of comparing the mean DSRs of the accessory enamel of S197 to those of the standard clinical sample. For all regions of the lateral enamel, the standard sample presented significantly faster DSRs. These were faster by a mean rate of 0.80µm/day (p<0.00) in the inner region, 0.98µm/day (p<0.00) in the mid region, and 0.59µm/day (p<0.00) in the outer region. Conversely, the accessory enamel sample presented significantly faster DSRs for the inner cuspal enamel region by a mean rate of 1.45µm/day (p<0.00).

Discussion

Inter-regional enamel growth of S197

The lateral enamel DSRs of the primary cusp were significantly faster than those of the accessory enamel in the inner and mid regions. Conversely, the accessory enamel cuspal DSRs were significantly faster than those of the primary cusp for the inner and mid regions (see Table 1). This finding goes against those of past research, which found

*Table 1. Results of the independent samples T-tests comparing the mean regional DSRs (µm/day) of the accessory enamel of Sample 197 to the primary cusp enamel of Sample 197. Significant results are marked in bold, *p<0.00.*

Enamel Region	Sample	N	Mean	Min	Max	S.D.	Sig.
Lateral Enamel							
Inner	Accessory	6	2.24	2.02	2.37	0.14	**0.00***
	Primary cusp	6	2.77	2.48	2.98	0.19	
Mid	Accessory	6	2.51	2.37	2.81	0.16	**0.01**
	Primary cusp	6	2.98	2.67	3.35	0.24	
Outer	Accessory	6	3.13	2.89	3.78	0.33	0.42
	Primary cusp	6	3.35	2.88	3.77	0.34	
Cuspal Enamel							
Inner	Accessory	6	4.65	4.30	4.98	0.21	**0.00***
	Primary cusp	6	2.51	2.14	2.78	0.12	
Mid	Accessory	6	3.91	3.37	4.41	0.37	**0.00***
	Primary cusp	6	2.89	3.44	2.40	0.25	
Outer	Accessory	6	3.71	3.09	4.14	0.46	0.81
	Primary cusp	6	3.84	3.48	4.24	0.27	

*Table 2. Results of the independent samples T-tests comparing the mean regional DSRs (µm/day) of the healthy samples to those collected from the primary cusp enamel of Sample 197. Significant results are marked in bold, *p<0.00.*

Enamel Region	Sample	N	Mean	Min	Max	S.D	Sig.
Lateral Enamel							
Inner	Primary cusp	6	2.77	2.48	2.98	0.19	**0.01**
	Healthy	12	3.04	2.56	3.32	0.21	
Mid	Primary cusp	6	2.98	2.67	3.35	0.24	**0.00***
	Healthy	12	3.49	2.86	3.80	0.27	
Outer	Primary cusp	6	3.35	2.88	3.77	0.34	**0.02**
	Healthy	12	3.72	3.14	4.06	0.25	
Cuspal Enamel							
Inner	Primary cusp	6	2.51	2.14	2.78	0.12	**0.00***
	Healthy	8	3.20	2.84	3.43	0.23	
Mid	Primary cusp	6	2.89	3.44	2.40	0.25	**0.00***
	Healthy	8	3.54	3.16	3.86	0.22	
Outer	Primary cusp	6	3.84	3.48	4.24	0.27	0.69
	Healthy	8	3.89	3.36	4.09	0.23	

*Table 3. Results of the independent samples T-tests comparing the mean regional DSRs (µm/day) of the healthy samples to those collected from the accessory enamel of Sample 197. Significant results are marked in bold, *p<0.00.*

Enamel Region	Sample	N	Mean	Min	Max	S.D	Sig.
Lateral Enamel							
Inner	Accessory	6	2.24	2.02	2.37	0.14	**0.00***
	Healthy	12	3.04	2.56	3.32	0.21	
Mid	Accessory	6	2.51	2.37	2.81	0.16	**0.00***
	Healthy	12	3.49	2.86	3.80	0.27	
Outer	Accessory	6	3.13	2.89	3.78	0.33	**0.00***
	Healthy	12	3.72	3.14	4.06	0.25	
Cuspal Enamel							
Inner	Accessory	6	4.65	4.30	4.98	0.21	**0.00***
	Healthy	8	3.20	2.84	3.43	0.23	
Mid	Accessory	6	3.91	3.37	4.41	0.37	0.05
	Healthy	8	3.54	3.16	3.86	0.22	
Outer	Accessory	6	3.71	3.09	4.14	0.46	0.74
	Healthy	8	3.89	3.36	4.09	0.23	

DSRs to remain similar between equivalent regions of different non-accessory cusps in typically multi-cusped teeth (Mahoney, 2008). This unusual variation in DSR differences between the cusps is the product of the cuspal DSRs of the accessory cusp slowing with distance from the enamel dentine junction (EDJ) along the enamel prism pathway. This trend also differs to that seen in past research, which has shown permanent enamel growth rates of non-accessory enamel to always accelerate with distance from the EDJ (e.g. Beynon et al., 1991, 1998; Reid et al., 1998; Lacruz & Bromage, 2006; Mahoney, 2008; Aris et al., 2020a, 2020b).

This finding, in particular, demands further investigation, primarily to identify if the reversed growth pattern in cuspal DSRs of accessory enamel growth is consistent in other human samples. Should this be the case then the expected principle notion of enamel growth rates increasing with distance, a principle formulated on teeth not presenting accessory enamel growth from the EDJ, would need to be addressed. It is plausible that this principle, highly supported by the data of past research (e.g. Beynon et al., 1991; Beynon et al., 1998; Reid et al., 1998; Lacruz & Bromage, 2006; Mahoney, 2008; Aris et al., 2020a, 2020b) can only accurately be applied to growth of non-accessory enamel. Further research on the growth rates of accessory enamel is therefore required in order to create an equivalent growth principle for non-accessory enamel.

Primary cusp enamel growth compared to standard sample

Despite being the primary cusp of S197 and displaying standard morphology for an upper permanent first incisor, the regional enamel DSRs varied significantly from the mean DSRs of the standard sample (Table 2). Mean DSRs of all lateral enamel regions, and the inner and mid cuspal regions, were significantly slower in S197. However, outer cuspal DSRs were slower by only a mean rate of 0.05µm/day in S197. Overall, while this research only presents a preliminary case study, the data suggests that such enamel will grow slower than the standard sample cohort of the same tooth type within the same population.

This finding primarily supports the use of teeth possessing no abnormal or excess enamel in past growth rate studies (e.g. Beynon et al., 1991; Beynon et al., 1998; Reid et al., 1998; Lacruz & Bromage, 2006; Mahoney, 2008; Aris et al., 2020a, 2020b), as there is now clear potential for significant differences between teeth that do and do not present accessory enamel growth as defined here. Perhaps more importantly, there is new incentive for future research to continue analysing the growth rates throughout all regions and types of enamel from all tooth types. Such research will serve to expand our knowledge of the growth rate patterns common in human dentition, by identifying if non-accessory enamel growth rates slow in the presence of accessory enamel on the same tooth, or if S197 is a unique case. Future research should also examine the growth rates of less extreme non-accessory enamel growth than that of S197. This would help ascertain whether the extremity of accessory enamel growth is related to the slowing growth rates of the non-accessory enamel.

Accessory cusp enamel growth compared to standard sample

The lateral enamel DSRs of the accessory cusp of S197 presented significantly slower rates compared to those of the standard sample (Table 3). Conversely, the inner cuspal DSRs of the accessory cusp were significantly faster. The mid cuspal region was also faster by a mean rate of 0.37µm/day, but the outer cuspal region presented minimal variation to the standard sample (Table 3). These results demonstrate the erratic and inconsistent growth patterns of the accessory enamel of S197. It is particularly unusual that the cuspal accessory enamel growth slowed from inner to outer regions, and that the outer region mean DSR climaxed at a similar rate to equivalent DSRs of the standard sample. Further research is required to ascertain whether this is a unique phenomenon or the standard growth pattern for accessory enamel.

However, it should be noted that accessory enamel manifestations differ between different dental non-metric traits whose etiology includes excess enamel formation. Future research investigating the growth of accessory enamel should therefore consider analysing growth rates of teeth grouped according to their diagnosed traits and tooth types, as it should not be assumed that accessory enamel grows at similar rates between these groups. This principle should be applied to all future research advised here to avoid inaccurately grouping the growth patterns of all non-accessory enamel types.

Conclusions

The inter-regional differences in the growth rates collected from S197 were erratic, and in some enamel regions in direct contradiction with those expected of human incisors and multi-cusped teeth. Firstly, the differences between the equivalent regional DSRs of the primary and secondary

cusp of S197 vary from the similarities observed in past research comparing non-accessory cusps of the same teeth. Secondly, the presence of extreme accessory enamel formation appeared to slow the growth rates of the non-accessory enamel when compared to the growth rates of a standard sample of teeth lacking accessory enamel growth. Finally, the DSRs from the accessory cusp of S197 highlight how accessory enamel growth rates will not necessarily follow the trend of increasing rates with distance from the EDJ. The lack of additional research greatly limits our understanding of these findings. Overall, it is clear that more research into the growth rates of accessory enamel, as well as non-accessory enamel of the same teeth, is needed. Ideally such research will analyse different tooth types, and teeth with different diagnosed non-metric traits, independently.

Acknowledgments

We would like to thank the University of Kent for granting permission to sample teeth from their clinical collection. Further thanks also go to Annie Robertson for her assistance and artistic talents. Thanks also go to the anonymous reviewer and editor for their invaluable feedback.

REFERENCES

Antoine, D. (2000). *Evaluating the periodicity of incremental structures in dental enamel as a means of studying growth in children from past human populations* (Doctoral dissertation, University College London).

Antoine, D., Hillson, S., & Dean, M. C. (2009). The developmental clock of dental enamel: a test for the periodicity of prism cross-striations in modern humans and an evaluation of the most likely sources of error in histological studies of this kind. *Journal of Anatomy*, *214*(1), 45-55.

Aris, C. (2020). The Histological Paradox: Methodology and efficacy of dental sectioning. *Papers from the Institute of Archaeology*, *29*(1), 1-16.

Aris, C., Mahoney, P., & Deter, C. (2020a). Enamel thickness and growth rates in modern human permanent first molars over a 2000 year period in Britain. *American Journal of Physical Anthropology, 173,* 141-157.

Aris, C., Mahoney, P., O'Hara, M. C., & Deter, C. (2020b). Enamel growth rates of anterior teeth in males and females from modern and ancient British populations. *American Journal of Physical Anthropology, 173,* 236-249.

Asper, H. (1916). Uber die ''braune Retzius'sche Parallelsteifung'' im Schmelz der menschlichen Zahne. *Schweiz Vjschr. Zahnhlk*, *26*(1), 275-314

Berkovitz, B. K. B., Holland, G. R., & Moxham, B. J. (2002). *Oral anatomy, embryology and histology*. Mosby Incorporated.

Beynon, A. D., Clayton, C. B., Ramirez Rozzi, F. V. R., & Reid, D. J. (1998). Radiographic and histological methodologies in estimating the chronology of crown development in modern humans and great apes: a review, with some applications for studies on juvenile hominids. *Journal of Human Evolution*, *35*(4), 351-370.

Beynon, A. D., Dean, M. C., & Reid, D. J. (1991). Histological study on the chronology of the developing dentition in gorilla and orangutan. *American Journal of Physical Anthropology*, *86*(2), 189-203.

Birch, W., & Dean, M. C. (2014). A method of calculating human deciduous crown formation times and of estimating the chronological ages of stressful events occurring during deciduous enamel formation. *Journal of Forensic and Legal Medicine*, *22*, 127-144.

Boyde, A. (1989). Enamel. In *Teeth* (pp. 309-473). Springer, Berlin, Heidelberg.

Boyde, A., (1990). Developmental interpretations of dental microstructure. In DeRousseau, J.C. (Ed.), *Primate Life History and Evolution (*pp. 229 -267). New York: Wiley-Liss.

Boyde, A. (1990). Developmental interpretations of dental microstructure. In DeRousseau, J.C. (Ed.), *Primate Life History and Evolution* (pp. 229 -267). New York: Wiley-Liss.

Bromage, T. G. (1991). Enamel incremental periodicity in the pig-tailed macaque: A polychrome fluorescent labeling study of dental hard tissues. *American Journal of Physical Anthropology*, *86*(2), 205-214.

Dean, M. C. (1995). The nature and periodicity of incremental lines in primate dentine and their relationship to periradicular bands in OH 16 (*Homo habilis*). In J. M. Cecchi (Ed.), *Aspects of dental biology: Paleontology, anthropology and evolution* (pp. 239–265). Florence: International Institute for the Study of Man.

Dean, M. C. (1998). A comparative study of cross striation spacings in cuspal enamel and of four methods of estimating the time taken to grow molar cuspal enamel in Pan, Pongo and Homo. *Journal of Human Evolution*, *35*(4), 449-462.

Dean, M. C., Beynon, A. D., Reid, D. J., & Whittaker, D. K. (1993a). A longitudinal study of tooth growth in a single individual based on long-and short-period incremental markings in dentine and enamel. *International Journal of Osteoarchaeology*, *3(*4), 249-264.

Edgar, H. J. H., Willermet, C., Ragsdale, C. S.,

O'Donnell, A., & Daneshvari, S. (2016). Frequencies of rare incisor variations reflect factors influencing precontact population relationships in Mexico and the American Southwest. *International Journal of Osteoarchaeology*, *26* (6), 987-1000.

FitzGerald, C. M. (1995). *Tooth crown formation and the variation of enamel microstructural growth markers in modern humans* (Doctoral dissertation, University of Cambridge).

FitzGerald, C. M. (1998). Do enamel microstructures have regular time dependency? Conclusions from the literature and a large-scale study. *Journal of Human Evolution*, *35*(4-5), 371-386.

FitzGerald, C. M., & Saunders, S. R. (2005). Test of histological methods of determining chronology of accentuated striae in deciduous teeth. *American Journal of Physical Anthropology*, *127*(3), 277-290.

Guatelli-Steinberg, D., & Lukacs, J. R. (1999). Interpreting sex differences in enamel hypoplasia in human and non-human primates: Developmental, environmental, and cultural considerations. *American Journal of Physical Anthropology*, *110*(S29), 73-126.

Gysi, A. (1931). Metabolism in adult enamel. *Dental Dig*, 37, 661-668

Holt, S. A., Reid, D. J., & Guatelli-Steinberg, D. (2012). Brief communication: premolar enamel formation: completion of figures for aging LEH defects in permanent dentition. *Dental Anthropology Journal*, *25*(1), 4-7.

Kajiyama, S. (1965). Total number of regular incremental lines (Regulare Parallelstreifen nach Asper) in the enamel of human permanent teeth. *Journal of Nihon University School of Dentistry*, *39*, 77-83.

Lukacs, J. R. (1991). Localized enamel hypoplasia of human deciduous canine teeth: prevalence and pattern of expression in rural Pakistan. *Human Biology*, *63*(4), 513-522.

Lukacs, J. R. (1992). Dental paleopathology and agricultural intensification in South Asia: new evidence from Bronze Age Harappa. *American Journal of Physical Anthropology*, *87*(2), 133-150.

Lukacs, J. R. (1999). Enamel hypoplasia in deciduous teeth of great apes: Do differences in defect prevalence imply differential levels of physiological stress?. *American Journal of Physical Anthropology*, *110*(3), 351-363.

Lacruz, R. S., & Bromage, T. G. (2006). Appositional enamel growth in molars of South African fossil hominids. *Journal of Anatomy*, *209*(1), 13-20.

Lukacs, J. R., & Guatelli-Steinberg, D. (1994). Daughter neglect in India: LEH prevalence and the question of female biological superiority. *American Journal of Physical Anthropology, Supplement*, *18*, 132.

Lukacs, J. R., & Joshi, M. R. (1992). Enamel hypoplasia prevalence in three ethnic groups of northwest India: A test of daughter neglect and a framework for the past. Recent contributions to the study of enamel developmental defects. *Journal of Paleopathology Monograms Publications*, *2*, 359-372.

Lukacs, J. R., & Pal, J. N. (1993). Mesolithic subsistence in North India: inferences from dental attributes. *Current Anthropology*, *34*(5), 745-765.

Lukacs, J. R., & Walimbe, S. R. (1998). Physiological stress in prehistoric India: new data on localized hypoplasia of primary canines linked to climate and subsistence change. *Journal of Archaeological Science*, *25*(6), 571-585.

Mahoney, P. (2008). Intraspecific variation in M1 enamel development in modern humans: implications for human evolution. *Journal of Human Evolution*, *55*(1), 131-147.

Massler, M., & Schour, I. (1946). Growth of the child and the calcification pattern of the teeth. *American Journal of Orthodontics and Oral Surgery*, *32*(9), 495-517.

Nanci, A. and Smith. C. E. (1992). Development and calcification of enamel. In E. Bonucci, (Ed.) *Calcification in Biological Systems* (pp 313-343). Boca Raton, FL: CRC Press.

Okada, M. (1943). Hard tissues of animal body. Highly interesting details of Nippon studies in periodic patterns of hard tissues are described. *Shanghai Evening Post. Medical Edition of September 1943*, 15-31.

Primeau, C., Arge, S. O., Boyer, C., & Lynnerup, N. (2015). A test of inter-and intra-observer error for an atlas method of combined histological data for the evaluation of enamel hypoplasia. *Journal of Archaeological Science: Reports*, *2*, 384-388.

Reid, D. J., Beynon, A. D., & Ramirez Rozzi, F. V. R. (1998). Histological reconstruction of dental development in four individuals from a medieval site in Picardie, France. *Journal of Human Evolution*, *35*(4-5), 463-477.

Reid, D. J., & Dean, M. C. (2006). Variation in modern human enamel formation times. *Journal of Human Evolution*, *50*(3), 329-346.

Schwartz, G. T., Mahoney, P., Godfrey, L. R., Cuozzo, F. P., Jungers, W. L., & Randria, G. F. (2005). Dental development in Megaladapis edwardsi (Primates, Lemuriformes): implications for understanding life history variation in subfossil lemurs. *Journal of Human Evolution*, *49* (6), 702-721.

Schwartz, G. T., Reid, D. J., & Dean, C. (2001). Developmental aspects of sexual dimorphism in hominoid canines. *International Journal of Primatology*, *22*(5), 837-860.

Smith, C. E., & Nanci, A. (2003). Overview of morphological changes in enamel organ cells associated with major events in amelogenesis. *International Journal of Developmental Biology*, *39*(1), 153-161.

Smith, T. M., Reid, D. J., Dean, M. C., Olejniczak, A. J., & Martin, L. B. (2007). New perspectives on chimpanzee and human molar crown development. In: *Dental perspectives on human evolution: state of the art research in dental paleoanthropology*. Springer, Dordrecht. pp. 177-192.

Zheng, J., Li, Y., Shi, M. Y., Zhang, Y. F., Qian, L. M., & Zhou, Z. R. (2013). Microtribological behaviour of human tooth enamel and artificial hydroxyapatite. *Tribology International*, *63*, 177-185.

The Impact of Hybridization on Upper First Molar Shape in Robust Capuchins (*Sapajus nigritus x S. libidinosus*)

Emma Ayres Kozitzky[1*]

[1] New York University

Keywords: geometric morphometrics; molar shape; hybridization; robust capuchins

ABSTRACT To better understand the impact of hybridization on development and morphology, I analyze an understudied phenotype in hybrid morphology research: tooth shape. I apply a 2D geometric morphometric approach to compare variation in first upper molar cusp tip positions and crown outline shape among 31 crested capuchins (*Sapajus nigritus*), 37 bearded capuchins (*S. libidinosus*), and 44 hybrids (*S. nigritus* x *S. libidinosus*). A principal components analysis shows that group membership accounts for a significantly greater proportion of variance along the first major axis of M^1 shape variation than does allometry. While most hybrids have *S. nigritus*-like M^1s, several possess a transgressive M^1 shape not observed in either parental species. Procrustes distances are greater in hybrids compared to the parental capuchins, and two-block partial least squares analyses show that hybrids exhibit weaker integration between cusp tip positions and crown outline shape. These results demonstrate that hybridization generates novel M^1 shapes and support the hypothesis that destabilized development results in elevated phenotypic variance in hybrids. Further studies of dental shape in hybrid primates will generate important data for on-going efforts to detect potential hybrids in the hominin fossil record and to understand the evolutionary outcomes of anthropogenic hybridization.

Hybridization, once viewed as rare and universally detrimental (Dobzhansky, 1940; Mayr, 1963), is increasingly viewed as a frequent and innovative evolutionary phenomenon (Ackermann et al., 2019; Arnold, 1997; Taylor & Larson, 2019). Adaptive hybridization and fertile hybrid populations have been observed in a wide array of animals and plants, such as Galápagos finches (Grant & Grant, 2020), toads (C. Chen & Pfennig, 2020), butterflies (Jiggins et al., 2008), and poplar trees (Chhatre et al., 2018). There is an especially rich body of literature on ancient and contemporary primate hybridization. Genetic analyses have demonstrated that hybridization events occurred in many primate lineages during their course of evolution (de Manuel et al., 2016; Fan et al., 2018; Kuhlwilm et al., 2019; Svardal et al., 2017; Tung & Barreiro, 2017; Zichello, 2018), including hominins (Browning et al., 2018; L. Chen et al., 2020; Durvasula & Sankararaman, 2020; Green et al., 2010; Huerta-Sánchez et al., 2014; Reich et al., 2011; Slon et al., 2018). A growing number of primate taxa are proposed to have hybrid origins (Burrell et al., 2009; Detwiler, 2019; Rogers et al., 2019; Roos et al., 2019; Thinh et al., 2010; Tosi et al., 2000; Wang et al., 2015). Hybridization continues to shape genetic and phenotypic variation in present-day primate populations in both natural and anthropogenic contexts (Alberts & Altmann, 2001; Bergman et al., 2008; E. L. Bynum et al., 1997; Cortés-Ortiz et al., 2007; Gligor et al., 2009; Jolly et al., 2011; Malukiewicz et al., 2015; Mather, 1992).

While genetic analysis has been crucial for exploring primate hybridization, there is a growing interest in understanding the impact of hybridization on morphology. Studies of hybrid primate morphology offer unique insight into the effect of

*Correspondence to:
Emma Ayres Kozitzky
Department of Anthropology
Center for the Study of Human Origins
New York University
New York, NY 10003
eak475@nyu.edu

This paper was the recipient of the Albert A. Dahlberg prize awarded by the Dental Anthropology Association in 2020.

rapid genetic recombination on phenotypic development and variation. Many studies have evaluated soft tissue phenotypes in contemporary hybrid populations using traits that are easy to observe in the field and can be measured non-invasively, such as pelage color and distribution, head shape, and tail carriage (Alberts & Altmann, 2001; N. Bynum, 2002; Kelaita & Cortés-Ortiz, 2013; Phillips-Conroy & Jolly, 1986). Researchers have also studied the relationship between hybrid ancestry and hard tissue phenotype, such as skeletodental size, shape, and non-metric trait variation (Ackermann et al., 2006; Ackermann & Bishop, 2010; Boel, 2016; Cheverud et al., 1993; Eichel & Ackermann, 2016; Ito et al., 2015; Kohn et al., 2001; Phillips-Conroy, 1978). The proximate aims of hybrid morphology research are to elucidate how hybrid morphology quantitatively and qualitatively differs from parental morphology and if different kinds of hybrids share diagnosable traits indicative of their hybrid ancestry (Ackermann, 2010; Ackermann et al., 2019).

The data derived from hybrid morphology research has important broader implications for primate conservation and paleoanthropology. Primate conservation biologists observe that the frequency of hybridization will likely increase as primate habitats are disturbed or destroyed by anthropogenic interference (Detwiler et al., 2005; Malukiewicz, 2019; Thompson et al., 2018). Rare, endangered primates may reproduce with more common heterospecifics if conspecific mates are difficult to find. Extensive admixture between divergent taxa may result in loss of genetic and phenotypic diversity and ultimately fuse two lineages (Seehausen et al., 2008), or it may generate novel diversity and prevent inbreeding depression (Arnold & Meyer, 2006). By studying the variation in hybrid phenotypes, conservation biologists may be able to understand if the outcomes of anthropogenic hybridization are harmful, neutral, or adaptive for endangered primate populations.

Paleoanthropologists acknowledge that hybrid hominins are likely present in the fossil record. Fossil evidence demonstrates that multiple hominin taxa cohabited Africa and Eurasia throughout the Pliocene and Pleistocene and could have hybridized where their ranges overlapped (Détroit et al., 2019; Grün et al., 2020; Herries et al., 2020; Spoor et al., 2015). The genetic evidence for hybridization events throughout hominin evolution is substantial (Durvasula & Sankararaman, 2020; Jacobs et al., 2019; Sankararaman et al., 2016; Skov et al., 2020; Villanea & Schraiber, 2019). The hybrid ancestry of several fossilized hominin individuals has been confirmed by ancient DNA analyses (Fu et al., 2015; Slon et al., 2018). However, ancient DNA preservation is rare in most of the hominin fossil record, so analyses of hard tissue phenotypes in extant hybrid primates can be used to assess the feasibility of using morphological indicators to identify hybrid hominin fossils (Ackermann et al., 2019). The identification of hybrid hominin fossils remains an outstanding issue for reconstructing hominin phylogenetic relationships, as most the commonly used phylogenetic frameworks assume evolutionary relationships are hierarchical rather than reticulate (Holliday, 2003).

Quantitative genetic theory states that in first-generation (F1) hybrids, phenotypic trait measurements controlled by additive genetic variation will be the midparental value (MPV), or the averaged parental measurements (Falconer & Mackay, 1997). Tests of this theory indicate that while some F1 hybrid primate phenotypes exhibit the expected MPV (Hamada et al., 2012), other traits in the same population may deviate from the expected phenotype (Ackermann et al., 2006; Cheverud et al., 1993; Eichel & Ackermann, 2016). Positive deviations from the MPV in F1 populations is referred to as heterosis, or hybrid vigor, while negative deviations are evidence of dysgenesis, or hybrid breakdown. Later-generation hybrids with higher genetic input from one parental taxon are expected to be more phenotypically like that parent, but some hybrids resemble one parent more than the other, regardless of parental genetic contribution (Boel et al., 2019; Ito et al., 2015). First- and later-generation hybrid populations sometimes exhibit transgressive phenotypes not observed in either parental population, such as extreme trait size, novel combinations of parental traits, or the presence of non-metric craniodental anomalies (Ackermann et al., 2014; Ackermann & Bishop, 2010; Jolly et al., 1997). Research on hybrid morphology in primates has documented a complex array of phenotypic outcomes that vary within and among hybrid populations (Alberts & Altmann, 2001). Importantly, these outcomes are not universally maladaptive (Charpentier et al., 2012) and may help hybrid populations occupy ecological niches unavailable to either parental population, thereby resulting in novel evolutionary lineages (Arnold, 1997; Zinner et al., 2011).

The high morphological variability observed within and among hybrid populations is thought to be the result of destabilized development (Clarke, 1993). The uniquely adapted developmen-

tal regimes of two distinct parental taxa are unlikely to merge seamlessly in offspring and could result in perturbations during hybrid morphogenesis. This is supported by the observation that deviations from predicted F1 midparental phenotypes tend to be more pronounced with increasing genetic distance between parental populations (Bernardes et al., 2017; Z. J. Chen, 2013; Stelkens & Seehausen, 2009). Researchers have tested the hypothesis that hybrids experience destabilized development using tests of morphological integration and fluctuating asymmetry (Alibert et al., 1994; Jackson, 1973; Klingenberg, 2003; Klingenberg & McIntyre, 1998). Tightly integrated trait complexes and highly symmetric bilateral trait measurements are hypothesized to reflect stable, canalized development. So, if hybridization results in developmental destabilization, hybrids are expected to exhibit weaker trait integration and greater fluctuating asymmetry between bilateral traits than parental taxa. Some hybrids do meet these expectations (Ackermann et al., 2014; Leary et al., 1985; Neff & Smith, 1979), but others do not differ from observed levels of parental trait integration or fluctuating asymmetry (Jackson, 1973; Pallares et al., 2016). In some cases, hybrid samples exhibit stronger trait integration and bilateral trait symmetry than parents, indicating that hybrid development is more stable than parental development (Alibert et al., 1994; Boel et al., 2019; Debat et al., 2000).

Despite growing interest in primate hybrid morphology, the relationships among hybrid ancestry, development, and phenotype remain unclear and difficult to predict. However, one of the most potentially informative anatomical regions for this research has also been one of the most understudied: the dentition. Several lines of evidence suggest that in-depth analyses of dental phenotypic variation will produce valuable data for hybrid morphology research. Anomalous dental non-metric traits are observed at high frequencies in some hybrid populations, such as supernumerary teeth, crown rotation and/or malformation, and dental crowding (Ackermann et al., 2010, 2014; Ackermann & Bishop, 2010; Goodwin, 1998; Heide-Jorgensen & Reeves, 1993). Intergeneric hybrids of *Theropithecus gelada* and *Papio hamadryas* ("geboon") exhibit combinations of parental traits in their dentitions, such as *T. gelada*-like enamel crenulation on *P. hamadryas*-like low-crowned molars, resulting in novel dental phenotypes (Jolly et al., 1997). Most of the geboon hybrids also exhibited maxillary cheektooth dimensions that exceeded the parental means. However, hybrids of more closely related baboon species *P. hamadryas* and *P. anubis* were not easily differentiable from parental species based on both metric and non-metric dental traits (Phillips-Conroy, 1978). Similarly, dental non-metric trait expression did not discriminate between closely related *Macaca fuscata*, *M. cyclopis*, and their hybrids (Boel et al., 2019). Further analyses of dental size, shape, and non-metric trait expression in extant primate hybrids would elucidate if hybrid primates exhibit shared patterns of dental trait variation.

Dental phenotypic analyses of hybrids also could help to understand if deviations from typical parental development generate the high variability observed in hybrid populations. Mammalian dental development is well-studied, and models of dental development have been tested in both extinct and extant primates (Evans et al., 2016; Hlusko et al., 2016; Jernvall & Jung, 2000; Ortiz et al., 2018; Paul et al., 2017). The iterative nature of dental development results in predictable patterns of dental trait integration both within the same tooth crown and among metameres. The patterning cascade model claims that the duration of tooth germ growth and the spatiotemporal distribution and strength of embryonic signaling centers within the germ constrain possible cusp configurations and crown size in the fully formed tooth (Jernvall, 2000). So, differences between parental and hybrid cusp configurations and accessory cusp expression likely reflect deviations in underlying patterning cascade pathways. Similarly, the inhibitory cascade model states that mammalian mandibular molar number and relative size are dictated by embryonic signaling strength and duration of odontogenesis, so differences between hybrid and parental molar size relationships and molar number likely reflect differences in this developmental pathway as well (Kavanagh et al., 2007). Indeed, in a hybrid baboon population, supernumerary mandibular molars are positively correlated with increased molar row length, which suggests that dental development is prolonged in the hybrids compared to parents (Ackermann et al., 2014).

Data derived from studies of hybrid dentitions is especially useful for conservation biologists and paleoanthropologists. Results derived from studies of hybrid skulls and postcrania are not easily applied in living primate populations, but the teeth of primates in hybrid zones can be evaluated, photographed, or molded and cast during trapping expeditions (Kelaita & Cortés-Ortiz, 2013; Phillips-Conroy, 1978). While skeletal data is certainly use-

ful for paleoanthropologists interested in determining the feasibility of identifying hybrid ancestry using fossil morphology, teeth tend to be better preserved and comprise most of the hominin fossil record (Bailey, 2002; Gómez-Robles et al., 2007; Martinón-Torres et al., 2012; Wood & Abbott, 1983).

The genus *Sapajus* is an excellent study taxon for hybridization research. The robust capuchin clade underwent rapid radiation and expansion during the Pleistocene, and species often interbreed where their ranges meet (Lima et al., 2018; Lynch Alfaro, Boubli, et al., 2012), making them an appropriate analog for understanding hominin hybridization. A sample of hybrids of *Sapajus nigritus* and *S. libidinosus* are housed at the Smithsonian National Museum of Natural History (NMNH). *Sapajus nigritus* and *S. libidinosus* shared a common ancestor approximately 2.6 Ma and belong to different clades within the genus, the former belonging to a more ancient clade endemic to the Atlantic Forest of Brazil, and the latter belonging to a recently evolved clade adapted to Brazilian dry shrublands (Lima et al., 2018; Wright et al., 2015). Both species are listed as 'near threatened' by the IUCN Red List of Threatened Species and both are known to occupy habitats disturbed by agricultural practices (Melo, Alfaro, et al., 2015; Melo, Fialho, et al., 2015). It is possible that anthropogenic hybridization could result in the loss of genetic and phenotypic diversity among robust capuchin species (Lynch Alfaro et al., 2014; Martins et al., 2017). A morphological analysis of hybrid robust capuchins would establish if phenotypic diversity is impacted by hybridization.

Here, I apply 2D geometric morphometric (2DGM) techniques to study variation in first upper molar (M^1) crown outline shape and cusp tip configuration among *Sapajus nigritus*, *S. libidinosus*, and their hybrids. Dental shape has been used to study population affinity and to characterize extinct and extant primate taxa (Bailey et al., 2016; Gamarra et al., 2016; Gómez-Robles et al., 2007, 2015; Rizk et al., 2013), including robust capuchins (Delgado et al., 2015), but has not yet been used to study patterns of morphological variation among hybrids and their parental taxa. The primary aims of this study are to explore variation and the factors driving variation in M^1 morphology in hybrids compared to *S. nigritus* and *S. libidinosus*; to determine if M^1 morphology can discriminate between hybrids and parental taxa; and to evaluate if hybrids exhibit evidence of destabilized dental development compared to parental taxa. Based on previous hybrid morphology research, I tested the following predictions:

1) M^1 shape is statistically distinct among *S. nigritus*, *S. libidinosus*, and their hybrids.
2) The mean shape of hybrid M^1s is the midparental value (the mean shape of the combined parental sample).
3) There is more variability in M^1 shape within the hybrid sample than within either parental sample.
4) Hybrids exhibit weaker covariation between cusp tip configuration and crown outline shape than parental taxa.

Materials and Methods

My sample includes *Sapajus nigritus* (n = 31), *S. libidinosus* (n = 37), and a hybrid sample of *S. nigritus* x *S. libidinosus* (n = 44). The dental sample comprises 112 right M^1s (Table 1). Only specimens with unworn or minimally worn M^1s were included.

Table 1. Number of M^1s included in this study.

	Female	Male	Total
Sapajus nigritus	16	15	31
S. nigritus x *S. libidinosus*	21	23	44
S. libidinosus	21	16	37
Total	58	54	112

I used a Nikon D500 DSLR digital camera fitted with a macro lens and attached to a copy stand to photograph M^1 occlusal surfaces. I positioned the M^1 cementoenamel junction (CEJ) parallel to the lens and included a scale placed at the same level as the occlusal plane (Bailey, 2004; Gómez-Robles et al., 2007). While directly referencing the specimen, I marked each of the four main M^1 cusp tips (the paracone, protocone, metacone, and hypocone) on the digital images using the GNU Image Manipulation Program version 2.10.12 (The GIMP Development Team, 2019). If a specimen exhibited slight wear, I marked the cusp tip in the center of the wear facet.

I uploaded the photographs to TpsDig2 version 2.31 to digitize a series of 2D landmarks (points of biological homology among specimens) and semi-landmarks (non-homologous points of morphological interest; Bookstein, 1997). Landmarks 1 through 4 were placed on the tips of the paracone, protocone, metacone, and hypocone (Figure 1). These landmarks capture variation in the position

of the main cusps relative to each other and relative to the crown outline. In order to examine variation in the shape of M^1 crown outlines, I placed 30 semilandmarks around the perimeter of the occlusal surface, starting at the point of maximum curvature where the buccal and mesial margins intersect. I drew a closed curve around the crown outline, and then appended 29 additional equidistant semilandmarks to the curve (see Figure 1). Finally, I exported all landmark and semilandmark coordinates as a .tps file to RStudio version 1.2.5033 for analysis.

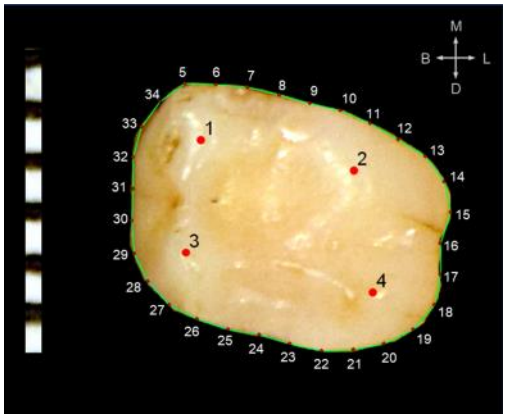

Figure 1. The landmark (1-4) and semilandmark (5-34) configuration used to analyze variation in M^1 cusp tip position and crown outline shape. M: mesial; D: distal; B: buccal; L: lingual.

All geometric morphometric analyses were performed using the R package geomorph (Adams et al., 2020). First, I defined semilandmarks 5 through 34 as sliding semilandmarks. Sliding semilandmarks can move along the crown outline between neighboring semilandmarks to optimize their position with respect to the average shape of the entire sample. This process removes random variation from the coordinate data introduced by the initial arbitrary placement of semilandmarks around the crown margin and converts semilandmarks 5 through 34 to homologous points statistically comparable to landmarks 1 through 4 (Gunz & Mitteroecker, 2013). Next, I performed a generalized Procrustes analysis (GPA) on the landmark and sliding semilandmark coordinates to remove the effects of specimen size, orientation, and position, leaving only variation related to shape. The GPA superimposes specimens by translating, scaling, and rotating the coordinates to generate an average shape, or consensus configuration, for the entire sample (Bookstein, 1997; Zelditch et al., 2012). I used the results of the GPA for all subsequent analyses.

To explore and compare major axes of M^1 shape variation among *S. nigritus*, *S. libidinosus*, and their hybrids, I conducted a principal components analysis (PCA). To visualize variation in shape space, I plotted PC 1 against PC 2 and PC 2 against PC 3. I included 95% confidence ellipses for each taxon to illustrate within-taxon variability. Then, to test the effect of allometry on M^1 shape, I constructed twelve linear models using results from the PCA (Table 2a). Each model tested the association between scores on PCs 1, 2, and 3 with taxonomic designation, logarithm-transformed centroid size, or a combination of both variables. The best-fitting model for PCs 1, 2, and 3 were selected using the function for Akaike's information criterion (AIC) in the R package bbmle (Bolker et al., 2020).

I used warp grids representing the mean shape for each taxon to visually evaluate if and how M^1 shape varies among groups. To statistically evaluate the extent to which M^1 shape is morphologically distinct among these groups by maximizing intergroup differences, I extracted the first ten PCs derived from the PCA (encompassing the majority of shape variation within the sample) for a discriminate function analysis (DFA). Then I used the results from the DFA for a cross-validated assignment test.

I measured within- and between-group variance using pairwise Procrustes distances (the Euclidean distance between two sets of shape coordinates; Spoor et al., 2015). A Procrustes distance equal to zero represents a pair of individuals with identical M^1 shape, while increasing distance reflects increasing dissimilarity in shape. I evaluated statistical differences in Procrustes distances among taxa using pairwise *t*-tests using Bonferroni correction for multiple comparisons.

I performed a two-block partial least squares analysis (2B PLS) to evaluate the level of covariation between the position of cusp tips (block 1: landmarks 1 through 4) and the shape of the crown outline (block 2: sliding semilandmarks 5 through 34), and implemented a permutation procedure (n = 1,000 permutations) to test the r-PLS correlation coefficients generated by the 2B PLS for statistical significance. Because calculation of the r-PLS statistic is dependent on sample size, I employed a standardized z-score converted to pairwise effect sizes to compare the strength of integration among groups (Adams & Collyer, 2016). Large pairwise effect sizes indicate that the level of morphological integration differs between the two samples.

Results

Mean M¹ shape in parental and hybrid taxa

The mean shapes for *S. nigritus*, *S. libidinosus*, and the hybrids compared to the pooled-sample consensus configuration are shown in Figures 2a, 2b, and 2c, respectively. Differences in mean shape are magnified by a factor of three to assist in visual interpretation. The average crown outline shape in *S. nigritus* is rhomboid, while that of *S. libidinosus* is more ovoid. The average crown outline in the hybrid sample is more mesiobuccally skewed than either parental taxon and has a waisted lingual margin. The two parental taxa exhibit similar intercusp distances relative to the crown outline, but the mean *S. nigritus* paracone, metacone and hypocone (landmarks 1, 3, and 4, see Figure 1) are buccally displaced compared to the consensus cusp tips. The average hybrid protocone, paracone, and metacone (landmarks 1 through 3, see Figure 1) are slightly mesially displaced compared to the consensus configuration. The average hybrid M¹ shape differs from the expected midparental shape. The midparental M¹ crown outline does not have the waisted lingual margin that is present in the hybrid mean outline, and the hybrid protocone, paracone, and metacone are mesially displaced compared to the expected midparental M¹ cusp configuration.

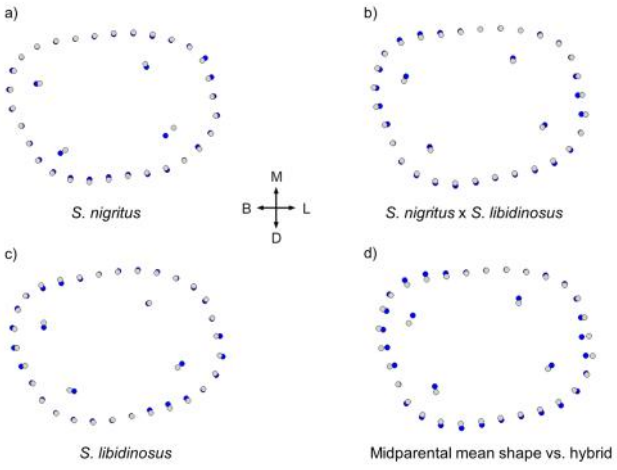

Figure 2. Pooled sample consensus M¹ shape (gray) compared to mean M¹ shape (blue) among (a) *S. nigritus,* (b) *hybrids*, and (c) *S. libidinosus*. Figure 2d illustrates the mean parental M¹ shape (*S. nigritus* and *S. libidinosus* combined, light gray) and the transformation of the mean parental M¹ shape into the mean hybrid shape (blue). All comparisons are magnified by a factor of 3 to aid in visual interpretation. M: mesial; D: distal; B: buccal; L: lingual.

Principal components analysis

The first three PCs account for approximately half (48.1%) of the variation in M¹ shape among *S. nigritus*, *S. libidinosus*, and *S. nigritus* x *S. libidinosus*. Principal component 1 explains 20.8% of shape variation, while PC 2 explains 16.6% (Figure 3a). The warp grids representing M¹ shape at extreme ends of variation along each PC illustrate that M¹s with low PC 1 scores have a mesiobuccally skewed rhomboid crown outline which tapers distally and a waisted lingual margin. The cusp tips are displaced towards the buccal margin. First molars with high PC 1 scores have squared, symmetrical outlines and roughly equidistant cusp tips. Along PC 2, M¹s with low scores have mesiobuccally skewed rhomboid outlines with cusp tips displaced towards the buccal margin, while M¹s with high scores have more symmetrical crown outlines, increased buccolingual distance between the two mesial cusps and between the two distal cusps, and lingual displacement of the lingual cusps. There is substantial overlap among the three taxa, but hybrids tend to have low PC 1 scores and high PC 2 scores, while the parental taxa tend to have high PC 1 scores and low PC 2 scores. The 95% confidence ellipse for hybrids is much broader than those of the parental taxa, reflecting greater variation in shape space.

Principal component 3 accounts for 11.2% of M¹ shape variation (Figure 3b). First molars with low PC 3 scores have symmetrical and ovoid crown outlines and a rhomboid cusp tip configuration. High scores on PC 3 correspond to M¹s with mesiobuccally skewed, rhomboid crown outlines with a waisted lingual margin, wide intercusp spacing, and all cusp tips displaced towards the periphery. There is very little separation among taxa in PC 2 vs. PC 3 shape space. The range of variation among *S. nigritus* individuals is almost entirely subsumed within the range of the hybrids. *S. libidinosus* tends to cluster on the low end of PC 2 away from *S. nigritus* and the hybrids. Based on shape and size of the 95% confidence ellipses projected onto tangent space for each taxon, the hybrids exhibit the highest variation in M¹ shape along PCs 2 and 3.

Regression analysis and allometry

The regression analysis demonstrated that taxonomic designation explains more variation in PC 1 scores than does M¹ size (Tables 2a and 2b). Approximately 20% ($p < 0.001$) of variation in PC 1 scores is explained by taxonomic designation. A post-hoc pairwise *t*-test using Bonferroni adjustment for multiple comparisons showed that hybrids had significantly lower scores on PC 1 than

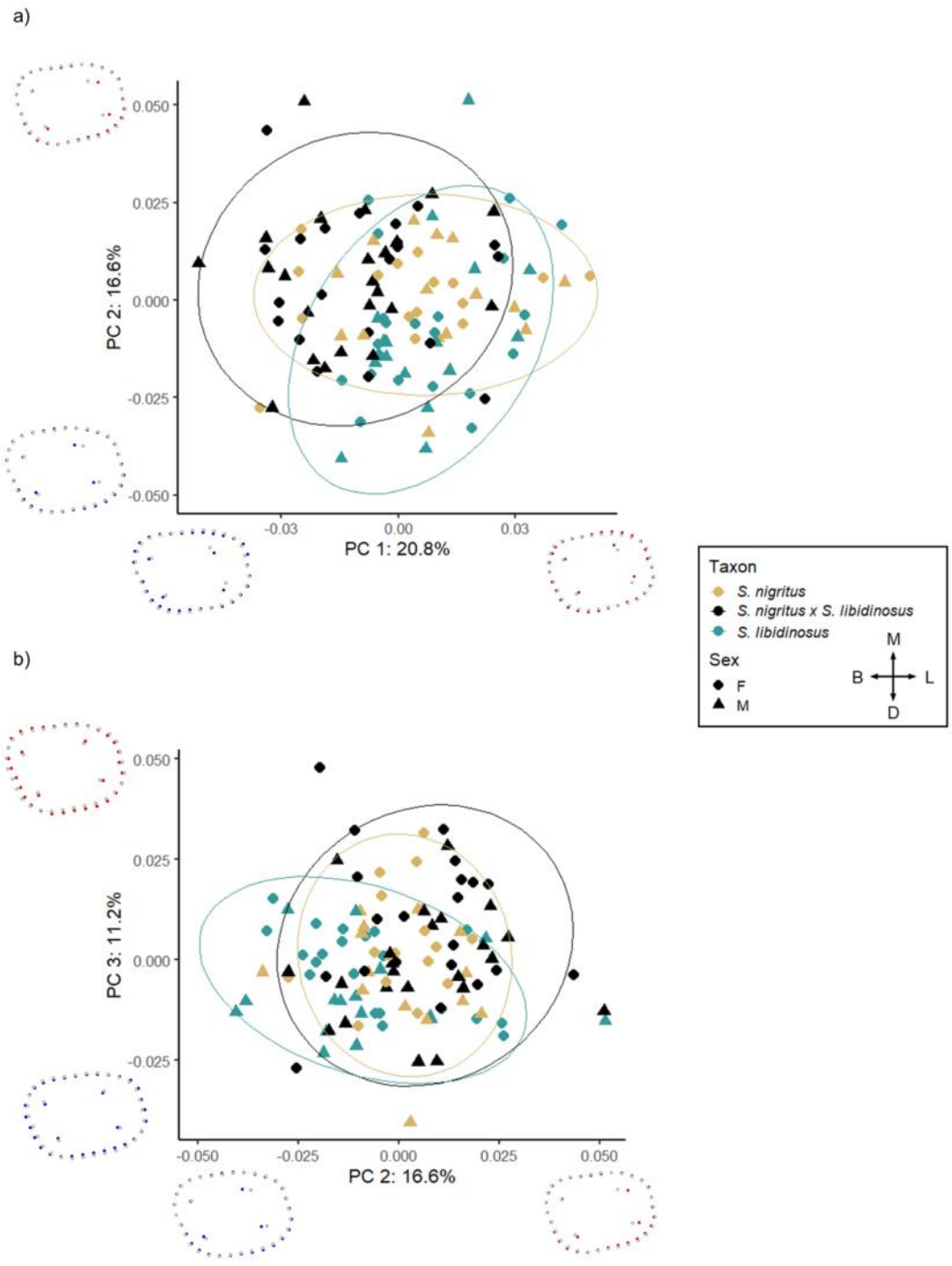

Figure 3. Scatter plots of (a) PC 1 against PC 2 scores, and (b) PC 2 scores against PC 3 scores derived from the PCA of M^1 shape. The warp grids illustrate the transformation of the consensus configuration (gray) into the shape of M^1s with the lowest (blue) and highest (red) scores along PCs 1 and 2. Ellipses represent 95% confidence intervals for each group. Note that, while there is considerable overlap among the groups, the hybrids tend to exhibit lower PC 1 and higher PC 2 scores than the parental taxa, corresponding to M^1s with skewed crown outlines, a waisted lingual margin, and wider intercusp distances. M: mesial; D: distal; B: buccal; L: lingual.

Table 2. Results of the regression analysis assessing the effect of taxonomic designation and allometry on variation in the first three principal component (PC) scores.

a)

Model #	Model Terms	R^2	*p*-value
1	PC 1 ~ log(centroid size)	0.02	0.20
2	**PC 1 ~ taxon**	**0.20**	**<0.001**
3	PC 1 ~ taxon + log(centroid size)	0.22	<0.001
4	PC 1 ~ taxon * log(centroid size)	0.22	<0.001
5	PC 2 ~ log(centroid size)	0.06	0.008
6	PC 2 ~ taxon	0.11	0.002
7	**PC 2 ~ taxon + log(centroid size)**	**0.17**	**<0.001**
8	PC 2 ~ taxon * log(centroid size)	0.18	<0.001
9	PC 3 ~ log(centroid size)	0.01	0.29
10	**PC 3 ~ taxon**	**0.07**	**0.02**
11	PC 3 ~ taxon + log(centroid size)	0.09	0.02
12	PC 3 ~ taxon * log(centroid size)	0.09	0.08

The best-fitting model for each PC is in bold.

b)

PC	Model #	AIC	dAIC	df	Weight
1	**2**	**-567.3**	**0.0**	**4**	**0.526**
	3	-566.7	0.6	5	0.383
	4	-563.8	3.5	7	0.091
	1	-546.3	21.1	3	<0.001
2	**7**	**-586.3**	**0.0**	**5**	**0.653**
	8	-584.6	1.7	7	0.284
	6	-581.3	5.0	4	0.054
	5	-577.4	8.9	3	0.007
3	**10**	**-619.6**	**0.0**	**4**	**0.478**
	11	-619.3	0.3	5	0.416
	12	-615.6	4.0	7	0.066
	9	-614.6	5.0	3	0.040

The best-fitting model for each PC is in bold.

both *S. nigritus* and *S. libidinosus* ($p = 0.003$ and $p < 0.001$, respectively), but no significant difference in PC 1 scores between *S. nigritus* and *S. libidinosus* ($p = 0.99$; Figure 4a). More complex models testing the effect of taxonomic designation on the relationship between PC 1 scores and M^1 size were non-significant. Change in M^1 shape along the main axis of variation is not driven by size alone. However, the next-best-fitting model according to AIC suggested that the average PC 1 score estimated from M^1 size varies by taxon.

A more complex model is required to explain variation in PC 2 scores. First molar size and taxonomic designation only explain 6% ($p = 0.008$) and 11% ($p = 0.002$) of variation in PC 2 scores, respectively, and a comparison of the two models indicates that PC 2 ~ taxon is a better fit than PC 2 ~ log(centroid size) ($F = 5.93$, $p = 0.02$). A post-hoc comparison of differences in PC 2 scores by taxon indicates that *S. libidinosus* has significantly lower PC 2 scores than the hybrids ($p = 0.001$; Figure 4b); all other pairwise comparisons are non-significant. A multivariate model combining the effect of taxonomic designation and M^1 centroid size explains 17% ($p < 0.001$) of variation in PC 2 scores and is a significantly better fit than PC 2 ~ taxon. There is no significant increase in explanatory power with the addition of an interaction term describing change in the slope of the relationship between M^1 shape and size among taxa ($F = 1.12$, $p = 0.33$). So, variation in shape along PC 2 is partly driven by size, but the average PC 2 score estimated from M^1 size differs by taxon.

As with PC 1, taxonomic designation explains the most variation in PC 3 scores rather than M^1 size. However, the amount of variation in PC 3 scores explained by taxonomic designation is small ($R^2 = 0.07$, $p = 0.02$), and a post-hoc comparison average PC 3 scores by taxon indicates that the only significant difference among taxa is between *S. libidinosus* and the hybrids ($p = 0.016$, Figure 4c). Comparisons with more complex models accounting for different size/shape relationships by taxon do not add significant explanatory power.

Discriminant function analysis

Results for the discriminant function analysis are illustrated in Figure 5. The DFA maximized differences in between-group variation, but there is little separation among parental species and their hybrids along linear discriminant functions (LDs) 1 and 2. Along LD 2, there is some separation between *S. libidinosus,* which clusters at the positive end, and *S. nigritus* and hybrids, which both cluster toward the negative end. Most of the hybrids have negative loadings on LD 1 and LD 2.

The results of the cross-validated assignment test are presented in Table 3. The percentage of individuals correctly classified to their *a priori* assigned taxon ranges from only slightly better than chance in *S. nigritus* (61.3%) to moderate in *S. libidinosus* (73.0%). In the hybrid group 70.5% were correctly assigned as such. Both *S. nigritus* and *S. libidinosus* misclassified individuals were more frequently assigned to the hybrid group than to the wrong parental taxon, reflecting higher variation in M^1 shape among hybrids.

Procrustes distances within and among taxa

The mean pairwise Procrustes distances in M^1 shape are listed in Table 4, and frequency distributions of pairwise Procrustes distances within and between taxa are visualized in Figure 6. The average distance for the entire sample is 0.06. Within-taxon shape variability is highest for the hybrids (distance = 0.059) compared to the parental taxa (*S. nigritus* = 0.055, *S. libidinosus* = 0.053). All three taxa have significantly different mean Procrustes distances ($p < 0.001$). The between-taxa comparisons show a greater degree of similarity between *S. libidinosus* and *S. nigritus* M^1 shape (distance = 0.058) than between each parental taxon and the hybrids, and there is approximately equal distance between the parental taxa and the hybrids (*S. nigritus* vs. hybrids = 0.061, *S. libidinosus* vs. hybrids = 0.062).

Table 3. Results of the cross-validated assignment test. The number of individuals correctly assigned to their a priori designated taxon are in bold.

	S. nigritus	*S. nigritus* x *S. libidinosus*	*S. libidinosus*	% Correct
S. nigritus	**19**	8	4	61.3
S. nigritus x *S. libidinosus*	5	**31**	8	70.5
S. libidinosus	4	6	**27**	73.0

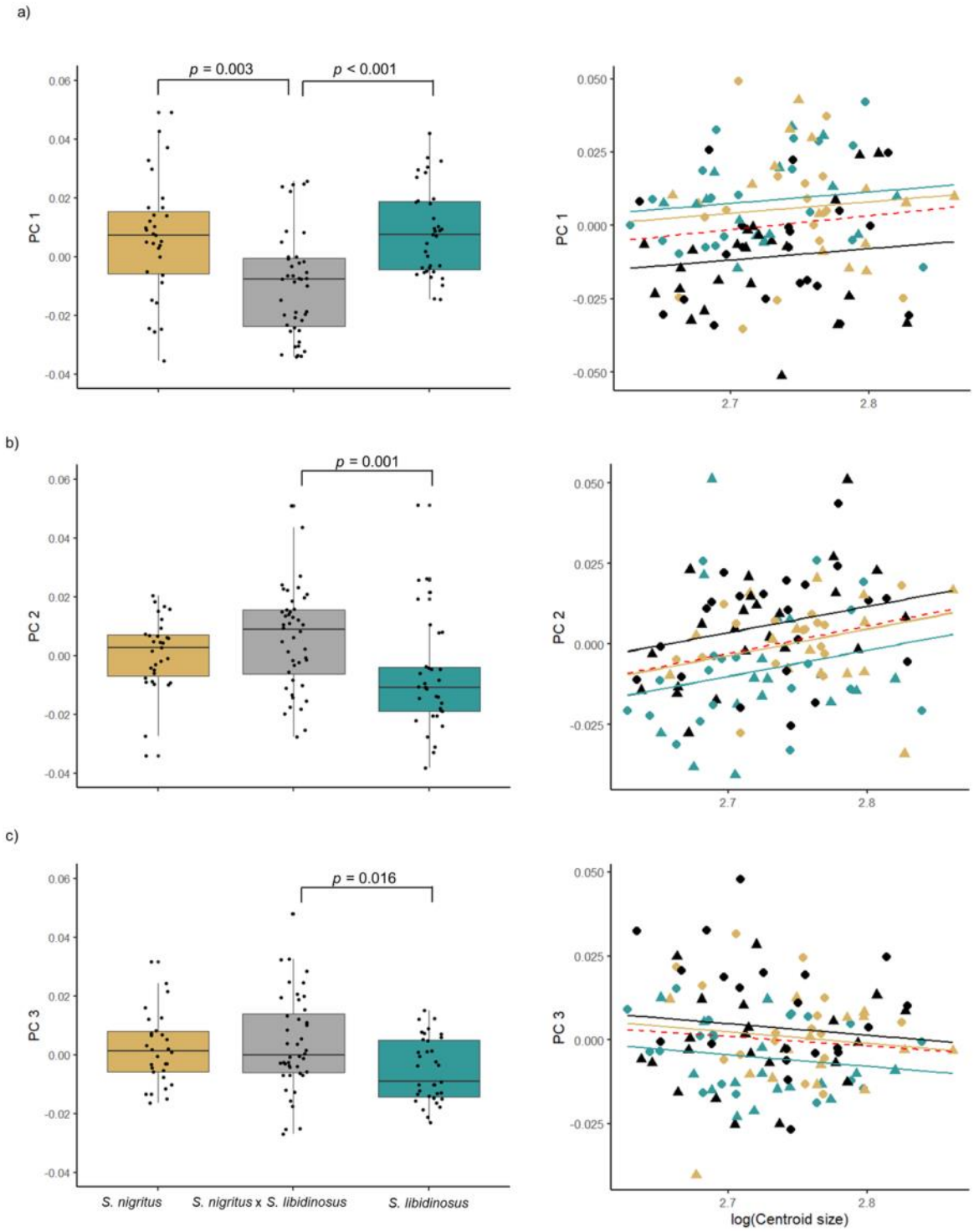

Figure 4. Box-and-whisker plots and scatterplots of comparing the relationship among taxonomic designation, log-transformed M^1 centroid size, and scores for (a) PC 1, (b) PC 2, and (c) PC 3. The *p*-values for significant differences in PC scores between groups are indicated above the brackets. The red dashed regression line on each scatterplot represents a simple PC score ~ log(centroid size) model. indicates the line of best fit for the pooled sample (PC 2 ~ log(Centroid size)). Based on Akaike's information criterion, the variation in PC 1 and 3 scores is best explained by taxonomic designation (Table 2b), while average PC 2 scores estimated from log(Centroid size) significantly differ among taxa (indicated by separate lines of best fit for each taxon; PC 2 ~ taxon + log(Centroid size)).

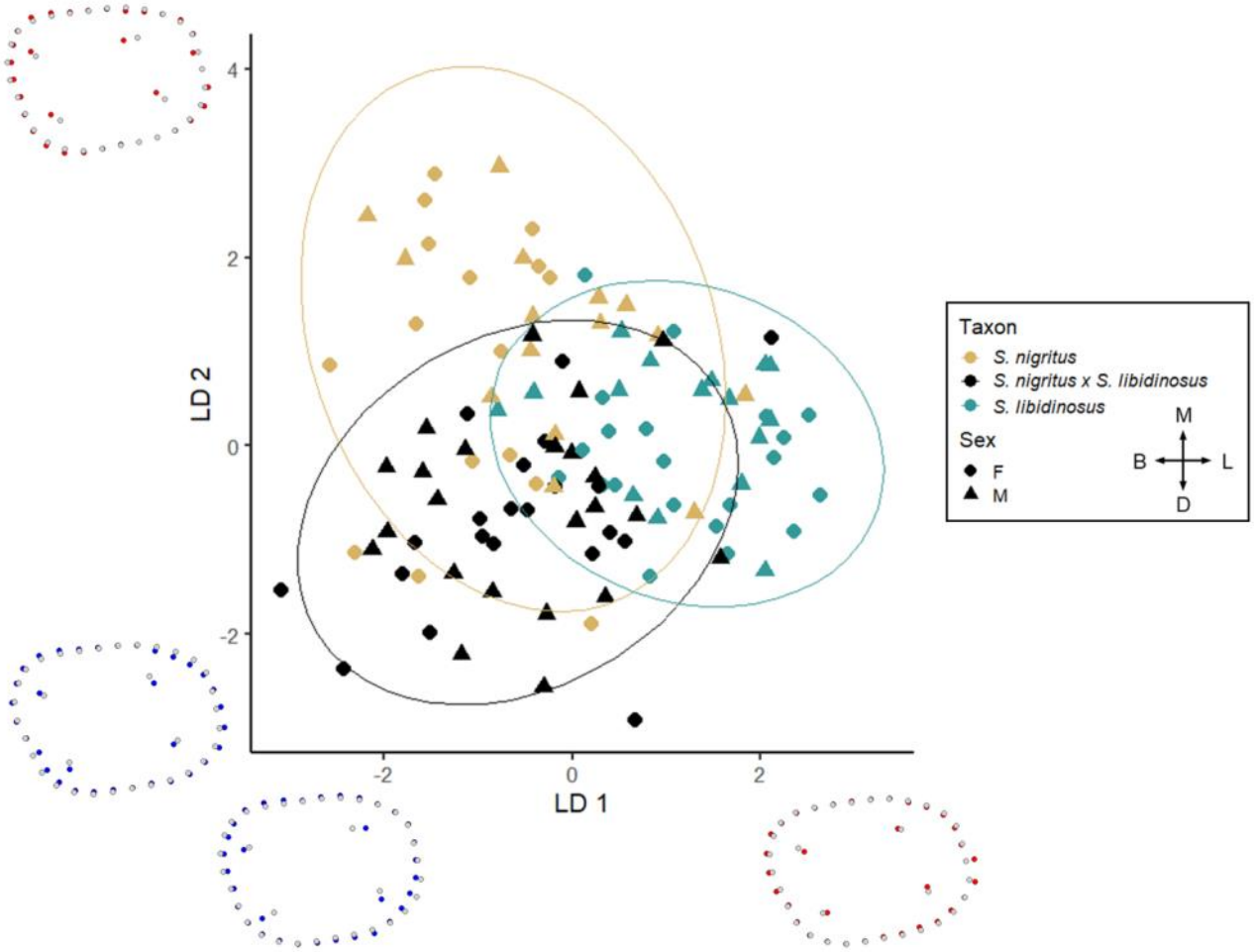

Figure 5. Scatter plot of LDs 1 and 2 derived from the linear discriminant function analysis, in which among-group differences in M^1 shape are maximized. Ellipses represent 95% confidence intervals for each group. First molar shapes along the low end of LDs 1 and 2 are shown in blue, while shapes for M^1 on the high end of LDs 1 and 2 are illustrated in red. M: mesial; D: distal; B: buccal; L: lingual.

Table 4. Mean pairwise Procrustes distances within and between taxa. A Procrustes distance value of 0 means that there is no difference in M^1 shape between two individuals.

	S. nigritus	*S. nigritus* x *S. libidinosus*	*S. libidinosus*
S. nigritus	0.055		
S. nigritus x *S. libidinosus*	0.061	0.059	
S. libidinosus	0.058	0.062	0.053

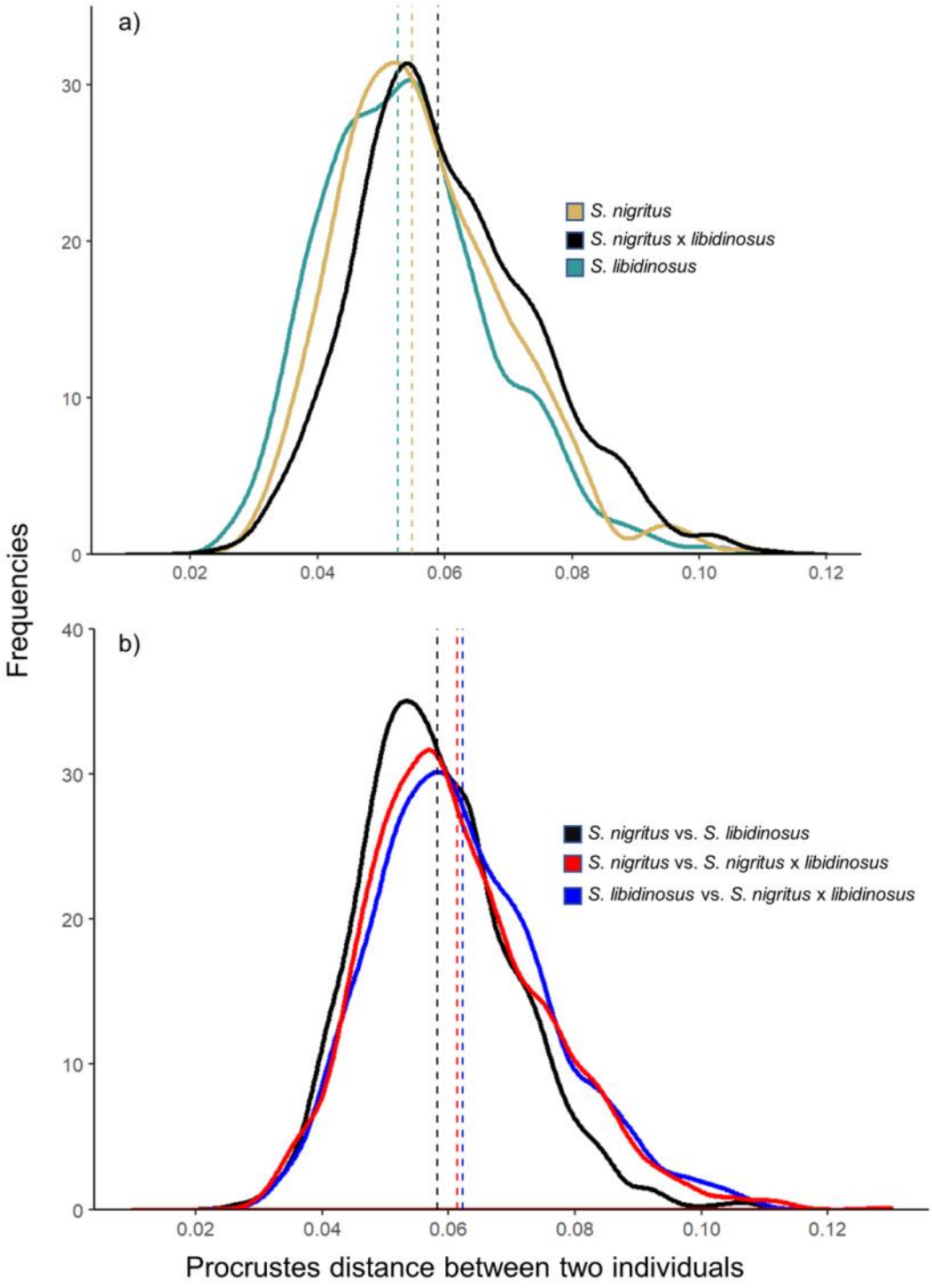

Figure 6. Frequency distributions of (a) within-group, and (b) between-group pairwise Procrustes distances, reflecting degree of similarity in M^1 shape between specimen pairs. Vertical dashed lines represent the mean pairwise Procrustes distance for each group. Note that the hybrids exhibit elevated within-group Procrustes distances, reflecting the higher morphological variability in this group compared to the parental taxa. Also, between-group comparisons between one parental taxon and the hybrids exhibit higher mean Procrustes distances compared to the pairwise distances between parental taxa.

Covariation between cusp tip configuration and crown outline shape

The results of the 2B PLS analysis are summarized in Table 5. There is a strong and statistically significant correlation between cusp tip configuration (block 1) and crown outline shape (block 2) for the combined sample (*r*-PLS = 0.66, *p* = 0. 001). There are differences in covariation between blocks 1 and 2 among the three taxonomic groups. The two parental taxa exhibit high and significant correlations between blocks 1 and 2 (*S. nigritus r*-PLS = 0.76, *p* = 0. 002; *S. libidinosus r*-PLS = 0.75, *p* = 0.001), while the hybrids exhibit weaker correlation between cusp configuration and crown outline shape (*r*-PLS = 0.63, *p* = 0.015). Effect sizes for each sample indicate that the hybrids, compared to the parental taxa, exhibit weaker integration than expected based on its permutated sampling distribution. However, pairwise statistical comparisons indicate that there is no statistically significant difference in the strength of integration among groups (although at *p* = 0.07, the difference in integration between the hybrids and *S. libidinosus* does approach significance; Table 5b).

Discussion

The impact of hybridization on primate hard tissue morphology is difficult to predict. While traits under additive genetic control are expected to exhibit the midparental state in F1 hybrid populations, studies reveal that F1 morphology often deviates from expectations (Ackermann et al., 2006; Ito et al., 2015). Frequently, F1 hybrid trait morphology is polytypic and individuals exhibit novel phenotypes not observed in either parental population (Bergman et al., 2008; Fuzessy et al., 2014; Jolly et al., 1997). Many commonly measured phenotypic traits are not under additive genetic control. Hybridization may affect non-additive trait expression, resulting in heterosis or dysgenesis (Z. J. Chen, 2013). The recombination of two divergently adapted parental genomes in hybrids may disrupt the interaction and expression of non-additive genes that control complex physiological and metabolic networks, including growth and development. This ultimately relaxes the constraints observed in parental developmental pathways and is associated with increased morphological variability in hybrids. Deviations from expected midpa-

Table 5. Results of the two-block partial least squares analysis.

a)

	r-PLS	*p*-value	Effect size
S. nigritus	0.76	0.002	3.01
S. nigritus x S. *libidinosus*	0.63	0.015	2.26
S. libidinosus	0.75	0.001	3.94
Taxa pooled	0.66	0.001	--

The r-PLS value reflects the degree of covariation between configuration of the cusp tips (block 1, landmarks 1 through 4) and the shape of the crown outline (block 2, sliding semilandmarks 5 through 34). Larger effect sizes are associated with stronger observed covariation between cusp tip and crown outline shape than expected based on the permutated sampling distribution.

b)

	S. nigritus	*S. nigritus* x *S. libidinosus*	*S. libidinosus*
S. nigritus	--	0.78	0.47
S. nigritus x *S. libidinosus*	0.79	--	0.07
S. libidinosus	0.60	1.44	--

Matrix of pairwise differences in 2B PLS effect size measuring difference in the strength of integration between samples in the lower triangle with corresponding p-values in the upper triangle.

rental morphology in F1 hybrids are positively associated with increasing parental genetic divergence (Allen et al., 2020; Bernardes et al., 2017; Stelkens & Seehausen, 2009). For example, there are fewer instances of cranial and postcranial trait heterosis in hybrids of recently diverged tamarin subspecies than between crosses of more anciently diverged tamarin subspecies (Cheverud et al., 1993; Kohn et al., 2001). Similarly, non-metric indicators of disrupted skeletodental development tend to be more frequently observed in primates with increasing parental divergence (Ackermann et al., 2014; Boel et al., 2019).

Beyond the first generation, hybrid morphology is expected to more closely resemble that of the parental population into which the hybrids have backcrossed (Falconer & Mackay, 1997). Continuous trait values in the backcrossed offspring of an F1 hybrid and an individual from the parental population are predicted to be the average of the parental value and the MPV. Some novel phenotypes observed in F1 hybrids persist in later-generation hybrids regardless of parental genetic contribution. *Macaca fuscata* x *M. cyclopis* macaques have enlarged, *M. fuscata*-like sinus size even in backcrossed individuals who derive most of their ancestry from *M. cyclopis* (Ito et al., 2015), and transgressive non-metric dental traits are observed in backcrossed *P. cynocephalus* x *P. anubis* individuals (Ackermann et al., 2014). The morphology of individuals in multigenerational hybrid zones depend on a combination of physiological, reproductive, and ecological selective pressures (Charpentier et al., 2008; Fourie et al., 2015; Jolly et al., 2011; Mourthe et al., 2019). These selection pressures structure the distribution of hybrid phenotypes across contact zones. For example, hybrids from the contact zone between *P. anubis* and *P. cynocephalus* in Amboseli, Kenya exhibit a continuous distribution of phenotypes ranging from more *P. anubis*-like to intermediate to more *P. cynocephalus*-like, while the phenotypic distribution of hybrids in the *P. anubis* x *P. hamadryas* contact zone in Awash, Ethiopia is bimodal with very few intermediate phenotypes (Alberts & Altmann, 2001; Wango et al., 2019). Phenotypically intermediate hybrids in Awash also exhibit reproductive behaviors intermediate to those observed in parental taxa, and are therefore thought to be at a reproductive disadvantage when backcrossing with *P. anubis* or *P. hamadryas* compared to hybrids with predominantly parental phenotypes and behaviors (Bergman et al., 2008). Hybrids in recently formed anthropogenic contact zones show more continuous phenotypic distributions and symmetrical contribution of parental genes into the contact zone (Malukiewicz, 2019). So, a biologically relevant understanding of phenotypic outcomes in hybrid populations requires information regarding a variety of endogenous and exogenous variables.

This study assumes that the NMNH is correct in its taxonomic designations of the specimens used. However, the hybrids and parental taxa studied here have not been genotyped, as is preferable in analyses examining the relationship between phenotype and degree of hybridity (Ackermann et al., 2006; Boel et al., 2019; Cheverud et al., 1993; Hamada et al., 2012). The assumption that the parental taxa are not themselves admixed may be particularly problematic for robust capuchins, as *Sapajus* species have a complex history of hybridization in secondary contact zones (Lima et al., 2018). In addition, there may be cryptic hybrids in the sample with a high degree of genetic admixture but no phenotypic indication of hybridity (Ackermann, 2010; Kelaita & Cortés-Ortiz, 2013). Regardless, the results of the analyses presented here, combined with results from previous research, allow for some predictions to be made regarding the genetic makeup of the robust capuchin hybrids.

My analyses indicate that, while hybrid M^1 shape largely falls within the range of variation observed in *S. nigritus* and *S. libidinosus*, some aspects of hybrid M^1 shape are unique compared to parental morphology. While PC 1 typically captures the allometric component of shape variation (Zelditch et al., 2012), in this study taxonomic designation explained a greater proportion of variation in PC 1 scores than did molar size (Table 2). Hybrids significantly differed from *S. nigritus* and *S. libidinosus* on the main axis of M^1 shape variation in the PCA. Hybrids had significantly lower PC 1 scores than both parental taxa and higher PC 2 scores than *S. libidinosus*, corresponding to M^1s with increased buccolingual distance between cusps and a waisted lingual crown margin (see Figures 3 and 4). However, hybrids and *S. nigritus* did not exhibit significantly different PC 2 or PC 3 scores. So, some hybrids exhibit a unique molar morphotype compared to parents, while others cluster with *S. nigritus*. This was reflected by the reasonably accurate classifications generated by the DFA assignment test (Table 3). *Sapajus nigritus* had the lowest correct assignment (61.3%), with more individuals misclassified as hybrids than *S. libidinosus* (Table 3). *Sapajus libidinosus* specimens also were more often misclassified as hybrids than *S. nigritus* but exhibited the highest percentage of

correctly classified individuals (73.0%).

The results of the PCA and DFA support recent revisions in capuchin taxonomy. Based on genetic and morphological data, the capuchins are proposed to contain two genera: the gracile *Cebus* capuchins and the robust *Sapajus* capuchins (Lynch Alfaro, de Sousa e Silva-Júnior, et al., 2012). The IUCN recognizes eight *Sapajus* species that can be subdivided into a more ancient clade that evolved in the Brazilian Atlantic forest and a clade that recently left the Atlantic Forest to spread throughout the Amazon (Lima et al., 2018). *Sapajus nigritus* belongs to the more ancient clade, and retains morphological features indicative of arboreal living, such as longer limbs and tails. *Sapajus libidinosus* belongs to the Amazonian clade but has recently evolved morphological traits for terrestrial life in the dry shrublands of the Brazilian Cerrado-Caatinga, including thickened molar enamel and shorter, more robust limbs (Wright et al., 2015). *Sapajus libidinosus* is therefore the most morphologically derived robust capuchin species (Wright et al., 2015). The results of the PCA and DFA presented here indicate that *S. nigritus* and *S. libidinosus* exhibit statistically significant differences in M^1 shape. Hybrids cluster more with *S. nigritus* rather than with the more derived *S. libidinosus*. Based on the tendency of the hybrids and *S. nigritus* to cluster along PCs 2 and 3, I would expect the hybrids to exhibit greater genetic affinity with *S. nigritus*. Tail length has been shown to track degree of hybridity in macaques (Hamada et al., 2012), so it would be interesting to test this in *S. nigritus* x *S. libidinosus* hybrids.

Mean hybrid M^1 shape in this study is not the MPV (see Figure 2). Compared to the expected shape, the observed hybrid M^1 mean shape exhibits buccolingual expansion and a waisted lingual margin. However, the MPV is expected only in F1 hybrids and only for traits under additive genetic control (Falconer & Mackay, 1997). It is highly unlikely that wild hybrid populations contain only F1 individuals (Kelaita & Cortés-Ortiz, 2013; Phillips-Conroy & Jolly, 1986). Additionally, it is known that the genetic architecture controlling M^1 size and shape is partly non-additive (Hardin, 2019; Hlusko et al., 2016). Combined, these observations indicate that the deviation from the expected mid-parental M^1 shape observed in this study are likely caused by the disruption of non-additive gene expression or epigenetic interactions in later-generation *S. nigritus* x *S. libidinosus* hybrids. This suggests that the morphological impact of hybridization persists beyond early hybrid generations, as has been demonstrated in baboons and macaques (Ackermann et al., 2014; Ito et al., 2015).

The *S. nigritus* x *S. libidinosus* hybrids exhibit evidence of destabilized dental development. Measured by pairwise Procrustes distances, hybrids exhibit statistically significant elevation of within-taxon variation in M^1 shape compared to both parental taxa. This variation may be driven by relaxed constraints during dental development (Fuzessy et al., 2014). Indeed, hybrids exhibit lower mean correlation between cusp tip configuration and crown outline shape (r-PLS = 0.63) compared to *S. nigritus* and *S. libidinosus* (r-PLS = 0.76 and r-PLS = 0.75, respectively). Hybrids tend to have wider intercusp distances and cusps positioned closer to the crown periphery than the parental taxa. Cusp tips correspond to the position of embryonic signaling centers in developing tooth germs. The distance between cusp tips is controlled by the relative strengths of activator and inhibitor molecules excreted by each signaling center and the duration of germ growth. Increased inhibitory signaling and/or prolonged germ growth are expected to result in fully formed teeth with widely spaced cusp tips (Guatelli-Steinberg et al., 2013; Jernvall, 2000). So, the wide intercusp distances and weaker correlation of cusp configuration and crown outline shape observed in *S. nigritus* x *S. libidinosus* hybrids are likely the result of prolonged dental development and/or deviation in levels of signaling molecules compared to those observed in parental dental development. Similarly, Ackermann et al. (2014) found that the presence of supernumerary distomolars is associated with increased molar row length in F1 hybrid *P. cynocephalus* x *P. anubis* individuals, suggesting that dental development is prolonged in hybrids compared to parents. Among other papionin hybrids, *Papio hamadryas* x *P. anubis* hybrids exhibit unique molar size relationships compared to parental taxa, suggesting that developmental pathways controlling hybrid baboon molar size may be destabilized compared to unadmixed baboons (Phillips-Conroy, 1978). However, based on frequencies of dental non-metric trait expression and fluctuating asymmetry of bilateral cranial traits, there is no evidence for destabilized dental development in early-generation *M. fuscata* x *M. cyclopis* macaques (Boel et al., 2019). It is possible that these observations support the prediction that the degree of developmental destabilization observed in hybrids is associated with parental divergence. *Sapajus nigritus* and *S. libidinosus* shared a common ancestor around 2.6 Ma (Lima et al., 2018); *P. cynocephalus*

and *P. anubis* diverged approximately 1.5 Ma while *P. hamadryas* and *P. anubis* diverged approximately 800 ka (Rogers et al., 2019); and *M. fuscata* and *M. cyclopis* are estimated to diverge as recently as 170 ka (Chu et al., 2007). A comparison of dental phenotypic variation and integration among these different hybrid populations would confirm the relationship between the degree of parental divergence and destabilized development in hybrids.

While non-metric dental anomalies are observed at high frequencies in some mammalian hybrid populations, this pattern is not shared by all extant primates. This calls into question the suggestion that certain dental non-metric traits, especially supernumerary distomolars or dental crowding, are evidence of significant hybrid ancestry in extinct hominins (Ackermann, 2010; Ackermann et al., 2019). However, continuous dental trait variation remains understudied, even though non-metric dental traits are often correlated with continuous trait variation (Ortiz et al., 2018) and a *Homo sapiens* fossil with substantial *H. neanderthalensis* ancestry exhibits extremely large upper third molars (Fu et al., 2015). The results presented here suggest that transgressive M^1 morphology that falls outside of the range of variation observed in well-defined hominin taxa may be indicative of hybrid ancestry in hominin fossils. Further analyses comparing molar shape variation in other extant primate hybrids would confirm if this is a valid prediction. In terms of primate conservation, this study did not indicate that hybridization reduced phenotypic variation among hybrids of *S. nigritus* and *S. libidinosus*. Rather, hybridization generated novel phenotypes not observed in either parental population. It remains to be determined if expanded intercusp distances in these hybrids facilitate ecological niche separation from other robust capuchin populations.

Conclusions

The dentition has been an anatomical region of interest in hybrid research, but previous work has predominantly studied non-metric dental trait variation rather than tooth shape. The results presented here suggest that a more in-depth analysis of the impact of hybridization on continuous dental phenotypes and development is warranted. The shape of the first upper molar is statistically distinct among *S. nigritus*, *S. libidinosus* and their hybrids, and hybrids exhibit morphological evidence of destabilized development, including elevated within-sample variance and weaker correlation between cusp tip configuration and crown outline shape. The same analyses used here applied to the rest of the postcanine teeth would likely uncover other significant differences between the hybrids and parental taxa. A more comprehensive understanding of the impact of hybridization on dental development could be gained by further comparisons of continuous trait integration between metameres and between occluding upper and lower molars; and by comparing levels of fluctuating asymmetry of continuous traits in left and right antimeres. The data derived from such studies would offer crucial information for attempts to diagnose hybrid ancestry from fossil morphology and to understand the evolutionary outcomes of hybridization among endangered primates in degraded habitats.

Acknowledgements

I thank Darrin Lunde for his assistance with accessing collections at the Smithsonian National Museum of Natural History. I also thank Shara Bailey for her guidance throughout the conception of this project and for her feedback on this manuscript.

REFERENCES

Ackermann, R. R. (2010). Phenotypic traits of primate hybrids: Recognizing admixture in the fossil record. *Evolutionary Anthropology: Issues, News, and Reviews*, *19*(6), 258–270.

Ackermann, R. R., Arnold, M. L., Baiz, M. D., Cahill, J. A., Cortés-Ortiz, L., Evans, B. J., Grant, B. R., Grant, P. R., Hallgrimsson, B., Humphreys, R. A., Jolly, C. J., Malukiewicz, J., Percival, C. J., Ritzman, T. B., Roos, C., Roseman, C. C., Schroeder, L., Smith, F. H., Warren, K. A., … Zinner, D. (2019). Hybridization in human evolution: Insights from other organisms. *Evolutionary Anthropology: Issues, News, and Reviews*, *28* (4), 189–209.

Ackermann, R. R., & Bishop, J. M. (2010). Morphological and molecular evidence reveals recent hybridization between *Gorilla* taxa. *Evolution*, *64* (1), 271–290.

Ackermann, R. R., Brink, J. S., Vrahimis, S., & de Klerk, B. (2010). Hybrid wildebeest (*Artiodactyla*: Bovidae) provide further evidence for shared signatures of admixture in mammalian crania. *South African Journal of Science*, *106*, 1–4.

Ackermann, R. R., Rogers, J., & Cheverud, J. M. (2006). Identifying the morphological signatures of hybridization in primate and human evolution. *Journal of Human Evolution*, *51*(6), 632–645.

Ackermann, R. R., Schroeder, L., Rogers, J., & Che-

verud, J. M. (2014). Further evidence for phenotypic signatures of hybridization in descendant baboon populations. *Journal of Human Evolution*, *76*, 54–62.

Adams, D. C., Collyer, M., & Kaliontzopoulou, A. (2020). *Geomorph: Software for geometric morphometric analyses. R package version 3.2.1*. https://cran.r-project.org/web/packages/geomorph/geomorph.pdf

Adams, D. C., & Collyer, M. L. (2016). On the comparison of the strength of morphological integration across morphometric datasets. *Evolution*, *70* (11), 2623–2631.

Alberts, S. C., & Altmann, J. (2001). Immigration and hybridization patterns of yellow and anubis baboons in and around Amboseli, Kenya. *American Journal of Primatology*, *53*(4), 139–154.

Alibert, P., Renaud, S., Dod, B., Bonhomme, F., & Auffray, J.-C. (1994). Fluctuating asymmetry in the *Mus musculus* hybrid zone: A heterotic effect in disrupted co-adapted genomes. *Proceedings of the Royal Society of London. Series B: Biological Sciences*, *258*(1351), 53–59.

Allen, R., Ryan, H., Davis, B. W., King, C., Frantz, L., Irving-Pease, E., Barnett, R., Linderholm, A., Loog, L., Haile, J., Lebrasseur, O., White, M., Kitchener, A. C., Murphy, W. J., & Larson, G. (2020). A mitochondrial genetic divergence proxy predicts the reproductive compatibility of mammalian hybrids. *Proceedings of the Royal Society B: Biological Sciences*, *287*(1928), 20200690.

Arnold, M. L. (1997). *Natural Hybridization and Evolution*. New York: Oxford University Press, USA.

Arnold, M. L., & Meyer, A. (2006). Natural hybridization in primates: One evolutionary mechanism. *Zoology*, *109*(4), 261–276.

Bailey, S. E. (2002). *Neandertal dental morphology: Implications for modern human origins* [Ph.D. Thesis]. Arizona State University.

Bailey, S. E. (2004). A morphometric analysis of maxillary molar crowns of Middle-Late Pleistocene hominins. *Journal of Human Evolution*, *47*(3), 183–198.

Bailey, S. E., Benazzi, S., Buti, L., & Hublin, J.-J. (2016). Allometry, merism, and tooth shape of the lower second deciduous molar and first permanent molar. *American Journal of Physical Anthropology*, *159*(1), 93–105.

Bergman, T. J., Phillips-Conroy, J. E., & Jolly, C. J. (2008). Behavioral variation and reproductive success of male baboons (*Papio anubis* × *Papio hamadryas*) in a hybrid social group. *American Journal of Primatology*, *70*(2), 136–147.

Bernardes, J. P., Stelkens, R. B., & Greig, D. (2017). Heterosis in hybrids within and between yeast species. *Journal of Evolutionary Biology*, *30*(3), 538–548.

Boel, C. (2016). *The Craniodental Morphology of Hybridising Macaques, and Implications for the Detection of Hybrids in the Human Fossil Record* [Ph.D. Thesis]. University of New South Wales.

Boel, C., Curnoe, D., & Hamada, Y. (2019). Craniofacial Shape and Nonmetric Trait Variation in Hybrids of the Japanese Macaque (*Macaca fuscata*) and the Taiwanese Macaque (*Macaca cyclopis*). *International Journal of Primatology*, *40*, 214–243.

Bolker, B., R Development Core Team, & Giné-Vázquez, I. (2020). *Bbmle* (1.0.23.1) [Computer software].

Bookstein, F. L. (1997). *Morphometric Tools for Landmark Data: Geometry and Biology*. Cambridge: Cambridge University Press.

Browning, S. R., Browning, B. L., Zhou, Y., Tucci, S., & Akey, J. M. (2018). Analysis of Human Sequence Data Reveals Two Pulses of Archaic Denisovan Admixture. *Cell*, *173*(1), 53–61.

Burrell, A. S., Jolly, C. J., Tosi, A. J., & Disotell, T. R. (2009). Mitochondrial evidence for the hybrid origin of the kipunji, *Rungwecebus kipunji* (Primates: Papionini). *Molecular Phylogenetics and Evolution*, *51*(2), 340–348.

Bynum, E. L., Bynum, D. Z., & Supriatna, J. (1997). Confirmation and location of the hybrid zone between wild populations of *Macaca tonkeana* and *Macaca hecki* in Central Sulawesi, Indonesia. *American Journal of Primatology*, *43*(3), 181–209.

Bynum, N. (2002). Morphological variation within a macaque hybrid zone. *American Journal of Physical Anthropology*, *118*(1), 45–49.

Charpentier, M. J. E., Fontaine, M. C., Cherel, E., Renoult, J. P., Jenkins, T., Benoit, L., Barthès, N., Alberts, S. C., & Tung, J. (2012). Genetic structure in a dynamic baboon hybrid zone corroborates behavioural observations in a hybrid population: Population structure in a baboon hybrid zone. *Molecular Ecology*, *21*(3), 715–731.

Charpentier, M. J. E., Tung, J., Altmann, J., & Alberts, S. C. (2008). Age at maturity in wild baboons: Genetic, environmental and demographic influences: Maturation in a hybrid baboon population. *Molecular Ecology*, *17*(8), 2026–2040.

Chen, C., & Pfennig, K. S. (2020). Female toads engaging in adaptive hybridization prefer high-quality heterospecifics as mates. *Science*, *367* (6484), 1377.

Chen, L., Wolf, A. B., Fu, W., Li, L., & Akey, J. M. (2020). Identifying and Interpreting Apparent Neanderthal Ancestry in African Individuals.

Cell, *180*(4), 677–687.

Chen, Z. J. (2013). Genomic and epigenetic insights into the molecular bases of heterosis. *Nature Reviews Genetics*, *14*(7), 471–482.

Cheverud, J. M., Jacobs, S. C., & Moore, A. J. (1993). Genetic differences among subspecies of the saddle-back tamarin (*Saguinus fuscicollis*): Evidence from hybrids. *American Journal of Primatology*, *31*(1), 23–39.

Chhatre, V. E., Evans, L. M., DiFazio, S. P., & Keller, S. R. (2018). Adaptive introgression and maintenance of a trispecies hybrid complex in range-edge populations of Populus. *Molecular Ecology*, *27*(23), 4820–4838.

Chu, J. H., Lin, Y. S., & Wu, H. Y. (2007). Evolution and dispersal of three closely related macaque species, *Macaca mulatta, M. cyclopis*, and *M. fuscata*, in the eastern Asia. *Molecular Phylogenetics and Evolution*, *43*(2), 418–429.

Clarke, G. M. (1993). The genetic basis of developmental stability. I. Relationships between stability, heterozygosity and genomic coadaptation. *Genetica*, *89*(1), 15–23.

Cortés-Ortiz, L., Duda Jr, T. F., Canales-Espinosa, D., García-Orduña, F., Rodríguez-Luna, E., & Bermingham, E. (2007). Hybridization in large-bodied New World primates. *Genetics Society of America*, *176*, 2421–2425.

de Manuel, M., Kuhlwilm, M., Frandsen, P., Sousa, V. C., Desai, T., Prado-Martinez, J., Hernandez-Rodriguez, J., Dupanloup, I., Lao, O., Hallast, P., Schmidt, J. M., Heredia-Genestar, J. M., Benazzo, A., Barbujani, G., Peter, B. M., Kuderna, L. F. K., Casals, F., Angedakin, S., Arandjelovic, M., … Marques-Bonet, T. (2016). Chimpanzee genomic diversity reveals ancient admixture with bonobos. *Science*, *354*(6311), 477–481.

Debat, V., Alibert, P., David, P., Paradis, E., & Auffray Jean-Christophe. (2000). Independence between developmental stability and canalization in the skull of the house mouse. *Proceedings of the Royal Society of London. Series B: Biological Sciences*, *267*(1442), 423–430.

Delgado, M. N., Galbany, J., Górka, K., & Pérez-Pérez, A. (2015). Taxonomic Implications of Molar Morphology Variability in Capuchins. *International Journal of Primatology*, *36*(4), 707–727.

Détroit, F., Mijares, A. S., Corny, J., Daver, G., Zanolli, C., Dizon, E., Robles, E., Grün, R., & Piper, P. J. (2019). A new species of *Homo* from the Late Pleistocene of the Philippines. *Nature*, *568*(7751), 181.

Detwiler, K. M. (2019). Mitochondrial DNA Analyses of *Cercopithecus* Monkeys Reveal a Localized Hybrid Origin for *C. mitis doggetti* in Gombe National Park, Tanzania. *International Journal of Primatology*, *40*(1), 28–52.

Detwiler, K. M., Burrell, A. S., & Jolly, C. J. (2005). Conservation Implications of Hybridization in African Cercopithecine Monkeys. *International Journal of Primatology*, *26*(3), 661–684.

Dobzhansky, T. (1940). Speciation as a Stage in Evolutionary Divergence. *American Society of Naturalists*, *74*(753), 312–321.

Durvasula, A., & Sankararaman, S. (2020). Recovering signals of ghost archaic introgression in African populations. *Science Advances*, *6*(7), eaax5097. https://doi.org/10.1126/sciadv.aax5097

Eichel, K. A., & Ackermann, R. R. (2016). Variation in the nasal cavity of baboon hybrids with implications for late Pleistocene hominins. *Journal of Human Evolution*, *94*, 134–145.

Evans, A. R., Daly, E. S., Catlett, K. K., Paul, K. S., King, S. J., Skinner, M. M., Nesse, H. P., Hublin, J.-J., Townsend, G. C., & Schwartz, G. T. (2016). A simple rule governs the evolution and development of hominin tooth size. *Nature*, *530*(7591), 477–480.

Falconer, D., & Mackay, T. (1997). *Introduction to Quantitative Genetics*. Dover Publications.

Fan, Z., Zhou, A., Osada, N., Yu, J., Jiang, J., Li, P., Du, L., Niu, L., Deng, J., Xu, H., Xing, J., Yue, B., & Li, J. (2018). Ancient hybridization and admixture in macaques (genus *Macaca*) inferred from whole genome sequences. *Molecular Phylogenetics and Evolution*, *127*, 376–386.

Fourie, N. H., Jolly, C. J., Phillips-Conroy, J. E., Brown, J. L., & Bernstein, R. M. (2015). Variation of hair cortisol concentrations among wild populations of two baboon species (*Papio anubis, P. hamadryas*) and a population of their natural hybrids. *Primates*, *56*(3), 259–272.

Fu, Q., Hajdinjak, M., Moldovan, O. T., Constantin, S., Mallick, S., Skoglund, P., Patterson, N., Rohland, N., Lazaridis, I., Nickel, B., Viola, B., Prüfer, K., Meyer, M., Kelso, J., Reich, D., & Pääbo, S. (2015). An early modern human from Romania with a recent Neanderthal ancestor. *Nature*, *524*(7564), 216–219.

Fuzessy, L. F., Silva, I. de O., Malukiewicz, J., Silva, F. F. R., Pônzio, M. do C., Boere, V., & Ackermann, R. R. (2014). Morphological Variation in Wild Marmosets (*Callithrix penicillata* and *C. geoffroyi*) and Their Hybrids. *Evolutionary Biology*, *41*(3), 480–493.

Gamarra, B., Nova Delgado, M., Romero, A., Gal-

bany, J., & Pérez-Pérez, A. (2016). Phylogenetic signal in molar dental shape of extant and fossil catarrhine primates. *Journal of Human Evolution*, *94*, 13–27.

Gligor, M., Ganzhorn, J. U., Rakotondravony, D., Ramilijaona, O. R., Razafimahatratra, E., Zischler, H., & Hapke, A. (2009). Hybridization between mouse lemurs in an ecological transition zone in southern Madagascar. *Molecular Ecology*, *18*(3), 520–533.

Gómez-Robles, A., Bermúdez de Castro, J. M., Martinón-Torres, M., Prado-Simón, L., & Arsuaga, J. L. (2015). A geometric morphometric analysis of hominin lower molars: Evolutionary implications and overview of postcanine dental variation. *Journal of Human Evolution*, *82*, 34–50.

Gómez-Robles, A., Martinón-Torres, M., Bermúdez de Castro, J. M., Margvelashvili, A., Bastir, M., Arsuaga, J. L., Pérez-Pérez, A., Estebaranz, F., & Martínez, L. M. (2007). A geometric morphometric analysis of hominin upper first molar shape. *Journal of Human Evolution*, *53*(3), 272–285.

Goodwin, H. T. (1998). Supernumerary teeth in Pleistocene, recent, and hybrid individuals of the *Spermophilus richardsonii* complex (Sciuridae). *Journal of Mammalogy*, *79*(4), 1161–1169.

Grant, P. R., & Grant, B. R. (2020). Triad hybridization via a conduit species. *Proceedings of the National Academy of Sciences*, *117*(14), 7888–7896.

Green, R. E., Krause, J., Briggs, A. W., Marcic, T., Stenzel, U., Kircher, M., Patterson, N., Li, H., Zhai, W., Fritz, M. H.-Y., Hansen, N. F., Durand, E. Y., Malaspinas, A.-S., Jensen, J. D., Marques-Bonet, T., Alkan, C., Prüfer, kay, Meyer, M., Burbano, H. A., … Siegemund..., M. (2010). A Draft Sequence of the Neandertal Genome. *Science, New Series*, *328*(5979), 710–722.

Grün, R., Pike, A., McDermott, F., Eggins, S., Mortimer, G., Aubert, M., Kinsley, L., Joannes-Boyau, R., Rumsey, M., Denys, C., Brink, J., Clark, T., & Stringer, C. (2020). Dating the skull from Broken Hill, Zambia, and its position in human evolution. *Nature*, *580*, 372–375.

Guatelli-Steinberg, D., Hunter, J. P., Durner, R. M., Moormann, S., Weston, T. C., & Betsinger, T. K. (2013). Teeth, morphogenesis, and levels of variation in the human Carabelli trait. In G. R. Scott & J. D. Irish (Eds.), *Anthropological perspectives on dental morphology: Genetics, evolution, variation*. (pp. 69–91). Cambridge University Press.

Gunz, P., & Mitteroecker, P. (2013). Semilandmarks: A method for quantifying curves and surfaces. *Hystrix, the Italian Journal of Mammalogy*, *24*(1). https://doi.org/10.4404/hystrix-24.1-6292

Hamada, Y., Yamamoto, A., Kunimatsu, Y., Tojima, S., Mouri, T., & Kawamoto, Y. (2012). Variability of tail length in hybrids of the Japanese macaque (*Macaca fuscata*) and the Taiwanese macaque (*Macaca cyclopis*). *Primates*, *53*(4), 397–411. https://doi.org/10.1007/s10329-012-0317-3

Hardin, A. M. (2019). Genetic contributions to dental dimensions in brown-mantled tamarins (*Saguinus fuscicollis*) and rhesus macaques (*Macaca mulatta*). *American Journal of Physical Anthropology*, *168*(2), 292–302.

Heide-Jorgensen, M. P., & Reeves, R. R. (1993). Description of an anomalous monodontid skull from West Greenland: A possible hybrid? *Marine Mammal Science*, *9*(3), 258–268.

Herries, A. I. R., Martin, J. M., Leece, A. B., Adams, J. W., Boschian, G., Joannes-Boyau, R., Edwards, T. R., Mallett, T., Massey, J., Murszewski, A., Neubauer, S., Pickering, R., Strait, D. S., Armstrong, B. J., Baker, S., Caruana, M. V., Denham, T., Hellstrom, J., Moggi-Cecchi, J., … Menter, C. (2020). Contemporaneity of *Australopithecus*, *Paranthropus*, and early *Homo erectus* in South Africa. *Science*, *368*(6486), eaaw7293.

Hlusko, L. J., Schmitt, C. A., Monson, T. A., Brasil, M. F., & Mahaney, M. C. (2016). The integration of quantitative genetics, paleontology, and neontology reveals genetic underpinnings of primate dental evolution. *Proceedings of the National Academy of Sciences*, *113*(33), 9262–9267.

Holliday, T. W. (2003). Species Concepts, Reticulation, and Human Evolution. *Current Anthropology*, *44*(5), 653–673.

Huerta-Sánchez, E., Jin, X., Asan, Bianba, Z., Peter, B. M., Vinckenbosch, N., Liang, Y., Yi, X., He, M., Somel, M., Ni, P., Wang, B., Ou, X., Huasang, Luosang, J., Cuo, Z. X. P., Li, K., Gao, G., Yin, Y., … Nielsen, R. (2014). Altitude adaptation in Tibetans caused by introgression of Denisovan-like DNA. *Nature*, *512*(7513), 194–197.

Ito, T., Kawamoto, Y., Hamada, Y., & Nishimura, T. D. (2015). Maxillary sinus variation in hybrid macaques: Implications for the genetic basis of craniofacial pneumatization. *Biological Journal of the Linnean Society*, *115*(2), 333–347.

Jackson, J. F. (1973). A Search for the Population Asymmetry Parameter. *Systematic Biology*, *22*(2), 166–170.

Jacobs, G. S., Hudjashov, G., Saag, L., Kusuma, P., Darusallam, C. C., Lawson, D. J., Mondal, M., Pagani, L., Ricaut, F.-X., Stoneking, M., Metspa-

lu, M., Sudoyo, H., Lansing, J. S., & Cox, M. P. (2019). Multiple Deeply Divergent Denisovan Ancestries in Papuans. *Cell*, *177*(4), 1010–1021.

Jernvall, J. (2000). Linking development with generation of novelty in mammalian teeth. *Proceedings of the National Academy of Sciences*, *97*(6), 2641–2645.

Jernvall, J., & Jung, H.-S. (2000). Genotype, phenotype, and developmental biology of molar tooth characters. *American Journal of Physical Anthropology*, *113*(s 31), 171–190.

Jiggins, C. D., Salazar, C., Linares, M., & Mavarez, J. (2008). Hybrid trait speciation and Heliconius butterflies. *Philosophical Transactions of the Royal Society B: Biological Sciences*, *363*(1506), 3047–3054.

Jolly, C. J., Burrell, A. S., Phillips-Conroy, J., E., Bergey, C., & Rogers, J. (2011). Kinda baboons (*Papio kindae*) and grayfoot chacma baboons (*P. ursinus griseipes*) hybridize in the Kafue river valley, Zambia. *American Journal of Primatology*, *73*(3), 291–303.

Jolly, C. J., Woolley-Barker, T., Beyene, S., Disotell, T. R., & Phillips-Conroy, J. E. (1997). Intergeneric Hybrid Baboons. *International Journal of Primatology*, *18*(4), 597–627.

Kavanagh, K. D., Evans, A. R., & Jernvall, J. (2007). Predicting evolutionary patterns of mammalian teeth from development. *Nature*, *449*(7161), 427–432.

Kelaita, M. A., & Cortés-Ortiz, L. (2013). Morphological variation of genetically confirmed *Alouatta Pigra* × *A. palliata* hybrids from a natural hybrid zone in Tabasco, Mexico. *American Journal of Physical Anthropology*, *150*(2), 223–234.

Klingenberg, C. P. (2003). Developmental instability as a research tool: Using patterns of fluctuating asymmetry to infer the developmental origins of morphological integration. In M. Polak (Ed.), *Developmental Instability: Causes and Consequences* (pp. 427–442). Oxford University Press.

Klingenberg, C. P., & McIntyre, G. S. (1998). Geometric Morphometrics of Developmental Instability: Analyzing Patterns of Fluctuating Asymmetry with Procrustes Methods. *Evolution*, *52*(5), 1363–1375.

Kohn, L. A. P., Langton, L. B., & Cheverud, J. M. (2001). Subspecific genetic differences in the saddle-back tamarin (*Saguinus fuscicollis*) postcranial skeleton. *American Journal of Primatology*, *54*(1), 41–56.

Kuhlwilm, M., Han, S., Sousa, V. C., Excoffier, L., & Marques-Bonet, T. (2019). Ancient admixture from an extinct ape lineage into bonobos. *Nature Ecology & Evolution*.

Leary, R. F., Allendorf, F. W., & Knudsen, K. L. (1985). Developmental instability and high meristic counts in interspecific hybrids of salmonid fishes. *Evolution*, *39*(6), 1318–1326.

Lima, M. G. M., de Sousa e Silva-Júnior, J., Černý, D., Buckner, J. C., Aleixo, A., Chang, J., Zheng, J., Alfaro, M. E., Martins, A., Di Fiore, A., Boubli, J. P., & Lynch Alfaro, J. W. (2018). A phylogenomic perspective on the robust capuchin monkey (*Sapajus*) radiation: First evidence for extensive population admixture across South America. *Molecular Phylogenetics and Evolution*, *124*, 137–150.

Lynch Alfaro, J. W., Boubli, J. P., Olson, L. E., Di Fiore, A., Wilson, B., Gutiérrez-Espeleta, G. A., Chiou, K. L., Schulte, M., Neitzel, S., Ross, V., Schwochow, D., Nguyen, M. T. T., Farias, I., Janson, C. H., & Alfaro, M. E. (2012). Explosive Pleistocene range expansion leads to widespread Amazonian sympatry between robust and gracile capuchin monkeys. *Journal of Biogeography*, *39*(2), 272–288.

Lynch Alfaro, J. W., de Sousa e Silva-Júnior, J., & Rylands, A. B. (2012). How Different Are Robust and Gracile Capuchin Monkeys? An Argument for the Use of *Sapajus* and *Cebus*. *American Journal of Primatology*, *74*(4), 273–286.

Lynch Alfaro, J. W., Izar, P., & Ferreira, R. G. (2014). Capuchin monkey research priorities and urgent issues. *American Journal of Primatology*, *76*(8), 705–720.

Malukiewicz, J. (2019). A Review of Experimental, Natural, and Anthropogenic Hybridization in *Callithrix* Marmosets. *International Journal of Primatology*, *40*, 72–98.

Malukiewicz, J., Boere, V., Fuzessy, L. F., Grativol, A. D., de Oliveira e Silva, I., Pereira, L. C. M., Ruiz-Miranda, C. R., Valença, Y. M., & Stone, A. C. (2015). Natural and Anthropogenic Hybridization in Two Species of Eastern Brazilian Marmosets (*Callithrix jacchus* and *C. penicillata*). *PLOS ONE*, *10*(6), e0127268.

Martinón-Torres, M., Bermúdez de Castro, J. M., Gómez-Robles, A., Prado-Simón, L., & Arsuaga, J. L. (2012). Morphological description and comparison of the dental remains from Atapuerca-Sima de los Huesos site (Spain). *Journal of Human Evolution*, *62*(1), 7–58.

Martins, W. P., Lynch Alfaro, J., & Rylands, A. B. (2017). Reduced range of the endangered crested capuchin monkey (*Sapajus robustus*) and a possible hybrid zone with *Sapajus nigritus*. *American Journal of Primatology*, *79*(10), e22696.

Mather, R. (1992). *A field study of hybrid gibbons in central Kalimantan, Indonesia* [Ph.D. Thesis]. University of Cambridge.

Mayr, E. (1963). *Animal species and evolution.* The Belknap Press of Harvard University Press.

Melo, F. R., Alfaro, J. L., Miranda, J. M. D., Rímoli, J., Alonso, A. C., Santos, M. C. dos, Ludwig, G., Martins, W. P., & Martins, J. N. (2015, January 26). *IUCN Red List of Threatened Species: Black-horned Capuchin*. IUCN Red List of Threatened Species. https://www.iucnredlist.org/en

Melo, F. R., Fialho, M. de S., Jerusalinsky, L., Laroque, P. de O., Alfaro, J. L., Montenegro, M. M. V., Bezerra, B. M., & Martins, A. B. (2015, January 26). *IUCN Red List of Threatened Species: Bearded Capuchin*. IUCN Red List of Threatened Species. https://www.iucnredlist.org/en

Mourthe, I., Trindade, R. A., Aguiar, L. M., Trigo, T. C., Bicca-Marques, J. C., & Bonatto, S. L. (2019). Hybridization Between Neotropical Primates with Contrasting Sexual Dichromatism. *International Journal of Primatology*, *40*(1), 99–113.

Neff, N. A., & Smith, G. R. (1979). Multivariate Analysis of Hybrid Fishes. *Systematic Zoology*, *28*(2), 176–196.

Ortiz, A., Bailey, S. E., Schwartz, G. T., Hublin, J.-J., & Skinner, M. M. (2018). Evo-devo models of tooth development and the origin of hominoid molar diversity. *Science Advances*, *4*(4), eaar2334. https://doi.org/10.1126/sciadv.aar2334

Pallares, L. F., Turner, L. M., & Tautz, D. (2016). Craniofacial shape transition across the house mouse hybrid zone: Implications for the genetic architecture and evolution of between-species differences. *Development Genes and Evolution*, *226*(3), 173–186.

Paul, K. S., Astorino, C. M., & Bailey, S. E. (2017). The Patterning Cascade Model and Carabelli's trait expression in metameres of the mixed human dentition: Exploring a morphogenetic model. *American Journal of Physical Anthropology*, *162*(1), 3–18.

Phillips-Conroy, J. E. (1978). *Dental Variability in Ethiopian Baboons: An Examination of the Anubis-Hamadryas Hybrid Zone in the Awash National Park, Ethiopia* [Ph.D. Thesis]. New York University.

Phillips-Conroy, J. E., & Jolly, C. J. (1986). Changes in the structure of the baboon hybrid zone in the Awash National Park, Ethiopia. *American Journal of Physical Anthropology*, *71*(3), 337–350.

Reich, D., Patterson, N., Kircher, M., Delfin, F., Nandineni, M. R., Pugach, I., Ko, A. M.-S., Ko, Y.-C., Jinam, T. A., Phipps, M. E., Saitou, N., Wollstein, A., Kayser, M., Pääbo, S., & Stoneking, M. (2011). Denisova Admixture and the First Modern Human Dispersals into Southeast Asia and Oceania. *The American Journal of Human Genetics*, *89*(4), 516–528. https://doi.org/10.1016/j.ajhg.2011.09.005

Rizk, O. T., Grieco, T. M., Holmes, M. W., & Hlusko, L. J. (2013). Using geometric morphometrics to study the mechanisms that pattern primate dental variation. *Anthropological Perspectives on Tooth Morphologies: Genetics, Evolution, Variation. Cambridge: Cambridge University Press. p*, 126–169.

Rogers, J., Raveendran, M., Harris, R. A., Mailund, T., Leppälä, K., Athanasiadis, G., Schierup, M. H., Cheng, J., Munch, K., Walker, J. A., Konkel, M. K., Jordan, V., Steely, C. J., Beckstrom, T. O., Bergey, C., Burrell, A., Schrempf, D., Noll, A., Kothe, M., … Baboon Genome Analysis Consortium. (2019). The comparative genomics and complex population history of *Papio* baboons. *Science Advances*, *5*(1), eaau6947. https://doi.org/10.1126/sciadv.aau6947

Roos, C., Liedigk, R., Thinh, V. N., Nadler, T., & Zinner, D. (2019). The Hybrid Origin of the Indochinese Gray Langur *Trachypithecus crepusculus* . *International Journal of Primatology*, *40*(1), 9–27.

Sankararaman, S., Mallick, S., Patterson, N., & Reich, D. (2016). The combined landscape of Denisovan and Neanderthal ancestry in present-day humans. *Current Biology*, *26*(9), 1241–1247.

Seehausen, O., Takimoto, G., Roy, D., & Jokela, J. (2008). Speciation reversal and biodiversity dynamics with hybridization in changing environments. *Molecular Ecology*, *17*(1), 30–44. https://doi.org/10.1111/j.1365-294X.2007.03529.x

Skov, L., Coll Macià, M., Sveinbjörnsson, G., Mafessoni, F., Lucotte, E. A., Einarsdóttir, M. S., Jonsson, H., Halldorsson, B., Gudbjartsson, D. F., Helgason, A., Schierup, M. H., & Stefansson, K. (2020). The nature of Neanderthal introgression revealed by 27,566 Icelandic genomes. *Nature*. https://doi.org/10.1038/s41586-020-2225-9

Slon, V., Mafessoni, F., Vernot, B., de Filippo, C., Grote, S., Viola, B., Hajdinjak, M., Peyrégne, S., Nagel, S., Brown, S., Douka, K., Higham, T., Kozlikin, M. B., Shunkov, M. V., Derevianko, A. P., Kelso, J., Meyer, M., Prüfer, K., & Pääbo, S.

(2018). The genome of the offspring of a Neanderthal mother and a Denisovan father. *Nature*, *561*(7721), 113–116.

Spoor, F., Gunz, P., Neubauer, S., Stelzer, S., Scott, N., Kwekason, A., & Dean, M. C. (2015). Reconstructed *Homo habilis* type OH 7 suggests deep-rooted species diversity in early *Homo*. *Nature*, *519*(7541), 83–86.

Stelkens, R., & Seehausen, O. (2009). Genetic Distance Between Species Predicts Novel Trait Expression in Their Hybrids. *Evolution*, *63*(4), 884–897.

Svardal, H., Jasinska, A. J., Apetrei, C., Coppola, G., Huang, Y., Schmitt, C. A., Jacquelin, B., Ramensky, V., Müller-Trutwin, M., Antonio, M., Weinstock, G., Grobler, J. P., Dewar, K., Wilson, R. K., Turner, T. R., Warren, W. C., Freimer, N. B., & Nordborg, M. (2017). Ancient hybridization and strong adaptation to viruses across African vervet monkey populations. *Nature Genetics*, *49*(12), 1705–1713.

Taylor, S. A., & Larson, E. L. (2019). Insights from genomes into the evolutionary importance and prevalence of hybridization in nature. *Nature Ecology & Evolution*, *3*(2), 170–177.

The GIMP Development Team. (2019). *GNU Image Manipulation Program* (2.10.12) [Computer software]. www.gimp.org

Thinh, V. N., Mootnick, A. R., Geissmann, T., Li, M., Ziegler, T., Agil, M., Moisson, P., Nadler, T., Walter, L., & Roos, C. (2010). Mitochondrial evidence for multiple radiations in the evolutionary history of small apes. *BMC Evolutionary Biology*, *10*(1), 74.

Thompson, K. A., Rieseberg, L. H., & Schluter, D. (2018). Speciation and the City. *Trends in Ecology & Evolution*, *33*(11), 815–826.

Tosi, A. J., Morales, J. C., & Melnick, D. J. (2000). Comparison of Y Chromosome and mtDNA Phylogenies Leads to Unique Inferences of Macaque Evolutionary History. *Molecular Phylogenetics and Evolution*, *17*(2), 133–144.

Tung, J., & Barreiro, L. B. (2017). The contribution of admixture to primate evolution. *Current Opinion in Genetics & Development*, *47*, 61–68.

Villanea, F. A., & Schraiber, J. G. (2019). Multiple episodes of interbreeding between Neanderthal and modern humans. *Nature Ecology & Evolution*, *3*(1), 39–44.

Wang, B., Zhou, X., Shi, F., Liu, Z., Roos, C., Garber, P. A., Li, M., & Pan, H. (2015). Full-length *Numt* analysis provides evidence for hybridization between the Asian colobine genera *Trachypithecus* and *Semnopithecus*: A *Numt* Clarifies a Colobine Hybridization Event. *American Journal of Primatology*, *77*(8), 901–910.

Wango, T. L., Musiega, D., Mundia, C. N., Altmann, J., Alberts, S. C., & Tung, J. (2019). Climate and Land Cover Analysis Suggest No Strong Ecological Barriers to Gene Flow in a Natural Baboon Hybrid Zone. *International Journal of Primatology*, *40*(1), 53–70.

Wood, B. A., & Abbott, S. A. (1983). Analysis of the dental morphology of Plio-Pleistocene hominids. I. Mandibular molars: Crown area measurements and morphological traits. *Journal of Anatomy*, *136*(Pt 1), 197–219. PubMed.

Wright, K. A., Wright, B. W., Ford, S. M., Fragaszy, D., Izar, P., Norconk, M., Masterson, T., Hobbs, D. G., Alfaro, M. E., & Lynch Alfaro, J. W. (2015). The effects of ecology and evolutionary history on robust capuchin morphological diversity. *Molecular Phylogenetics and Evolution*, *82*, 455–466.

Zelditch, M. L., Swiderski, D. L., & Sheets, H. D. (2012). *Geometric Morphometrics for Biologists: A Primer*. Amsterdam: Elsevier.

Zichello, J. M. (2018). Look in the trees: Hylobatids as evolutionary models for extinct hominins. *Evolutionary Anthropology: Issues, News, and Reviews*, *27*(4), 142–146.

Zinner, D., Arnold, M. L., & Roos, C. (2011). The strange blood: Natural hybridization in primates. *Evolutionary Anthropology: Issues, News, and Reviews*, *20*(3), 96–103.

Permanent Molar Trait Expression in the Late Neolithic Cave Burials of the Meuse Basin, Belgium

Frank L'Engle Williams[1*] and Rebecca L. George[2]

[1] Georgia State University
[2] University of Nevada, Reno

Keywords: Hastière Caverne M, Hastière Trou Garçon C, Sclaigneaux, Bois Madame, Maurenne Caverne de la Cave

ABSTRACT At least 250 cave burials along the Meuse river basin of Belgium yield prehistoric remains, and most date from the Late Neolithic period. Several of these collective burials have been radiocarbon dated, including the early/late Neolithic deposits of Hastière Caverne M and Hastière Trou Garçon C and the final/late Neolithic caves of Sclaigneaux and Bois Madame. An additional cave burial, Maurenne Caverne de la Cave, has been radiocarbon dated to the Middle Neolithic and final/late Neolithic periods, circa 4,635 to 3,830 years BP, which encompasses the entire range of dates for the other collective burials. Individuals (n = 127) are represented by fragmentary gnathic remains with *in situ* dental elements. Although the remains have been studied in detail, researchers have yet to compare dental morphology across cave sites. Arizona State University Dental Anthropology System (ASUDAS) scores of permanent molar morphology are employed to examine whether differences within and between the cave burials exist, and whether chronology and geography can account for the variation in traits. Affirming our expectations, the final/late Neolithic cave of Sclaigneaux, the most geographically distant cave burial, and secondarily Hastière Caverne M, possibly the earliest site, emerge as the most distinctive. The final/late Neolithic sites of Sclaigneaux and Bois Madame exhibit the greatest variability of trait expression. This research contributes to the understanding of the relatedness of early farming communities, and these findings bear on the mobility and continuity of human groups in the Meuse basin of Belgium during the terminus of the Neolithic before the onset of the Bronze Age in northern Europe.

The Meuse River basin of central Belgium extends along a semi-continuous karstic uplift featuring numerous cliff walls, rock formations and at least 3,000 caverns. More than 250 of these caves preserve the remains of prehistoric humans. Although these caves have been known for centuries, formal exploration of the sites commenced in the winter of 1829-1830 and has continued to the present (Polet, 2011). Close to 200 of these funerary sites have been radiocarbon dated to the Late Neolithic period (Toussaint et al., 2001). Many of these are collective burials and contain five to 15 individuals (Polet, 2011), however, some are larger, such as the caves of Bois Madame and Sclaigneaux (Dumbruch, 2003; De Paep & Polet, 2007). Only eight percent of these funerary sites contain between 55 and 60 individuals (Polet, 2011).

Hundreds of skeletal fragments and dental elements have been investigated from Hastière Caverne M (Hastière M), Hastière Trou Garçon C (Trou Garçon), Sclaigneaux, Bois Madame and Maurenne Caverne de la Cave (Maurenne) (Figure 1), and adults of both sexes and children are represented, suggesting familial, kin or descent groups used the caves for burial. These five cave deposits are all radiocarbon dated to the Late Neolithic (Table 1). However, Maurenne is associated with three dates from the terminus of the Late Neolithic (4,160 ± 45; 3,950 ± 70; 3,830 ± 90 years BP), and one date, 4,635 ± 45 years BP, from the Middle Neolith-

*Correspondence to:
Frank L'Engle Williams
Department of Anthropology
Georgia State University
P.O. Box 3998
Atlanta, GA, 30302-3998
United States
frankwilliams@gsu.edu

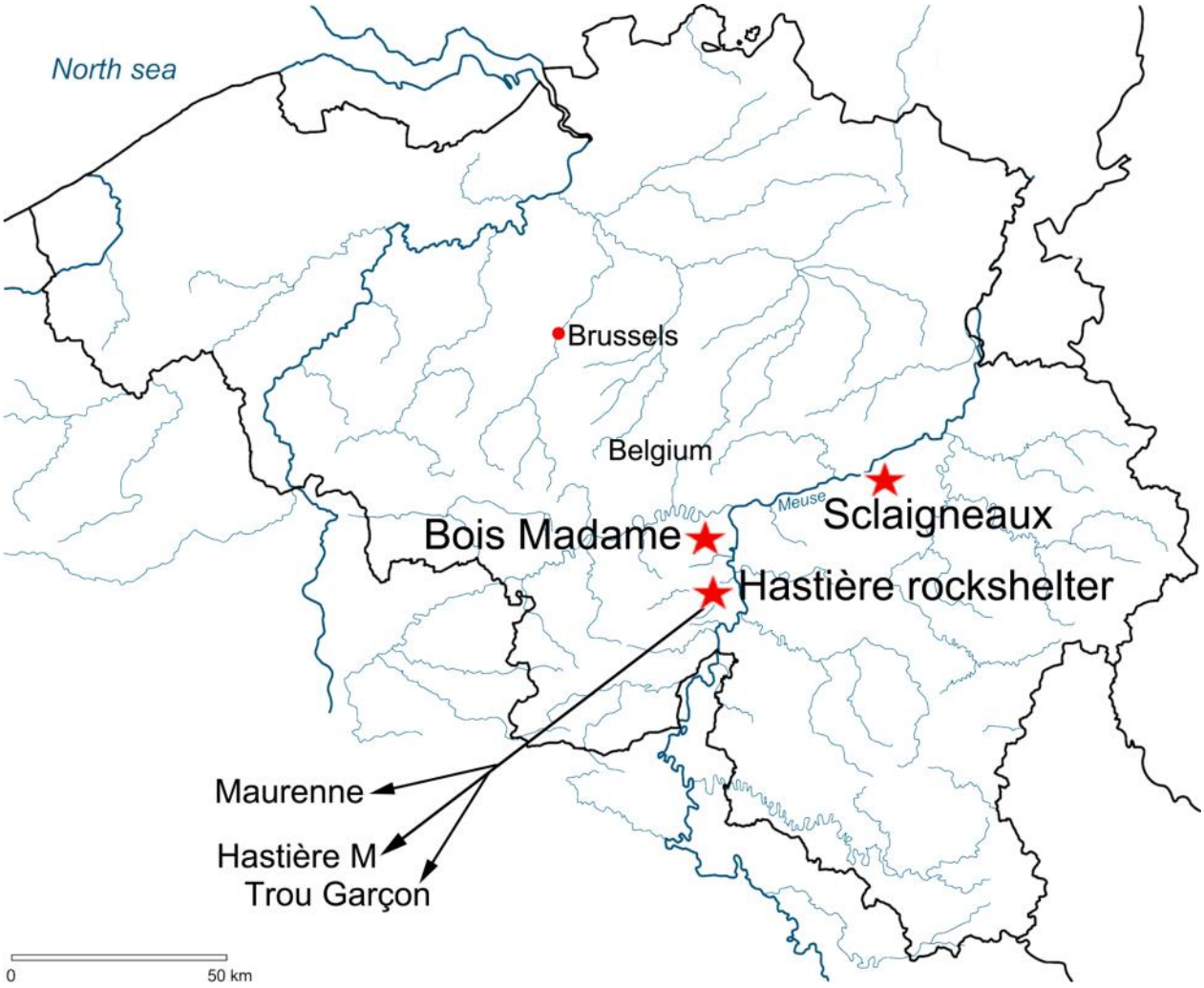

Figure 1. Map of Belgium showing the location of five Late Neolithic collective burials along the Meuse River system.

Table 1. Radiocarbon dates associated with five Neolithic collective burials of Belgium, arranged by site and by distance from Hastière rockshelter; dating was conducted using Accelerated Mass Spectrometry (AMS) at Oxford University, UK (OxA) and the University of Groningen (GrA), and conventional methods at the University of Louvain, Belgium (Lv).

Collective burial	Sample number	Dates in years BP	Reference
Hastière M	AMS OxA-6558	4,345 ± 60[a]	Bronk-Ramsey et al. (2002)
Trou Garçon	AMS OxA-6853	4,220 ± 45[a]	Bronk-Ramsey et al. (2002)
Maurenne	AMS OxA-9025	4,635 ± 45[b]	Bronk-Ramsey et al. (2002)
Maurenne	AMS OxA-9026	4,160 ± 45[c]	Bronk-Ramsey et al. (2002)
Maurenne	Lv-1483	3,950 ± 70[c]	Toussaint (2007)
Maurenne	Lv-1482	3,830 ± 90[c]	Toussaint (2007)
Bois Madame	AMS OxA 10831	4,075 ± 38[c]	Dumbruch (2003)
Bois Madame	AMS OxA 10830	3,910 ± 40[c]	Dumbruch (2003)
Sclaigneaux	GrA-32975	4,155 ± 35[c]	De Paepe & Polet (2007)

[a] early/late Neolithic; [b] Middle Neolithic; [c] final/late Neolithic

ic, implying its use for more than 800 years (Vanderveken, 1997; Bronk-Ramsey et al., 2002; Toussaint, 2007).

The Maurenne burial is adjacent to Hastière rockshelter formation (see Figure 1). Two other collective burials at this site include Hastière M and Trou Garçon. Hastière M is one of the oldest Late Neolithic cave sites and dates to 4,345 ± 60 years BP, followed by Trou Garçon, which has yielded a date of 4,220 ± 45 years BP (Bronk-Ramsey et al., 2002; Toussaint, 2007). These two can be described as early/late Neolithic.

Two large, well-studied final/late Neolithic cave burials are Sclaigneaux and Bois Madame. Sclaigneaux is associated with a single radiocarbon date of 4,155 ± 35 years BP (De Paepe, 2007; De Paepe & Polet 2007). At Bois Madame in the Burnot Valley, two dates have been obtained. Both of these derive from the boundary of the fourth millennium prior to the Bronze Age, 4,075 ± 38 years BP and 3,910 ± 40 years BP, suggesting the collective burial of Bois Madame may have been utilized for more than 150 years (Bronk-Ramsey et al., 2002; Dumbruch, 2003, 2007).

Funerary context

Given the scarcity of habitation sites, these prehistoric peoples are primarily known from their remains in funerary caves and rockshelters. A range of burial practices has been inferred, including cremation, burial, a simple deposition of individuals on cave floors and cu-marks with flint implements. Comingled remains comprise a majority of the funerary deposits (Toussaint et al., 2001; Toussaint, 2007; Polet, 2011). At some caves, such as Bois Madame, the bones are found in a haphazard order as if the individuals were left unburied and later disturbed by human or non-anthropogenic agents (Dumbruch, 2003). The mixture of individuals within these collective burials could have arisen from bioturbation. However, the deliberate movement, occasional regrouping and comingling of bodies is more likely to be the result of burial rites, reburial and/or adding additional individuals (Toussaint et al., 2001; Toussaint, 2007).

Comparing individuals across cave burials

Although several well-preserved Late Neolithic crania are present, most individuals are represented by fragmentary gnathic remains with associated molars *in situ*, permitting an investigation of variation within and between sites in nonmetric dental trait expression using the Arizona State University Dental Anthropology System (ASUDAS) (Turner et al., 1991; Scott and Irish, 2017). Prior studies of the inhabitants of these Late Neolithic caves have found a lack of differentiation in diet (Garcia Martín, 1999; Semal et al., 1999), internment behavior (Vanderveken, 1997; Toussaint et al., 2001, 2003) and stature was estimated to be largely unimodal (Orban et al., 2000). However, chronological distinctions are apparent from radiocarbon dating. On the basis of chronology, we expect the early/late Neolithic sites to be more similar to each other in dental morphological expression than to the final/late cave burials, and vice versa. The three final/late Neolithic dates from Maurenne suggest this collective burial is more likely to resemble later sites than earlier ones.

It is also possible that differences in dental morphology will be patterned with respect to geography. Based on distance, individuals from Hastière rockshelter (Hastière M and Trou Garçon) and Maurenne should be more similar to one another, and secondarily to Bois Madame, whereas Sclaigneaux should be the most distinctive (see Figure 1).

Materials and Methods

A total of 127 individuals from the five caves were examined (Vanderveken, 1997; Toussaint et al.,

Table 2. Neolithic samples by cave, element, and number of individuals.

Neolithic cave site	Maxillae	Mandibles	Total
Hastière M	10	10	20
Trou Garçon	6	1	7
Maurenne	9	21	30
Bois Madame	13	15	28
Sclaigneaux	12	30	42
Total	50	77	127

2001; Dumbruch, 2003; De Paep, 2007; Toussaint, 2007; Williams and Polet, 2017; Table 2). Gnathic fragments were chosen on the basis of completeness and only relatively unworn crowns were examined. No isolated teeth were included to avoid errors in attribution. Given the lack of anterior teeth preserved *in situ*, and the inconsistent preservation of premolars, only molars were observed. Preference was given to young adults and subadults with relatively unworn cusps of permanent molars to increase the likelihood of accurate scoring, and included Smith (1984) wear stages 1 to 4. Individuals who exhibited substantial attrition, exceeding stage 4 (Smith, 1984), were excluded from the analysis (Turner et al., 1991; Scott and Irish, 2017).

Dental cast preparation

Dental casts were created from dental impressions of the original Neolithic material housed at the Royal Belgian Institute of Natural Sciences in Brussels. To create the dental molds, the dentition was cleaned and a thin layer of dental molding material, polyvinylsiloxane (President Jet Plus Regular Body, Coltène-Whaledent) was applied to the occlusal surface of the molars and allowed to air dry. Dental casts were created at Georgia State University by pouring centrifuged epoxy resin and hardener (Buehler) onto the dental impressions, which were placed into putty crucibles—stabilized with hardener (Buehler)—to catch the excess mixture. The casts dried for 24 hours before extraction.

Analysis

Dental morphology has been shown to be highly heritable (Turner et al., 1991; Scott and Turner, 1997; Irish, 2006; Hanihara, 2008; Scott and Irish, 2017; Scott et al., 2018). Dental casts, supplemented with photographic images, were scored by a single observer (RLG) to avoid issues of interobserver error (Turner and Scott, 1997; Hardin and Legge, 2013). Previously conducted intraobserver error analyses on 34 dental morphological traits found trait agreement at levels of 0.621 or above (McHugh, 2012). Since single-sided gnathic fragments were available for the great majority of the individuals, dental antimeres could not be examined to identify the maximum expression of any trait. It is possible that some of the maxillary and mandibular fragments belonged to the same individuals. However, given the preservation of the remains, pairing these elements was not possible. If some elements are indeed associated, then the total sample size of 127 would be smaller. Since 77 mandibular and 50 maxillary fragments are included, a potential minimum number of individuals (MNI) is 77 (Table 2). These associations are likely irrelevant in the current study as maxillary and mandibular molar traits are discussed separately

Another potential problem from the lack of matching elements might have arisen from inadvertently scoring antimeres from the same individual. However, this is unlikely for several reasons. First, only *in situ* molars rather than isolated elements were scored. Second, the range of dental attrition and dental ages suggests each gnathic fragment can be considered unique. Therefore, each fragment was treated as an individual (Hardin and Legge, 2013) as shown in Table 2, and the dental morphological traits were discussed independently. Score frequencies for each trait with respect to each cave site were calculated. Statistical analyses were not attempted due to the small and idiosyncratic sample sizes.

Results

All scores ascribed to individuals are presented in the context of the ASUDAS.

Maxillary molars

Metacone

For M^1, individuals from Hastière M and Trou Garçon often exhibit a metacone with a score of 4 (see Table 3). Fewer individuals have a larger metacone with a score of 5. In contrast, individuals from Maurenne and Bois Madame frequently present a metacone with a score of 5 and have a lower frequency of individuals with a score of 4. Sclaigneaux shows an equal prevalence of individuals with metacone scores of 4 and 5.

For the second molar (M^2), the dominant pattern across sites is a score of 3 or 4, though there is some variation in expression (Table 3). For instance, Hastière M and Trou Garçon are nearly divided equally between these two scores, whereas the final/late Neolithic burials present a greater tendency for a metacone with a score of 4. Individuals from Bois Madame show a greater range of expression in their metacone scores as they range from 2 to 5.

Although the sample size for M^3 is limited, the individual from Hastière M has a large metacone with a score of 5, whereas individuals from both Maurenne and Bois Madame exhibit a smaller cusp and have scores of 3. The other two sites are intermediate and have scores of 4 for the M^3 metacone (Table 3).

Table 3. Frequencies of maxillary traits.

Site	*n*	Trait & Tooth	Frequency of score							
			0	1	2	3	4	5	6	7
Hastière M	8	Metacone (M^1)					0.875	0.125		
Trou Garçon	5						0.800	0.200		
Sclaigneaux	10						0.500	0.500		
Maurenne	8						0.250	0.750		
Bois Madame	11						0.273	0.727		
Hastière M	5	Metacone (M^2)				0.600	0.400			
Trou Garçon	4					0.500	0.500			
Sclaigneaux	6					0.167	0.833			
Maurenne	3					0.333	0.667			
Bois Madame	8				0.125	0.125	0.375	0.375		
Hastière M	1	Metacone (M^3)						1.000		
Trou Garçon	2					0.500	0.500			
Sclaigneaux	3					0.333	0.667			
Maurenne	1					1.000				
Bois Madame	2					1.000				
Hastière M	7	Hypocone (M^1)					0.429	0.571		
Trou Garçon	4						0.500	0.500		
Sclaigneaux	10						0.400	0.600		
Maurenne	8						0.125	0.875		
Bois Madame	11					0.273	0.364	0.364		
Hastière M	6	Hypocone (M^2)			0.167	0.667	0.167			
Trou Garçon	2					1.000				
Sclaigneaux	4					0.500	0.500			
Maurenne	3				0.333		0.667			
Bois Madame	8				0.125	0.750	0.125			
Hastière M	1	Hypocone (M^3)				1.000				
Trou Garçon	1						1.000			
Sclaigneaux	3		0.333		0.333	0.333				
Maurenne	4						1.000			
Bois Madame	2			0.500		0.500				
Hastière M	5	Metaconule (M^1)	0.800		0.200					
Trou Garçon	3		0.667		0.333					
Sclaigneaux	8		1.000							
Maurenne	6		0.833	0.167						
Bois Madame	9		0.667		0.333					
Hastière M	8	Metaconule (M^2)	0.500	0.250	0.125	0.125				
Trou Garçon	4		0.500	0.250	0.250					
Sclaigneaux	4		1.000							
Maurenne	2		0.500	0.500						
Bois Madame	7		0.714	0.286						
Hastière M	1	Metaconule (M^3)	1.000							
Trou Garçon	2		0.500				0.500			
Sclaigneaux	2		1.000							
Maurenne	1		1.000							
Bois Madame	2		0.500	0.500						
Hastière M	3	Carabelli's Trait (M^1)	0.333	0.667						
Trou Garçon	2		0.500	0.500						
Sclaigneaux	3		0.333					0.333	0.333	
Maurenne	2		1.000							
Bois Madame	5				0.200	0.200	0.200	0.200		0.200
Hastière M	3	Carabelli's Trait (M^2)	1.000							
Trou Garçon	1		1.000							
Sclaigneaux	2			0.500		0.500				
Maurenne	3		1.000							
Bois Madame	2				0.500	0.500				
Hastière M	4	Parastyle (M^1)	1.000							
Trou Garçon	3		1.000							
Sclaigneaux	3		0.667			0.333				
Maurenne	2		1.000							
Bois Madame	8		1.000							
Hastière M	5	Parastyle (M^2)	1.000							
Trou Garçon	3		0.667	0.333						
Sclaigneaux	4		0.750		0.250					
Bois Madame	7		1.000							

Hypocone
The M^1 hypocone is primarily scored as a 4 or 5 nearly evenly across three of the sites (see Table 3). Most individuals from Maurenne, though, are scored as 5 and more than a quarter of the M^1 samples from Bois Madame (27.3%) exhibit a smaller hypocone and are characterized by scores of 3.

For M^2, the hypocone tends to be expressed most strongly at Maurenne and Sclaigneaux as most individuals at these sites have scores of 4. For Bois Madame and Hastière M, a smaller hypocone with a score of 3 is the most frequent expression, with considerable variation (see able 3).

The M^3 hypocone is variably expressed at Sclaigneaux and Bois Madame. In comparison, the M^3 hypocone is most frequently larger at Trou Garçon and Maurenne with scores of 4 (see Table 3).

Metaconule (Cusp 5)
The metaconule is absent at Sclaigneaux across the molars (see Table 3). This is not the case at the other sites with the exception of M^3 in which individuals from Hastière M and Maurenne also lack Cusp 5. For M^1, three individuals from Bois Madame present small metaconules with a score of 2. The early/late Neolithic cave burials of Hastière M and Trou Garçon both exhibit substantial variation in the expression of the metaconule across the molars (see Table 3). Variation at the early/late Neolithic sites is particularly marked for the M^2 at Hastière M where the expression of Cusp 5 ranges from absent in half of the individuals to moderately expressed with scores of 1-3 in the other half. Trou Garçon is mostly associated with scores of 1 and 2. Maurenne and Bois Madame are similar in their low to absent expression of the metaconule on M^2 and M^3 (Table 3). In contrast, a prominent metaconule is expressed on the M^3 of Hastière M 29, presenting a score of 5 (Figure 2).

Carabelli's trait
Carabelli's trait is relatively well represented across these Neolithic sites on M^1 and M^2 but is absent entirely on M^3 (see Table 3). However, there is considerable variation within and between burials (Figures 3 and 4). For M^1, Bois Madame exhibits the strongest expression of this trait, with one individual having a prominent Carabelli's cusp with a score of 7. Bois Madame present the greatest degree of variation, with expressions ranging from 2-5. One individual from Sclaigneaux has a large Carabelli's trait with a score of 5 and another is even larger with a score of 6 (Figure 4). In comparison, this trait on M^1 is expressed as a 1 or absent altogether at the early/late Neolithic sites of Hastière M and Trou Garçon (see Table 3).

For M^2, Hastière M and Trou Garçon C lack expressions of Carabelli's trait while the final/late sites of Sclaigneaux and Bois Madame show substantial variation ranging from scores 1-3 (see Table 3). Maurenne resembles the Hastière M and Trou Garçon, in lacking evidence of a Carabelli's trait on M^2 (see Table 3).

Parastyle
As at other locations worldwide (Scott et al. 2018), the expression of a parastyle is rarely observed in these Neolithic collective burials and is completely absent on M^3 (see Table 3). However, a large M^1 parastyle is scored as a 3 on Sclaigneaux 119. A smaller M^2 parastyle is scored as a 2 on Sclaigneaux 99. In addition, a limited expression of a parastyle is noted for one M^2 from Trou Garçon (I.G. 3873) characterized as a buccal pit (score of 1).

Mandibular molars
Anterior fovea
The anterior fovea on M_1 is most frequently expressed as a score of 1 across the cave burials when it is present (Table 4; Figure 5). There is one individual, Maurenne 92, who presents a larger anterior fovea with a score of 3.

Groove pattern
The groove pattern for M_1 is primarily the Y pattern, with the exception of one individual from Hastière M and another from Sclaigneaux that exhibit an X pattern. The near ubiquity of the Y pattern, particularly at the final/late Neolithic cave burials, is further evidenced by the relatively large number of individuals with this configuration. This includes all of the Maurenne (n = 12) and Bois Madame (n = 8) assemblages, and nine out of 10 individuals from Sclaigneaux (see Table 4).

The groove patterns for M_2 and M_3 are more variable (see Table 4). For M_2, the groove pattern for the early/late Neolithic cave burial of Trou Garçon presents as an X. Individuals from Hastière M most often exhibit the plus groove pattern with some expression of the Y pattern. At Maurenne, all three groove pattern variants are evident (see Table 4). For M_3, Hastière M 10 exhibits an X groove pattern, as do most individuals from Maurenne.

The final/late Neolithic sites exhibit more variability in groove patterning for both M_2 and M_3 than is observed for these teeth in the earlier cave burials. All three configurations are visible at Sclaigneaux, although the Y pattern is the least

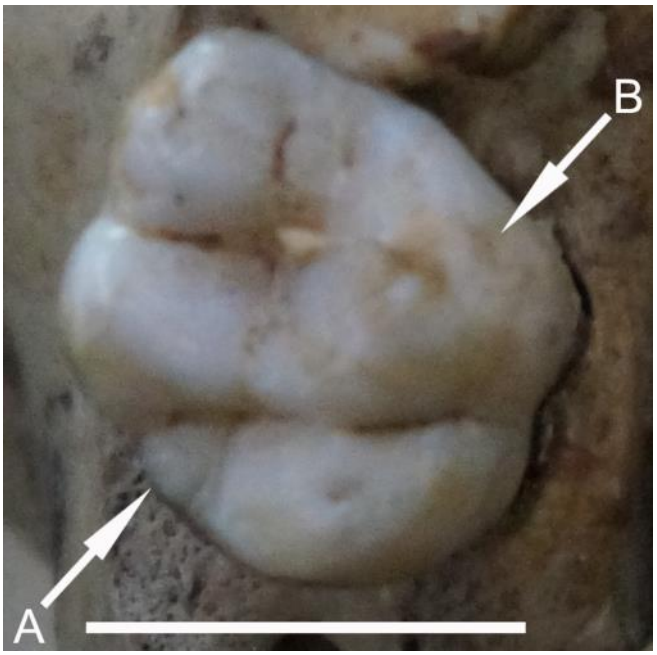

Figure 2. Hastière Trou Garçon C 20Z, a right M^1 shows (a) a large metaconule or Cusp 5 (ASUDAS score = 2) and (b) a pit form of Carabelli's trait (ASUDAS score = 1); scale bar = 1 cm.

Figure 3. Bois Madame, BM Mx 11, a right maxillary fragment, demonstrates a large Carabelli's trait (ASUDAS score = 7), identified by a white arrow on M^1; scale bar = 1 cm.

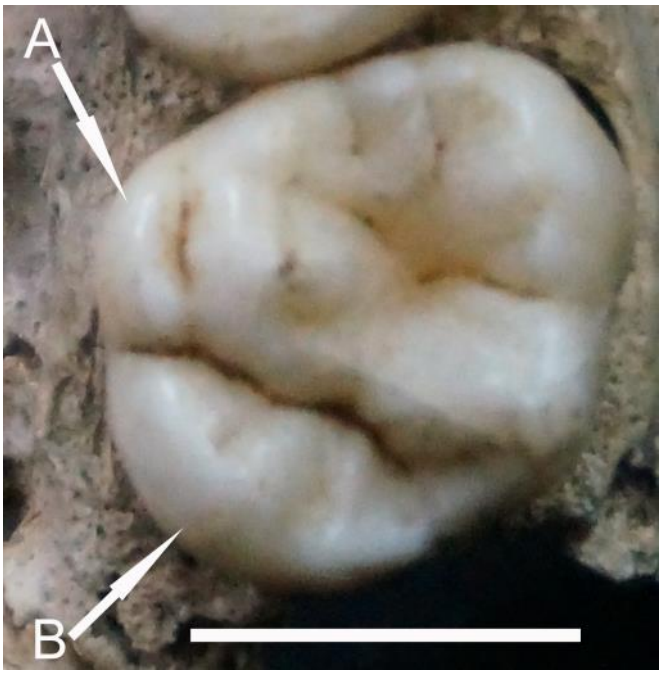

Figure 4**.** Sclaigneaux 119, a left M^1, exhibits (a) a pronounced Carabelli's cusp (ASUDAS score = 6), and (b) a large metacone (ASUDAS score = 4); scale bar = 1 cm.

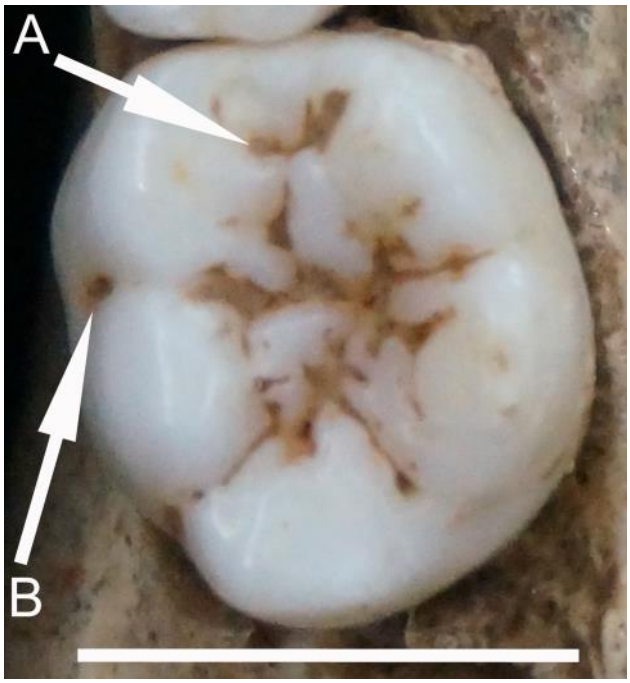

Figure 5. Bois Madame BM Md 32, a left M_1, shows (a) an anterior fovea (ASUDAS score = 1) and (b) a protostylid (ASUDAS score = 1), both of which are commonly found across cave sites; scale bar = 1 cm.

Table 4. Frequencies of mandibular traits.

			Frequency of score									
Site	***n***	**Trait & tooth**	**0**	**1**	**2**	**3**	**4**	**5**	**6**	**X**	**Y**	**+**
Hastière M	2	Anterior Fovea (M_1)		1.000								
Sclaigneaux	4		0.750	0.250								
Maurenne	8		0.625	0.250		0.125						
Bois Madame	4		0.500	0.500								
Hastière M	1	Groove Pattern (M_1)								1.000		
Sclaigneaux	10									0.100	0.900	
Maurenne	12										1.000	
Bois Madame	8										1.000	
Hastière M	4	Groove Pattern (M_2)									0.250	0.750
Trou Garçon	1									1.000		
Sclaigneaux	15									0.400	0.067	0.533
Maurenne	7									0.143	0.143	0.714
Bois Madame	8									0.375	0.250	0.375
Hastière M	1	Groove Pattern (M_3)								1.000		
Sclaigneaux	5									0.200	0.600	0.200
Maurenne	3									0.667		0.333
Bois Madame	2									0.500		0.500
Hastière M	4	Cusp Number (M_1)						0.750	0.250			
Sclaigneaux	11						0.091	0.727	0.182			
Maurenne	12						0.333	0.583	0.083			
Bois Madame	9							0.778	0.222			
Hastière M	5	Cusp Number (M_2)					0.600	0.400				
Trou Garçon	1						1.000					
Sclaigneaux	12						0.750	0.250				
Maurenne	8						1.000					
Bois Madame	7						0.714	0.286				
Hastière M	1	Cusp Number (M_3)					1.000					
Sclaigneaux	7						0.429	0.429	0.143			
Maurenne	3						1.000					
Bois Madame	2						0.500	0.500				
Hastière M	5	Mid-Trigonid Crest (M_2)	1.000									
Trou Garçon	1		1.000									
Sclaigneaux	12		0.917	0.083								
Maurenne	7		0.857	0.143								
Bois Madame	5		1.000									
Hastière M	1	Mid-Trigonid Crest (M_3)	1.000									
Sclaigneaux	9		0.889	0.111								
Maurenne	3		1.000									
Bois Madame	1		1.000									
Hastière M	5	Protostylid (M_1)	0.400	0.600								
Trou Garçon	1		1.000									
Sclaigneaux	10			1.000								
Maurenne	13		0.538	0.462								
Bois Madame	7		0.143	0.857								
Hastière M	4	Protostylid (M_2)	0.500	0.500								
Trou Garçon	1					1.000						
Sclaigneaux	9		0.222	0.778								
Maurenne	8		0.250	0.750								
Bois Madame	5		0.400	0.600								
Hastière M	1	Protostylid (M_3)	1.000									
Sclaigneaux	7		0.429	0.571								
Maurenne	2		0.500						0.500			
Bois Madame	1		1.000									
Hastière M	2	Hypoconulid (M_1)				0.500	0.400					
Sclaigneaux	11		0.091	0.091	0.182	0.091	0.091	0.455				
Maurenne	13		0.308			0.308	0.154	0.231				
Bois Madame	9					0.333	0.222	0.444				
Hastière M	5	Hypoconulid (M_2)	0.600	0.200		0.200						
Trou Garçon	1		1.000									
Sclaigneaux	13		0.769			0.154	0.077					
Maurenne	8		1.000									
Bois Madame	7		0.714	0.143				0.143				
Hastière M	1	Hypoconulid (M_3)	1.000									
Sclaigneaux	7		0.429	0.286			0.143	0.143				
Maurenne	3		1.000									
Bois Madame	2		0.500				0.500					
Hastière M	4	Entoconulid (M_1)	0.750		0.250							
Sclaigneaux	11		0.818	0.182								
Maurenne	12		0.917		0.083							
Bois Madame	9		0.778		0.111	0.111						
Hastière M	1	Entoconulid (M_3)	1.000									
Sclaigneaux	7		0.857		0.143							
Maurenne	3		1.000									
Bois Madame	2		1.000									

prevalent on M_2 and the most frequent expression on M_3 (see Table 4). All three groove patterns are present at Bois Madame for M_2 as they are at Sclaigneaux and Maurenne. However, only at Sclaigneaux are the three groove patterns present on M_3.

Cusp number

Only five or six cusps are observed on M_1 at the early/late Neolithic cave burial of Hastière M and the final/late site of Bois Madame, whereas Sclaigneaux and Maurenne both present 4-6 cusps. However, the predominant number is five cusps across the cave burials (see Table 4).

This pattern differs for M_2 in which four cusps is the most frequently observed. For the individuals from Maurenne (n = 8) and the individual from Trou Garçon, this is the only pattern observed for M_2. In comparison, there are some M_2 from Hastière M, Sclaigneaux and Bois Madame that present five cusps (see Table 4).

For M_3, there are primarily four cusps, with the exception of Maurenne and Sclaigneaux in which the expression of four and five cusps are equally represented (Table 4). Furthermore, at Sclaigneaux, more variation is observed for M_3 cusp number which includes the expression of four, five and six cusps.

Mid-trigonid crest

The mid-trigonid crest is eliminated for M_1 since no presence was recorded across sites for this molar. The mid-trigonid crest is also largely absent on M_2 and M_3 at these Neolithic cave burials. One exception is at Sclaigneaux where it is present, although rarely, on both M_2 and M_3. The only other site where a mid-trigonid crest is observable is at Maurenne and only the M_2 of Maurenne 18 (see Table 4).

Protostylid

A buccal pit (score of 1) is common at these Neolithic cave deposits and across the mandibular molar row (Figure 5). At Sclaigneaux, the buccal pit is found on all individuals examined (n = 10). Similarly, a buccal pit is more often present than absent on M_1 at Hastière M and Bois Madame. In contrast, at Maurenne a buccal pit on M_1 is more often absent than present; this feature is also absent in the single individual from Trou Garçon (Table 4).

On M_2, a buccal pit is visible at all sites and is more often expressed than not, particularly at Sclaigneaux and Maurenne (see Table 4). One exception is Trou Garçon 3, where a protostylid is scored as a 3.

Any variation of the protostylid is less frequently exhibited on M_3 than on the other molars. At Sclaigneaux, it is expressed as a buccal pit across the molar row. A much stronger expression of a protostylid is evidenced on one individual, Maurenne 15, where it is scored as a 6.

Hypoconulid (Cusp 5)

For M_1, Hastière M exhibits a moderate to large hypoconulid, expressed at scores of 3 and 4. Sclaigneaux presents the greatest degree of variation in the expression of the hypoconulid, ranging across the full spectrum of scores from 0-5, although the majority of individuals from this site are skewed towards the higher end of the scoring spectrum. This variation is similar at Bois Madame and Maurenne where the scores range from 0-5. However, most individuals from Bois Madame exhibit a larger hypoconulid with a correspondingly higher score and nearly a third of the individuals from Maurenne lack a cusp 5 entirely (see Table 4).

For M_2, the hypoconulid is more often absent than present across cave burials, and at Maurenne and Trou Garçon it is absent altogether. When it is expressed, the final/late Neolithic caves of Sclaigneaux and Bois Madame both show greater variation and the presence of a larger cusp 5. For example, when the hypoconulid is expressed at Hastière M, it ranges in score from 1-3. At the final/late Neolithic sites of Sclaigneaux and Bois Madame, a larger hypoconulid is evident, reflected in one individual from each site scoring a 4 and 5, respectively (see Table 4).

Like M_2, the variation in M_3 is more variable than observed in M_1, especially for the final/late Neolithic cave burials. The hypoconulid is completely absent in the one individual from Hastière M and the three individuals from Maurenne. In contrast, at the final/late Neolithic cave of Sclaigneaux, the greatest extent of variation is observed, with scores ranging from a low of 1 to a high of 5. Bois Madame has similar variability of expression of the hypoconulid, with scores extending from 0-4.

Entoconulid (Cusp 6)

An entoconulid is expressed on M_1 across the cave burials but at low frequencies. However, its expression varies. The most common expression of the entoconulid, or cusp 6, is a score of 2, as observed at Hastière M, Maurenne and Bois Mad-

ame. Sclaigneaux presents an entoconulid with a score of 1. At the other extreme is Bois Madame in which a larger entoconulid is scored as a 3. Thus, the final/late Neolithic caves of Sclaigneaux and Bois Madame are distinct in the expression of cusp 6 as compared to the other sites.

The entoconulid on M_2 was eliminated from the results because it is not observed across the sites. For M_3, the entoconulid is entirely absent with the exception of Sclaigneaux. This final/late Neolithic cave burial presents one individual (Sclaigneaux 19) out of seven with an entoconulid on M_3 that is scored as a 2.

Metaconulid (Cusp 7)
Frequencies for the metaconulid (Cusp 7) are excluded since only a single tooth fully expressed this trait in the available Neolithic sample, the left M_1 of Boise Madame BM Md 13 (Figure 6).

Discussion
Based on an earlier study of deciduous molar morphology (Williams et al., 2018), it was predicted that the early/late Neolithic cave burial of Hastière M would be distinctive and should differ from the final/late sites of Sclaigneaux and Bois Madame. Although this prediction was confirmed for some traits, the deciduous molar morphology of Hastière M is more distinctive compared to the permanent molars. The observation that deciduous molars are better at identifying relatedness (Paul and Stojanowski, 2017) may also apply to these Neolithic cave burials.

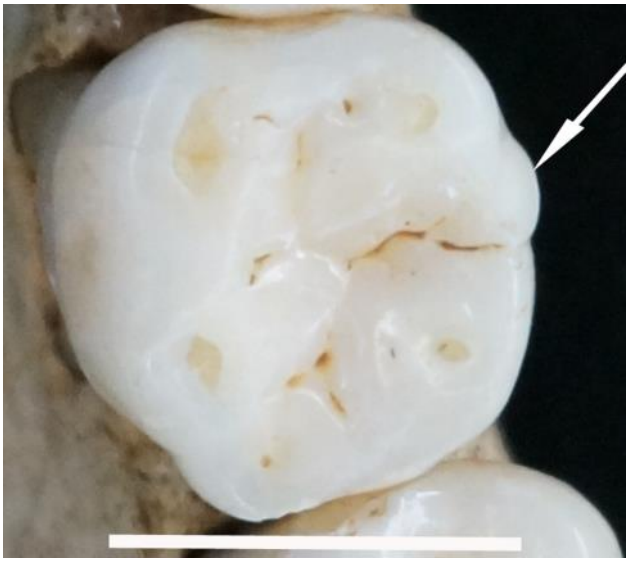

Figure 6. Left mandibular fragment of BM Md 13, presents the only fully expressed metaconulid (Cusp 7) observed (ASUDAS score = 2), demarcated by the white arrow on M_1; scale bar = 1 cm.

It was also anticipated that Sclaigneaux—situated about 35 km from the Hastière rockshelter—would be distinct if differences in morphology can be explained by geographic distance (Figure 1). Sclaigneaux does differ from the other cave burials in some respects, for example, showing the Y groove pattern for M^2. However, like the other final/late Neolithic site of Bois Madame, Sclaigneaux is quite variable in the expression of traits. These findings suggest variability is more pronounced in the final/late than the early/late Neolithic. The final/late Neolithic sites exhibit greater variation in the expression of traits, particularly the hypoconulid, protostylid, parastyle and Carabelli's trait across the molar row. However, the sample sizes are also substantially larger at the final/late Neolithic sites. This is particularly true of Sclaigneaux. It is unknown the extent to which the uneven sample sizes influenced the results.

It was expected that the two early/late Neolithic cave burials of Hastière M and Trou Garçon should resemble one another as they are similar chronologically and geographically. Yet there is no convincing evidence that they are similar. In fact, it appears that Trou Garçon resembles the final/late Neolithic sites of Bois Madame and secondarily Maurenne more than these individuals resemble Hastière M. Trou Garçon has a greater number of whole crania available but is represented by a smaller number of individuals compared to the other sites (Table 2). The limited sample size for Trou Garçon precludes definitive statements on its relationship to the other cave burials. However, Trou Garçon individuals are at times extreme in the expression of traits which separates this site from the others, such as a large protostylid on M_2 in Trou Garçon 3. Meanwhile, Hastière M is an outlier in other ways, such as the pronounced metaconule on M^3 in Hastière M 29.

The prediction that Maurenne would resemble the final/late Neolithic sites of Sclaigneaux and Bois Madame more than Hastière M was largely confirmed by the results. For this reason, it is more likely that the individuals buried at Maurenne are primarily associated with the three final/late Neolithic radiocarbon dates. The single Middle Neolithic date obtained from Maurenne may be an exception. Supporting this assertion is the observation of similarities between Maurenne and Bois Madame. Three of the dates for the former and the two dates for the latter overlap one another and the two burial chambers are about 10 km from one another suggesting, perhaps, closer contact existed between these two groups than between the earlier

and the more geographically distant individuals living close to Sclaigneaux cave.

There are also similarities between the caves, such as the large prevalence of a protostylid and Carabelli's trait, and the near absence of a metaconulid. There are most frequently five cusps on M_1 but often four on M_2 and M_3. The lack of discrete differences in these Belgian Neolithic caves is supported by archaeological evidence that suggests common lifeways, an undifferentiated economy and phenotypic homogeneity. Carbon and nitrogen isotopes imply similarities in diet across the Late Neolithic period in which terrestrial resources were relied upon more than aquatic ones (Semal et al., 1999). The dental microwear of several Late Neolithic caves suggests similarities in diet which comprised a large amount of vegetable fiber (Garcia-Martín, 2000), but fish may have also been consumed (Toussaint et al., 2001). Stature regression formulae from available Neolithic long bones and the first metatarsal indicate that most of the individuals were of short stature. It is also possible that the majority of the long bones come from a single sex (female) as the sample lacks a bimodal distribution of values typical of recent Belgians of both sexes (Orban et al., 2000).

Comparison with other prehistoric burials

A number of studies have been conducted using dental morphology as a proxy for affinity at Neolithic and other prehistoric sites. Studies of kinship within and across burials and cemeteries rely on phenotypic similarity as a proxy for genetic relationships and rare traits are often utilized to identify familial relations (Bentley, 1991; Howell and Kintigh, 1996; Alt et al., 1997; Jacobi, 1997; Corruccini and Shimada, 2002; Stojanowski & Schillaci, 2006; Pilloud, 2009; Lukacs & Pal, 2013). Familial, and possibly sibling relations among a triple burial at Dolní Věstonice from the Upper Paleolithic of the Czech Republic were evidenced by a sharing of groove pattern, number of cusps, accessory cusps and the presence of an entoconulid and parastyle for at least two of the three individual for each trait (Alt et al., 1997). The Neolithic cave burials of Belgium probably do not represent individuals from the same family as noted at Dolní Věstonice. In fact, it appears that there is a greater degree of variation within the Belgian Meuse Neolithic burials than between them.

Dental traits of early Neolithic Mediterranean sites

The dental morphology of several burial sites in the Mediterranean region have been explored. For example, at early Neolithic Çatalhöyük in Turkey, the protostylid, Carabelli's cusp, groove pattern, the hypoconulid, entoconulid, hypocone and deflecting wrinkle are significantly different from expected (Pilloud, 2009; Pilloud and Larsen, 2011). Iberian and Italian Neolithic burials differ in Carabelli's trait and the protostylid among other dental traits (López-Onaindia & Subirà, 2017). The protostylid on M_2 and M_3, the hypoconulid of M_1 and M_2, and the entoconulid on M_2 and to a lesser extent, groove pattern and cusp number on M_2, are suggested to be the most informative in separating Iberian from Italian Neolithic burials (López-Onaindia et al., 2018). The Neolithic cave burials of Belgium exhibit substantial variation in all of these traits, particularly the size of the hypocone and the expression of Carabelli's trait, and remarkable uniformity in the presence of a protostylid.

Dental morphology of Late Neolithic cave burials of Eurasia

Numerous Late Neolithic collective burials exist across Eurasia, such as the Late Neolithic-Chalcolithic collective tombs of Catalonia in which natural crevices and recesses include adults of both sexes and all ages with few grave goods (López-Onaindia et al., 2018). However, the dental morphology of only a few Late Neolithic sites have been studied in detail. An important exception concerns those surrounding Lake Baikal, Siberia where an increasingly greater percentage of Carabelli's trait occurs during the Neolithic period (Waters-Rist et al., 2016). Compared to the Late Neolithic collective burials of Belgium, a lower expression of this trait is observed and only at Bois Madame and Sclaigneaux is a large Carabelli's cusp evident (Table 3). Hastiére M and Bois Madame have higher frequencies of a Y groove pattern on M_2 (0.250) compared to those observed in Late Neolithic Siberians (0.140) (Waters-Rist et al., 2016), although Sclaigneaux has a much lower value of 0.067 (see Table 4). For cusp number of M_2, 71.4% of the Siberian Late Neolithic peoples of Lake Baikal exhibit 5+ cusps whereas the Late Neolithic burials from Belgium can be characterized as expressing fewer cusps on the second mandibular molar. In fact, mostly only four cusps are observed on M_2. However, Hastiére M, and to a lesser extent, Bois Madame and Sclaigneaux, show some expression of five cusps on M_2, ranging from 0.400 to 0.250 (see Table 4). Expression of a protostylid on M_1 is present in half of Late Neolithic peoples of Lake Baikal, Siberia (Waters-Rist et al., 2016), whereas for this temporal period in the Meuse Riv-

er basin of Belgium is it present more often than it is absent, and at Sclaigneaux it is observed in 100% of individuals (n = 10) (Table 4). More than a quarter of individuals (27%) of the Late Neolithic of Siberia exhibit an entoconulid (Cusp 6) on M_1 (Waters-Rist et al., 2016). Comparable frequencies for the collective burials of Late Neolithic Belgium for this trait exist at Hastiére M and to a lesser extent, Bois Madame (Table 4). Unlike their counterparts to the east who exhibit a low occurrence of a metaconulid (Cusp 7) on M_1 at 6.5% (Waters-Rist et al., 2016), at the Late Neolithic caves of Belgium, it is nearly absent with the exception of BM Md 13 from Bois Madame (Figure 6).

Conclusions

The five well-studied collective burials examined are somewhat discrete in terms of chronology based on radiocarbon dates. Although only limited samples are available for each cave burial, it appears that our predictions were confirmed. Hastière M is only partly distinct from the other cave deposits in the expression of traits, corroborating an analysis of deciduous molar morphology from the Late Neolithic caves of the Belgian Meuse basin (Williams et al., 2018). The final/late collective burials of Sclaigneaux and Bois Madame exhibit a greater range of expression of the hypoconulid, entoconulid, protostylid, Carabelli's cusp, metacone and metaconulid. Although differences between the final/late Neolithic cave burials of Sclaigneaux and Bois Madame and the others from Hastière rockshelter are evidenced by dental morphology, these sites likely represent ephemeral communities that experienced only limited continuity over time and were perhaps bounded as a function of distance, and to a lesser degree, by chronology. Alternatively, this lack of partitioning of discrete dental traits per burial location may signal that internment was not strictly kin-based as is observed at Neolithic Çatalhöyük (Pilloud & Larsen, 2011), though larger sample sizes to conduct statistical analyses would be necessary for an investigation into potential kin relations based on dental morphology. In this study, the very low frequencies of a metaconulid and the mid-trigonal crest characterize the burials. Furthermore, the expression of Carabelli's cusp on M^1 and M^2 joins Sclaigneaux and Bois Madame and secondarily Hastiére M and Trou Garçon. The greater degree of variation observed for the final/late Neolithic cave burials of Sclaigneaux and Bois Madame may have been the result of a slow but steady influx of peoples, perhaps along waterways, from other locations as a prelude to the population restructuring that occurred concomitantly with the onset of the Bronze Age. This seems to be the case at other locations in Eurasia (Subirà et al., 2014; Waters-Rist et al., 2016; López-Onaindia et al., 2018).

Acknowledgments

Permission to examine these Neolithic remains in Belgium was kindly provided by Patrick Semal, Chief of the Scientific Heritage Service, Royal Belgian Institute of Natural Sciences. Many thanks to William Anderson and Laura Aday for assisting in the creation of the epoxy resin dental casts. At the Royal Belgian Institute of Natural Sciences, we thank Caroline Polet for generously assisting with the Neolithic collections, and Laurence Cammaert who skillfully created the topographical map of Belgium featured in Figure 1, which we use with permission. We thank Marin Pilloud and the anonymous reviewers for valuable comments that significantly improved the manuscript. Support for this research was provided by Fulbright-Belgium and the Commission for Educational Exchange between the USA, Belgium, and Luxembourg.

REFERENCES

Alt, K. W., Pichler, S., Vach, W., Klima, B., Vlček, E. & Sedlmeier, J. (1997). Twenty-five thousand-year-old triple burial from Dolní Věstonice: an Ice-Age family? *American Journal of Physical Anthropology, 102*, 123-131.

Bailey, S. E. (2008). Inter- and intra-specific variation in *Pan* tooth crown morphology: implications for Neandertal taxonomy. In J. D. Irish & G. C. Nelson (Eds.), *Technique and application in dental anthropology* (pp. 293-316). Cambridge, U.K.: Cambridge University Press.

Bentley, G. R. (1991). A bioarchaeological reconstruction of the social and kinship systems at early Bronze Age Bab Edh-Dhra', Jordan. In S. A. Gregg (Ed.), *Between bands and states* (pp. 5-34). Carbondale: Center for Archaeological Investigations, Southern Illinois University at Carbondale Occasional Paper No.9.

Bronk-Ramsey, C., Higham, T. F. G., Owen, D. C., Pike, W. G. & Hedges, R. E. M. (2002). Radiocarbon dates from the Oxford AMS system: datelist 31. *Archaeometry, 44*(3) Supplement 1, 1-149.

Corruccini, R. S. & Shimada, I. (2002). Dental relatedness corresponding to mortuary patterning at Huaca Loro, Peru. *American Journal of Physical Anthropology, 117*, 118-121.

De Paepe, M. (2007). Studie van de laat-

neolithische menselijke resten uit een collectief graf te Sclaigneaux (provincie Namen, B.). MA thesis, Universiteit Gent.

De Paepe, M. & Polet, C. (2007). 'Numerous and tall': A revision of the Late Neolithic human remains found in a collective burial site at Claigneaux (prov. Namr), Belgium. *Notæ Præhistoricæ, 27*, 163-168.

Dumbruch, I. (2003). *Edute du site de l'abri-sous-roche du "Bois-Madame", Néolithique, à Arbre, dans la vallée du Burnot (Province de Namur). Etude anthropologique et archéologique, Volume I et II*. MA thesis, Université Libre de Bruxelles.

Dumbruch, I. (2007). Le Site de l'Abri-sous-Roche du "Bois-Madame" à Arbre (Province de Namur, Belgique). *Archæologia Mosellana, 7*, 609-612.

García-Martín, C. (2000). *Reconstitution du régime alimentaire par l'étude des micro-traces d'usure dentaire.* Master Européen en Anthropologie, Université Libre de Bruxelles.

Hardin, A. M. & Legge, S. S. (2013). Geographic variation in nonmetric dental traits of the deciduous molars of *Pan* and *Gorilla*. *International Journal of Primatology, 34*, 1000-1019.

Howell, T. L. & Kintigh, K. W. (1996). Archaeological identification of kin groups using mortuary and biological data: an example from the American Southwest. *American Antiquity, 61*, 537-554.

Irish, J. D. (2006). Who were the ancient Egyptians? Dental affinities among Neolithic through postdynastic peoples. *American Journal of Physical Anthropology, 22*, 529-543.

Jacobi, K. P. (1997). Dental genetic structuring of a colonial Maya cemetery, Tipu, Belize. In S. L. Whittington & D. M. Reed (Eds.), *Bones of the Maya: studies of ancient skeletons* (pp. 138-153). Washington: Smithsonian Institution Press.

López-Onaindia, D. & Subirà, M. E. (2017). Prehistoric funerary complexity in northern Iberia studied using dental morphology. *Homo: Journal of Comparative Human Biology, 68*, 122-133.

López-Onaindia, D., Coca, M., Gibaja, J. F. & Subirà, M. E. (2018). Biological differences related to cultural variability during the Neolithic in a micro-geographical area of the Iberian Peninsula. *Archaeological and Anthropological Sciences, 10*, 1957-1969.

Lukacs, J. R. & Pal, J. N. (2013). Dental morphology of early Holocene foragers of North India: non-metric trait frequencies and biological affinities. *Homo: Journal of Comparative Human Biology, 64*, 411-436.

McHugh, M. L. (2012). Interrater reliability: the kappa statistic. *Biochemica Medica* 22, 276-282.

Orban, R., Polet, C., Semal, P. & Leguebe, A. (2000). La stature des Néolithiques mosans. *Bulletin de l'Institut Royal des Sciences Naturelles de Belgique-Sciences de la Terre,* 70, 207-222.

Pilloud, M. A. (2009). *Community structure at Neolithic Çatalhöyük: biological distance analysis of household, neighborhood, and settlement*. Ph.D. dissertation. The Ohio State University.

Pilloud, M. A. & Larsen, C. S. (2011). "Official" and "practical" kin: inferring social and community structure from dental phenotype at Neolithic Çatalhöyük, Turkey. *American Journal of Physical Anthropology, 145*, 519-530.

Polet, C. (2011). Les squelettes néolithiques découverts dans les grottes du basin mosan. In N. Cauwe, A. Hauzeur, I. Jadin, C. Polet & B. Vanmontfort (Eds.), *5200-2000 av. J.- C. Premiers Agriculteurs en Belgique* (pp. 85-94). Éditions du Cedarc.

Scott, G. R. & Turner, C. G., II (1997). *The anthropology of modern human teeth: dental morphology and its variation in recent human populations.* Cambridge, U.K.: Cambridge University Press.

Scott, G. R., Turner, C. G., II, Townsend, G. C. & Martinón-Torres, M. (2018). *The anthropology of modern human teeth: dental morphology and its variation in recent and fossil Homo sapiens*, 2nd ed. Cambridge, U.K.: Cambridge University Press.

Semal, P., García Martín, C., Polet, C. & Richards, M. P. (1999). Considération sur l'alimentation des Néolithiques du Bassin mosan: usures dentaires et analyses isotopiques du collagène osseux. *Notæ Præhistoricæ, 19*, 127-135.

Smith, B. H. (1984). Patterns of molar wear in hunter-gatherers and agriculturalists. *American Journal of Physical Anthropology, 63*, 39-56.

Stojanowski, C. M., & Schillaci, M. A. (2006). Phenotypic approaches for understanding patterns of intracemetery biological variation. *Yearbook of Physical Anthropology, 49*, 49-88.

Subirà, M. E., López-Onaindia, D. & Yll, R. (2014). Cultural changes in funeral rites during the Neolithic in the northeast of the Iberian Peninsula? The Cave of Pantà de Foix (Barcelona). *International Journal of Osteoarchaeology, 26*, 104-113.

Toussaint, M. (2007). Les sépultures Néolithiques du basin mosan Wallon et leurs relations avec les bassins de la Seine et du Rhin. *Archaeologia Mosellana, 7*, 507-549.

Toussaint, M., Orban, R., Polet, C., Semal, P., Bocherens, H., Masy, P. & García Martín, C. (2001). Apports récents sur l'anthropologie des Mésolithiques et des Néolithiques mosans. *Anthropologica et Præhistorica, 112*, 91-105.

Toussaint, M., Lacroix, P., Lambermont, S., Lemarie, J. -F., Bruzzese, L. & Beaujean, J. –F. (2003). La sépulture d'enfant néolithique des nouveaux réseaux du Trou du Moulin, à Goyet (Gesves, province de Namur). *Anthropologica et Præhistorica, 116*, 179-210.

Turner, C. G., II, Nichol, C. & Scott, G. R. (1991). Scoring procedures for key morphological traits of the permanent dentition: the Arizona State University dental anthropology system. In M. A. Kelley & C. S. Larsen (Eds.), *Advances in dental anthropology* (pp. 13–31). New York: Wiley-Liss.

Vanderveken, S. (1997). Etude anthropologique des sépultures néolithiques de Maurenne et Hastière (province de Namur). MA thesis, Université Libre de Bruxelles.

Vanderveken, S. (2007). Les ossements humans néolithiques de Maurenne et Hastière (Province de Namur). *Notæ Præhistoricæ, 17*, 177-184.

Waters-Rist, A., Bazaliiskii, V. I., Goriunova, O. I., Weber, A. W. & Katzenberg, M. A. (2016). Evaluating the biological discontinuity hypothesis of Cis-Baikal Early versus Late Neolithic-Early Bronze Age populations using dental nonmetric traits. *Quaternary International, 405*, 122-133.

Williams, F. L., George, R. L. & Polet, C. (2018). Deciduous molar morphology from the Neolithic caves of the Meuse River Basin, Belgium. *Dental Anthropology, 31*, 18-26.

A Morphofunctional Hypothesis for Selection on EDAR V370A and Associated Elements of Sinodonty

Robert Dudley[1,2 *]

[1] University of California, Berkeley
[2] Smithsonian Tropical Research Institute

Keywords: agriculture, China, diet, EDAR V370A, shoveling

ABSTRACT The phenomenon of Sinodonty refers to a suite of dental characters shared between East Asian and Native American populations, and most prominently to the presence of shoveled incisors. Although this syndrome is a conspicuous aspect of dental differentiation among extant human populations, elements of which have been recent subject of detailed genetic analysis, adaptive consequences of shoveled incisors and related features remain unclear. Here, I hypothesize that many of the associated differences in dentition (along with reduction in mandibular length and increases in salivary gland branching) arose in parallel with the opportunistic consumption of wild rice and millet in central and northern China, respectively, and with their subsequent domestication in the Upper Paleolithic. More efficient mastication and digestion of plant grains (and of other starchy foods obtained via broad-spectrum foraging) would potentially have been enabled by these traits, yielding greater rates of nutritional intake as wild crops were progressively domesticated. This functional hypothesis, although not mutually exclusive relative to other proposed selective factors, matches the estimated timeline in China for both origin and time to fixation of the associated allele (EDAR V370A), and is consistent with chronic energetic gain and fitness benefits independent of any assumptions for concurrent climatic conditions.

Lingually shoveled incisors, an anatomical feature first described by Hrdlička (1920, 1921), are a salient characteristic of the phenomenon now termed Sinodonty, a suite of dental characters common between Native American and East Asian populations, but occurring at much lower frequencies in non-Sinodont populations (Turner, 1971, 1976, 1986, 1990; see also Mizoguchi, 1985; Scott & Turner, 1988; Stojanowski et al., 2013; Scott et al., 2018). This disjunct geographical distribution has historically provided strong indirect support for hypothesized Old World origins of New World human populations (e.g., Turner & Bird, 1981). Anatomically, the condition of Sinodonty refers primarily to the presence of posteriorly shoveled incisors, single-rooted upper premolars, and three-rooted lower molars, and is strongly heritable (Hanihara et al., 1974; Blanco and Chakraborty, 1976), but is also likely to be polygenic in origin. Genetically, presence of the allele EDAR V370A significantly influences the condition of incisor shoveling along with a variety of other ectodermic features, including increased thickness of scalp hairs (see Bryk et al., 2008; Fujimoto et al., 2008; Chang et al., 2009; Kimura et al., 2009). Increased tooth crown size also associates with EDAR V370 (Kimura et al., 2009; Park et al., 2012), and its greater expression in mice furthermore reduces mandibular length (Adhikari et al., 2016). Pleiotropic effects of this allele are thus substantial.

Positive selection on EDAR V370A has been intense in humans, consistent with its very high frequencies in East Asian and Native American populations relative to other groups (see Sabeti et al., 2007; Bryk et al., 2008; Kamberov et al., 2013; Hlusko et al., 2018). Demic modelling based on extant frequencies of EDAR V370A in primarily Asian populations (Kamberov et al., 2013) indicates geographical origins of the allele in central and north China, within a region broadly congruent with the extensive alluvial plains of the Yellow, Huai, and

*Correspondence to:
Robert Dudley
Department of Integrative Biology
University of California, Berkeley;
Smithsonian Tropical Research Institute
Balboa, Republic of Panama
wings@berkeley.edu

Yangtzi (Changjiang) Rivers. This demic model also places time of origination for the allele between ~40,000 and ~13,000 years BP, with a modal value of 35,300 years BP. A parallel approach to allele age using maximum likelihood estimation for data from modern Han Chinese places origination between ~38,000 and ~35,000 years BP (see Kamberov et al., 2013). Finally, the modal value for fixation time of EDAR V370A has been estimated (using haplotype data from 23 individuals of Chinese descent) as 10,740 years BP (Bryk et al., 2008). These estimates for origination and fixation of EDAR V370A within East Asia are recent relative to the age of our species, and are also suggestive of powerful selective forces at play over a short time interval.

Because scalp hair density is increased by EDAR V370A, various authors have suggested that thermoregulatory and water balance would be influenced by this morphological change, particularly in the cooler and drier climates of the Upper Paleolithic (see Yuan et al., 2004; Chang et al., 2009). An alternative hypothesis links increased eccrine (sweat) gland density to greater evaporative heat loss in a humid monsoonal climate (Kamberov, et al., 2013). Mammary duct density also increases in the presence of EDAR V370A, raising the possibility of enhanced maternal milk delivery and associated fitness benefits (Hlusko et al., 2018). Concomitant changes in dentition may thus have derived pleiotropically from selection on other traits.

However, Sinodonty by definition refers to tooth anatomy, which broadly reflects diet in mammals (Ungar, 2010; Pineda-Munoz et al., 2017). It is therefore parsimonious to consider dietary shifts concurrent with the rise of EDAR V370A and associated elements of Sinodonty that may have been the target of natural selection. In particular, the timeline for fixation of this allele, along with its inferred geographical region of origin, correspond well to archaeological data that indicate foraging of wild rice and millet in China, along with their subsequent domestication. The origins of prominent features of Sinodonty, in other words, correlate temporally with a major dietary shift associated with the emergence of cultivated crops in East Asia. I hypothesize that this specialized human dentition, along with other related phenotypic effects of EDAR V370A, were advantageous for the mastication and subsequent digestion of sympatric wild grains, and thus yielded energetic advantage during the extended process of crop domestication.

Timeline for rice and millet domestication in China

Domesticated rice in East Asia refers to a single subspecies (*Oryza rufipogon* ssp. *japonica*) derived from a wild ancestor, whereas millet refers to two species domesticated from different grass genera (broomcorn millet: *Panicum miliaceum*; foxtail millet: *Setaria italica*). Phylogenetic reconstruction places rice domestication in China at ~13,500–8200 BP (Molina et al., 2011), a range congruent with corroborative archeological evidence (see Liu et al., 2007; Gross & Zhao, 2014). Similarly, archeological finds are consistent with the domestication and cultivation of millet nearly 10,000 years ago (Lu et al., 2009; Yang et al., 2012; Bestel et al., 2014).

Foraging on wild grains would have necessarily preceded their domestication. For example, processing with grinding stones of wild grass seeds (including possibly ancestral millets) occurred as early as ~24,000 years BP (see Liu et al., 2013; Liu et al. 2018). The oldest known sites for pottery in China date to ~20,000–10,000 years BP, possibly marking the emergence of agriculture (see Wang & Sebillaud, 2019). Starchy foods more generally became increasingly prevalent through the Upper Paleolithic in China, as suggested by increased usage of nuts, beans, and tubers (see Liu et al., 2013). Archeological records cannot capture in detail the spectrum of foraging and cultivation behaviors carried out over millennia, and across a geographical mosiac, during the process of crop domestication (see Fuller et al., 2014; Larson et al., 2014). Nonetheless, the overlap between estimated timelines for the origin and fixation of EDAR V370A, and for the domestication of rice and millet, is substantial (Figure 1).

Functional consequences of Sinodonty

Shoveled incisors and related features of Sinodonty may influence chewing dynamics and masticatory efficiency. It has long been suggested that shoveling increases tooth strength and resistance to bending (see Hrdlička, 1921; Dahlberg, 1963). Specific effects of incisor shoveling and changes in premolar and molar root numbers are unknown for mastication, which is associated with diverse features of jaw kinematics (see Ross et al., 2012). Also relevant is the substantial reduction in mandibular length associated with expression of the EDAR allele (by 5–10% in mice; see Adhikari et al., 2016). In human agriculturalists, mandible dimensions are reduced relative to non-agricultural populations, consistent with relaxation of masticatory demand (see von Cramon-Taubadel, 2011; Noback &

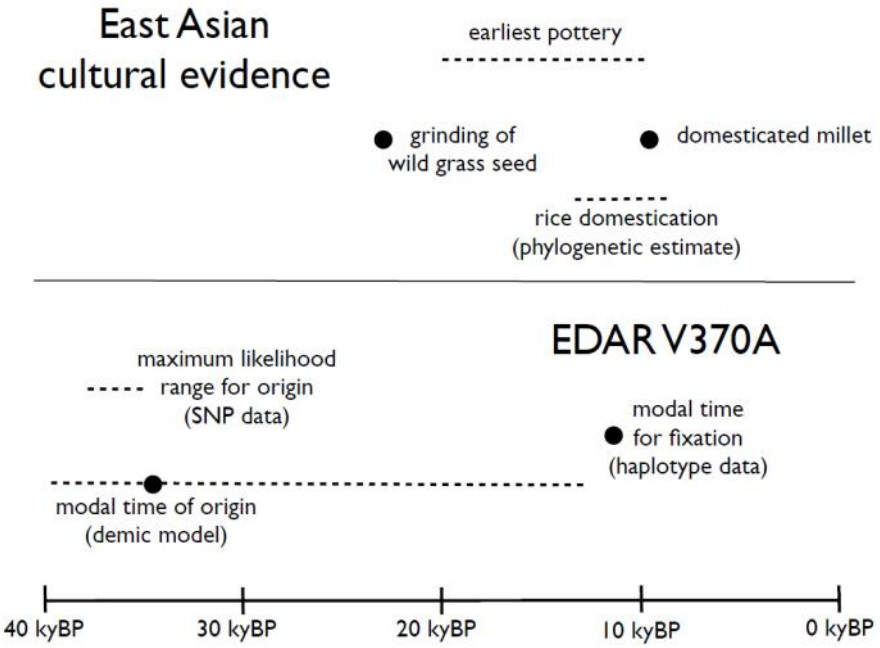

Figure 1. Timelines for estimated origin and fixation of EDAR V370A, and for relevant archaeological data and estimates of crop domestication. Dashed lines indicate approximate temporal ranges; see text for details and relevant citations.

Harvati, 2015; Katz et al., 2017). Paleontological data are not available to document the tempo of mandibular reduction across the rice and millet domestication sequence in East Asia, but a causal link with EDAR V370A cannot be excluded.

Interestingly, another consequence of enhanced EDAR expression in mice is to increase branching of adult salivary glands (by ~25%; Chang et al., 2009), which may in turn increase rates of saliva production and thereby facilitate starch digestion in the mouth (Valdez & Fox, 1991). This mechanism would provide a direct linkage between anatomical changes associated with EDAR V370A expression in humans, and advantageous physiological outcome as starchy crops were domesticated. An analogous argument was advanced by Hlusko et al. (2018) relative to increases in mammary duct density and lactation; such effects on gland density could moreover be complementary in some contexts (e.g., greater energy uptake would enable increased milk production), and would pertain independently of any specific climatic conditions. Pleiotropic changes in teeth, mandibular bone, and salivary gland density resulting from EDAR V370A can therefore influence human nutritional physiology in diverse ways.

Discussion and Conclusions

Various alleles alternative to EDAR V370A may contribute to tooth shoveling and other features characteristic of Sinodonty, and do not necessarily correspond to specific dietary adaptations. Prominent incisor shoveling in Neanderthals, for example, well precedes the origin of EDAR V370A, and does not associate with increased masticatory stresses (Clement et al., 2012). Similarly, a 3-rooted lower second molar has been described from a Denisovan mandible from western China, dated at ~160,000 BP (Bailey et al., 2019), although identification of this tooth has been challenged (see Scott et al., 2020; Bailey et al., 2020). The age of this specimen nonetheless well precedes the 38,000–35,000 BP estimated origination time for EDAR V370A (see Kamberov et al., 2013), and its features presumably derive from different genetic origins. Incisor shoveling in Native Americans likely derives genetically from their Eurasian source populations in northeastern Siberia (see Flegontov et al., 2019; Mathieson, 2020), but the oldest known human dentition from this latter region (~31,000 BP) is unfortunately incomplete with unknown occurrence of Sinodonty (see Sikora et al., 2019). The increased incidence of shoveling in Down syndrome

(see Cohen et al., 1970) is not yet characterized at the allelic level. Finally, an additional EDAR variant is found in south China and southeast Asia, but has not apparently been the target of positive selection (Riddell et al., 2020).

A pressing empirical need to evaluate any functional hypothesis relating to Sinodonty and to effects of EDAR V370A is to obtain a quantitative assessment of tooth and mandibular variation through time in East Asia. Changes in dentition and mandibular dimensions across the Paleolithic in China are not currently available, although there was a substantial reduction in mandibular dimensions from the Neolithic through the Bronze Age (Li et al., 2012). Incisor shoveling incidence in western European populations (which is low relative to that found in East Asia) has declined since the Neolithic (Brabant, 1971), a trend which may derive from genetic drift. Quantitative measurements of tooth morphology (e.g., Carayon et al., 2018) would enable better characterization of the shoveling phenotype and associated variation through time and among human populations, along with finite-element modeling of tooth bending mechanics. Similarly, consequences of changes in mandibular geometry can be inferred from mechanical modeling, although functional outcomes can be complex and not necessarily predictable from linear data (Sella-Tunis et al., 2018), to which end three-dimensional structural modelling using finite-element analysis would be appropriate (see Morales-García et al., 2019).

Multiple hypotheses pertain to the possible selective advantages of EDAR V370A, and none of these are mutually exclusive. Recognition of the temporal correlation between allele age and the timelines for wild grain consumption and domestication in East Asia, however, provides a linkage between diet and nutritional gain during the transition to agriculture. Worldwide, this transition has been associated with diverse changes in human behavior and morphological features, and is suggestive of powerful selective forces at play. For example, an allele for a highly active form of alcohol dehydrogenase originated in central China in parallel with rice domestication, prompting speculation as to increased dietary exposure to ethanol derived from carbohydrate fermentation (Peng et al., 2010). The pleiotropic effects of EDAR V370A are multifaceted, and unifactorial explanations for associated selective forces are likely to be incomplete. Nonetheless, chronic energetic benefits concurrent with grain domestication in East Asia have not previously been envisioned for this allele, and may have been of considerable advantage.

Acknowledgments

I thank Professor Li Liu and two anonymous reviewers for helpful comments on the manuscript.

REFERENCES

Adhikari, K. et al. (2016). A genome-wide association scan implicates *DCHS2*, *RUNX2*, *GLI3*, *PAX1* and *EDAR* in human facial variation. *Nature Communications, 7*, 11616.

Bailey, S.E., Hublin, J.-J., & Antón, S.C. (2019). Rare dental trait provides morphological evidence of archaic introgression in Asian fossil record. *Proceedings of the National Academy of Sciences USA, 116*, 14806-14807.

Bailey, S.E., Kupczik, K., Hublin, J.-J., & Antón, S.C. (2020). A closer look at the 3-rooted lower second molar of an archaic human from Xiahe. *Proceedings of the National Academy of Sciences USA, 117*, 39-40.

Bestel, S., Crawford, G.W., Liu, L., Shi, J., Song, Y., & Chen, X. (2014). The evolution of millet domestication, Middle Yellow River Region, North China: Evidence from charred seeds at the late Upper Paleolithic Shizitan Locality 9 site. *The Holocene, 24*, 261-265.

Blanco, R., & Chakraborty, R. (1976). The genetics of shovel shape in maxillary central incisors in man. *American Journal of Physical Anthropology, 44*, 233-236.

Brabant, H.E. (1971). The human dentition during the Megalithic era. In A.A. Dahlberg (Ed.): *Dental Morphology and Evolution* (pp. 283-297). Chicago: University of Chicago Press.

Bryk, J., Hardouin, E., Pugach, I., Hughes, D., Strotmann, R., Stoneking, M., & Myles, S. (2008). Positive selection in East Asians for an *EDAR* allele that enhances NF-κB activation. *PLoS ONE 3*, e2209.

Carayon, D. et al. (2018). A geometric morphometric approach to the study of variation of shovel-shaped incisors. *American Journal of Physical Anthropology, 168*, 229-241.

Chang, S.H., Jobling, S., Brennan, K., & Headon, D.J. (2009). Enhanced Edar signalling has pleiotropic effects on craniofacial and cutaneous glands. *PLoS ONE, 4*, e7591.

Clement, A.F., Hillson, S.W., & Aiello, L.C. (2012). Tooth wear, Neanderthal facial morphology and the anterior dental loading hypothesis. *Journal of Human Evolution, 62*, 367-376.

Cohen, M.M., Blitzer, F.J., Arvystas, M.G., and

Bonneau, R.H. (1970). Abnormalities of the permanent dentition in trisomy G. *Journal of Dental Research, 49*, 1386-1393.

Dahlberg, A.A. (1963). Dental evolution and culture. *Human Biology, 35*, 237-249.

Flegontov, P. et al. (2019). Palaeo-Eskimo genetic ancestry and the peopling of Chukokta and North America. *Nature, 570*, 236-240.

Fujimoto, A., Ohashi, J., Nishida, N., Miyagawa, T., Morishita, Y., Tsunoda, T., Kimura, R., & Tokunaga, K. (2008). A replication study confirmed the *EDAR* gene to be a major contributor to population differentiation regarding head hair thickness in Asia. *Human Genetics, 124*, 179-185.

Fuller, D.Q. et al. (2014). Convergent evolution and parallelism in plant domestication revealed by an expanding archeological record. *Proceedings of the National Academy of Sciences USA, 111*, 6147 -6152.

Gross, B.L., & Zhao, Z. (2014). Archaeological and genetic insights into the origins of domesticated rice. *Proceedings of the National Academy of Sciences USA, 111*, 6190-6197.

Hanihara, K., Masuda, T., & Tanaka, T. (1974). Family studies of the shovel trait in the maxillary central incisor. *Journal of the Anthropological Society of Nippon, 83*, 107-112.

Hlusko, L.J. et al. (2018). Environmental selection during the last ice age on the mother-to-infant transmission of vitamin D and fatty acids through breast milk. *Proceedings of the National Academy of Sciences USA, 115*, E4426-E4432.

Hrdlička, A. (1920). Shovel-shaped teeth. *American Journal of Physical Anthropology, 3*, 429-465.

Hrdlička, A. (1921). Further studies of tooth morphology. *American Journal of Physical Anthropology, 4*, 141-176.

Kamberov, Y.G. et al. (2013). Modeling recent human evolution in mice by expression of a selected EDAR variant. *Cell, 152*, 691-702.

Katz, D.C., Grote, M.N., & Weaver, T.D. (2017). Changes in human skull morphology across the agricultural transition are consistent with softer diets in preindustrial farming groups. *Proceedings of the National Academy of Sciences USA, 114*, 9050-9055.

Kimura, R., Yamaguchi, T., Takeda, Y., Kondo, O., Toma, T., Haneji, K., Hanihara, T., Matsukura, H., kawamura, S., Maki, K., et al. (2009). A common variation in EDAR is a genetic determinant of shovel-shaped incisors. *American Journal of Human Genetics, 85*, 528-535.

Larson, G. et al. (2014). Current perspectives and the future of domestication studies. *Proceedings of the National Academy of Sciences USA, 111*, 6139 -6146.

Li, H., Zhuan, Q., & Zhu, H. (2012). The size variation and related implications of mandibles in northern China in the past 7000 years. *Chinese Science Bulletin, 57*, 387-394.

Liu, L., Lee, G.-A., Jiang, L., & Zhang, J. (2007). Evidence for the early beginning (c. 9000 cal. BP) of rice domestication in China: a response. *The Holocene, 17*, 1059-1068.

Liu, L. et al. (2018). Harvesting and processing wild cereals in the Upper Palaeolithic Yellow River Valley, China. *Antiquity, 92*, 603-619.

Liu, L., Bestel, S., Shi, J., Song, Y., & Chen, X. (2013). Paleolithic human exploitation of plant foods during the last glacial maximum in North China. *Proceedings of the National Academy of Sciences USA, 110*, 5380-5385.

Lu, H. et al. (2009). Earliest domestication of common millet (*Panicum miliaceum*) in East Asia extended to 10,000 years ago. *Proceedings of the National Academy of Sciences USA, 106*, 7367-7372.

Mathieson, I. (2020). Limited evidence for selection at the *FADS* locus in Native American populations. *Molecular Biology and Evolution, 37*, 2029-2033.

Mizoguchi, Y. (1985). *Shovelling: A Statistical Analysis of its Morphology*. Tokyo: University of Tokyo Press.

Molina, J. et al. (2011). Molecular evidence for a single evolutionary origin of domesticated rice. *Proceedings of the National Academy of Sciences USA, 108*, 8351-8356.

Noback, M.L., & Harvati, K. (2015). The contribution of subsistence to global human cranial variation. *Journal of Human Evolution, 80*, 34-50.

Park, J.-H. et al. (2012). Effects of an Asian-specific non-synonymous EDAR variant on multiple dental traits. *Journal of Human Genetics, 57*, 508-514.

Peng, Y. et al. (2010). The ADH1B Arg47His polymorphism in East Asian populations and expansion of rice domestication in history. *BMC Evolutionary Biology*, *10*, 15.

Pineda-Munoz, S., Lazagabaster, I.A., Alroy, J., & Evans, A.R. (2017). Inferring diet from dental morphology in terrestrial mammals. *Methods in Ecology and Evolution, 8*, 481–491.

Riddell, J., Mallick, C.B., Jacobs, G.S., Schoenebeck, J.J, & Headon, D.J. (2020). Characterisation of a second gain of function EDAR variant, encoding EDAR380R, in East Asia. *European Journal of*

Human Genetics, doi.org/10.1038/s41431-020-0660-6.

Ross, C.F., Iriarte-Diaz, J., & Nunn, C.L. (2012). Innovative approaches to the relationship between diet and mandibular morphology in primates. *International Journal of Primatology, 33*, 632-660.

Sabeti, P.C. et al. (2007). Genome-wide detection and characterization of positive selection in human populations. *Nature, 449*, 913-919.

Scott, G.R. & Turner, C.G. (1988). Dental anthropology. *Annual Review of Anthropology, 17*, 99-126.

Scott, G.R., Irish, J.D., & Martinón-Torres, M. (2020). A more comprehensive view of the Denisovan 3-rooted lower second molar from Xiahe. *Proceedings of the National Academy of Sciences USA, 117*, 37-38.

Scott, G.R., Turner, C.G., Townsend, G.C., & Martinón-Torres, M. (2018). *The Anthropology of Modern Human Teeth: Dental Morphology and its Variation in Recent and Fossil Homo sapiens*. Cambridge; New York, NY: Cambridge University Press.

Sella-Tunis, T., Pokhojaev, A., Sarig, R., O'Higgins, P., & May, H. (2018). Human mandibular shape is associated with masticatory muscle force. *Scientific Reports, 8*, 6042.

Stojanowski, C.M., Johnson, K.M., & Duncan, W.N. (2013). Sinodonty and beyond: hemispheric, regional, and intracemetery approaches to studying dental morphological variation in the New World. In G.R. Scott and J.D. Irish (Eds.), *Anthropological Perspectives on Tooth Morphology: Genetics, Evolution, Variation* (pp. 408-452). Cambridge: Cambridge University Press.

Turner, C.G. (1971). Three-rooted mandibular first permanent molars and the question of American Indian origins. *American Journal of Physical Anthropology, 34*, 229-241.

Turner, C.G. (1976). Dental evidence on the origins of the Ainu and Japanese. *Science, 193*, 911- 913.

Turner, C.G. (1986). Dentochronological separation estimates for Pacific rim populations. *Science*, *232*, 1140-1142.

Turner, C.G. (1990). Major features of Sundadonty and Sinodonty, including suggestions about East Asian microevolution, population history, and late Pleistocene relationships with Australian Aboriginals. *American Journal of Physical Anthropology, 82*, 295-317.

Turner, C.G., & Bird, J. (1981). Dentition of Chilean paleo-Indians and peopling of the Americas. *Science, 212*, 1053-1055

Ungar, P.S. (2010). *Mammal teeth*. Baltimore: Johns Hopkins University Press.

Valdez, I.H., & Fox, PC. (1991). Interactions of the salivary and gastrointestinal systems. I. The role of saliva in digestion. *Digestive Diseases, 9*, 125-132.

von Cramon-Taubadel, N. (2011). Global mandibular variation reflects differences in agricultural and hunter-gatherer subsistence strategies. *Proceedings of the National Academy of Sciences USA, 108*, 19546-19551.

Wang, L., & Sebillaud, P. (2019). The emergence of early pottery in East Asia: new discoveries and perspectives. *Journal of World Prehistory, 32*, 73-110.

Yang, X., Wan, Z., Perry, L., Lu, H., Wang, Q., Zhao, C., Li, J., Xie, F., Yu, J., Cui, T., Wang, T., Li, M., Ge, Q. (2012). Early millet use in northern China. *Proceedings of the National Academy of Sciences USA, 109*, 3726-3730.

BOOK REVIEW

A World View of Bioculturally Modified Teeth. Edited by Scott E. Burnett and Joel D. Irish. University Press of Florida. 2017. 368 pp., $110.00 (hardcover). ISBN: 9780813054834.

There is great public and academic interest in intentional body modification. Interest is largely driven by the glimpse that bodily alterations offer into the belief systems of past and present societies. In focusing on the myriad populations that practice(d) intentional modification of the teeth, the edited volume, *A World View of Bioculturallu Modified Teeth*, offers readers a fascinating collection of chapters that illustrate the worldwide and temporal variation of an ancient practice. Four main types of intentional dental modification are discussed across 20 chapters: ablation (intentional tooth removal), filing, notching and incising, inlays (drilling the tooth to insert precious stones or metal), and tooth dyeing. The volume editors, Scott Burnett and Joel Irish, have the expertise and network to move such research in a much needed direction with the aim of pulling together population-level data rather than case studies of single individuals or sites, which have dominated the scholarly literature up to now. This approach fosters greater understanding of the social implications and biological consequences of intentional dental modification.

The book is divided into four sections covering different geographic regions: I) Africa, II) Europe and Northeast Asia, III) Southeast Asia, Australia, and Oceania, and, IV) the Americas. South America is, unfortunately, missing, though an Introduction written by Burnett and Irish provides a useful overview and ample references to work done in this region. Geographic coverage by the volume is, nonetheless, expansive. It is fitting that a foreword by Clark Spencer Larsen and a conclusion chapter by George Milner bookend the volume, as they published a widely read and highly regarded review of archaeological cases of dental modification in 1991.

There is a nice mix of early, mid- and late career scholars such that the volume contains chapters by the 'who's who' of dental anthropology but also brings newer researchers into the fold. As well, the authors come from different professional environments, including government ministries, museum curators, private companies, and various universities. Within the overarching theme of population perspective, the chapters have different aims, which exposes the reader to a broad range of methods that are used to explore diverse questions. The chapters are well written, clearly organized and blessedly concise. The most commonly discussed topics are (i) improved diagnostic methods (especially to distinguish causes of tooth ablation), (ii) the possibility that tooth ablation in some African groups was done because tetanus or infantile fever caused lockjaw, (iii) the effect of dental modification on oral health, (iv) the tools and methods used to modify teeth along with the proficiency of the person who performed the procedure, (v) the association of modification with sex, age, status, family/lineage, population and other identity categories, (vi) the role of modification as a physical signal to people/groups within (intra-) vs. outside (inter-) the population, (vii) the origin of the practice especially in regard to cultural diffusion vs. independent invention, and (viii) the use of spatiotemporal patterns of modification to infer movement and interaction amongst past populations.

The book is best suited to readers with some basic (bio)archaeological knowledge, but for the most part can also be understood by those without such knowledge. Most chapters contain evocative photographs of modified teeth and, if anything, one could wish for more of these. Other depictions of tooth modification are also compelling, including an image from the ancient Egyptian Tablet of Terura depicting a man being fed through a hollow tube placed in an opening possibly left by ablated teeth that were removed because of lockjaw (in the chapter by Bolhofner about Ancient Nubia) and a picture of an approximately 2000-year-old stone rain deity mask with clear evidence of inlays in the anterior teeth (in the chapter by Mayes and colleagues about Oaxaca, Mexico). Harvey and colleagues created useful drawings that reconstruct the face and smile of Jomon individuals from Japan with tooth ablation (to 'flesh out the skulls'). Many chapters include fascinating and informative accounts of tooth modification by past indigenous peoples and those with whom they came into contact (from sub-Saharan Africa, Southeastern Australia, Western Micronesia, Mesoamerica, and ancient Nubia) and the chapters on Taiwan, by Pietrusewsky and colleagues, and Bali, by Artaria, even include photographs of recent people undergoing tooth modification.

A valuable feature of this book is two chapters that explore intentional dental modification in modern populations, one living in Cape Town, South

Africa, in a chapter by Friedling, and the other living on the island of Java in Indonesia, in a chapter by Artaria. The ability to ask people why they chose to modify their teeth provides tremendous insight into what is often the most elusive question we have of past populations, which is "why did they do that?" Respondents gave a variety of reasons for removing or filing their teeth, most commonly involving notions of beauty, identity, and custom. I would have appreciated a chapter about modern-day dental procedures common in Western and other societies, often termed 'cosmetic dentistry', and including teeth straightening, whitening, replacement (i.e. veneers, caps including decorative gold crowns, bridges, dentures, etc.) and even the wearing of dental grills. Such chapters would serve to lessen the 'othering' that can happen with a book like this, as many readers will associate the examples with foreign places and peoples, and not think about dental modification for non-therapeutic purposes as a practice that is common in their own society.

The most common finding across populations that practiced dental modification is its occurrence during adolescence (circa 10-25 years of age), with the physical changes of puberty most closely tied to ceremonial events. Other findings common across populations proved elusive, as the association of dental modification with sex, status, and other identity groups is quite variable. An unexplored avenue is the comparison of skeletal markers of repetitive physical activity, such as long-bone cross-sectional geometry or muscle entheses, among those with and without dental modification, to identify different task or occupation groups, especially involving differential mobility. As well, at sites with skeletons suitable for radiocarbon dating, Bayesian modelling of each individual could illuminate fine-scale temporal patterns in dental modification.

The chapters that explored the effect of dental modification on oral health, perhaps surprisingly, did not always find a significant increase in caries or infection rates, although authors note these findings need to be substantiated with tooth specific data and by taking into account confounding factors such as age, diet, and dental wear. Radiographic and microscopic methods proved useful in detecting changes in the inner tooth layers (dentine and pulp) and alveolar bone. A future avenue to explore the impact of dental modification on oral health is via human and microbial biomolecules (proteins and DNA) in calculus deposits.

This volume demonstrates that isotopic methods can elucidate relationships between dental modification and aspects of identity, as shown by Kusaka who used stable carbon and nitrogen isotopes to reconstruct dietary differences among different Jomon sites; Hedman and colleagues who used strontium isotope ratios to determine the birthplace of individuals with dental modification at Cahokia; and Newton and Domett who reference oxygen and strontium isotope work being done to detect immigrants at several Southeast Asian sites. While there were no chapters in this volume that used ancient DNA data to explore genetic affinity and dental modification patterns, such work has recently been done and will no doubt become more common in the future.

All in all, the reader will undoubtedly come away with an appreciation of the wide range of insights, ranging from the 'how' to the 'why', that can be drawn by studying intentional dental modification. The editors and authors aptly demonstrate the utility of population-level investigations. As is often the case in bioarchaeology, much of the research raises just as many questions as answers. Yet, with new research broaching ever more sophisticated questions, as seen in this volume, our understandings are sure to grow and improve.

REFERENCE

Milner, G. R., & Larsen, C. S. (1991). Teeth as artifacts of human behavior: intentional mutilation and accidental modification. In M.A. Kelley & C.S. Larsen (Eds.), *Advances in dental anthropology* (pp. 357-378). New York: Wiley-Liss.

ANDREA L. WATERS-RIST
Department of Anthropology
University of Western Ontario

Dental Anthropology

Volume 34, Issue 01, 2021

Case Study

Growth Rates of Accessory Human Enamel: A Histological Case Study of a Modern-Day Incisor from Northern England
Christopher Aris and Emma Street 3

Research Articles

The Impact of Hybridization on Upper First Molar Shape in Robust Capuchins (*Sapajus nigritus* x *S. libidinosus*)
Emma Ayres Kozitzky 13

Permanent Molar Trait Expression in the Late Neolithic Cave Burials of the Meuse Basin, Belgium
Frank L'Engle Williams and Rebecca L. George 35

Commentary

A Morphofunctional Hypothesis for Selection on EDAR V370A and Associated Elements of Sinodonty
Robert Dudley 49

Book Review

Book Review: *A World View of Bioculturally Modified Teeth*
Andrea L. Waters-Rist 55

Published at:
The University of Nevada, Reno
1664 North Virginia, Reno, Nevada, 89557-0096 U.S.A.